An investigation into the structure and performance of a glass fibre size

Michael P. McGravey

An investigation into the structure and performance of a glass fibre size

Michael P. McGravey

Chemistry Department

Durham University

Durham, U.K.

DH1 3LE

Acknowledgements

From Celanese I would like to thank Shayel Ahmed for his unstinting support in this project and also Marc van Boxtel for continuing this support upon Shayel's departure from Celanese. Special thanks should also go to Rian van Straeten for the wet-out rate analysis work and for providing me with a moment of clarity mid-way through the project which helped reassess my goals for the project and how I could achieve them.

From Leeds I would like to thank Peter Hine for his invaluable help with all of the mechanical testing undertaken.

From Durham I would like to thank Lian Hutchings for his help with the GPC analysis and Laurent Porres for similar help with the UV-Vis absorption analysis. I would also like to thank Julian Bent and Sarah Green for help with photon correlation spectroscopy analysis, Christine Richardson for SEM analysis and Stephen Collins for assistance with DMA. Special thanks should go to Stuart Eggleston who has helped me with goniometry, ATR-FTIR and ESEM on many occasions and also to Richard Thompson for his help with IBA. I would also like to thank everyone who has been in the office during my time in Durham for making it a great place to study in.

Very special thanks should also go to both Linda and Adam for their unstinting support and for putting up with me throughout and also to Andrew for giving me a new, upcoming challenge.

Finally I would like to thank Neil for giving me the opportunity to do this project and for all his help and advice throughout.

Neil and I are grateful to Celanese and St. Gobain Vetrotex for their financial support.

Executive Summary

Batches of film-formers were created via emulsion polymerisation from a formulation supplied by Celanese. These film-formers were then incorporated into a formulation as supplied by St. Gobain Vetrotex which is used in industry to produce a working glass fibre size.

Initial studies were undertaken to determine the location of the constituent species present in the size to produce an image of its structure. The film-former formulation was then altered to produce a range of physical properties. The performance of sizes produced from these film-formers were then investigated in the areas of clarity, film formation, wetting ability and strength. Alterations to the size formulation was then undertaken to determine whether this produced any effect in the performance of the size over some of the same areas of investigation. The conclusions drawn are listed below:

- The coupling agent species present in the size formulation migrates to the glass interface of the size during drying.
- A minor amount of lubricant migrates to the air interface of the size during drying.
- Migration of species in the size only occurs during drying when the size is in its liquid state.
- The molecular weight and particle size of a film-former is directly related to the initiator and first stage monomer concentrations respectively.
- The molecular weight of a film-former does not alter the size's ability to form a continuous film if dried under suitable conditions.

- Film-formers with large particle sizes produce inhomogeneous films due to incomplete diffusion occurring during film formation.
- The inhomogeneity of films with larger particle sizes present produces an increasingly optically active film with an increased wet-out rate.
- The molecular weight and particle size of a film-former do not alter the corresponding sizes ability to wet a bare glass fibre due to the large amount of water present in the size formulation.
- A size can be redistributed following successive re-wetting and drying under certain conditions.
- The stiffness of a size is directly related to the molecular weight of the sizes film-former.
- An inhomogeneous, discontinuous size will be formed with excessive deviation from the size formulation.
- An excess of coupling agent is present in the standard size formulation.

Table of Contents

Chapter 1

Introduction

1.1 Glass Fibres

1.1.1 Introduction

Glass fibres were first introduced at the 1883 world's fair although it took more than 50 years for them to become commercially available. In 1939, the Owens-Corning Fibreglass Corporation introduced them as a method of insulating houses, and a few years later they were used to produce textiles. In the late 1940's fine diameter glass fibres, used in filtration systems, were also made available commercially. [1]

Nowadays about 1.5 million tons of glass fibres are consumed each year to be used as the primary materials for the production of reinforced plastics which are then used in a wide variety of applications. [2]

Glass fibres belong to a family of materials known as synthetic vitreous fibres (SVF) also known as man-made vitreous fibres (MMVF); other members of this family include mineral wool and refractory cement. Glass fibres differ from other SVFs due to the presence of high amounts of sodium (Na) and potassium (K). As well as this, the melting points of glass fibres are much lower than those of other SVFs and, therefore, glass fibres are only used in environments which will not exceed 200°C (although some are designed to be used in environments in excess of 500°C).[1]

1.1.2 The Manufacture of Glass

1.1.2.1 Introduction

In the production of glass fibres it is essential that the raw glass must be of a very high quality, as any imperfections in the glass would result in a breakage of the filament. Many different reasons can produce these imperfections, including a low melt temperature, the presence of dust particles in the glass mixture, and glass inhomogeneity. In the latter case the raw materials do not mix together efficiently. This causes sudden changes in the melt viscosity which, when drawn into filaments, causes the fibres to snap.

1.1.2.2 Grades of Glass

The common structural composition of glass is based around a silicon tetraoxide (SiO_4) tetrahedron with repeating silicon dioxide (SiO_2) units.[3] However, other metal oxides are also present in the glass which may produce a break in the polymer-like bond to produce terminal bonds, see figure 1.1.

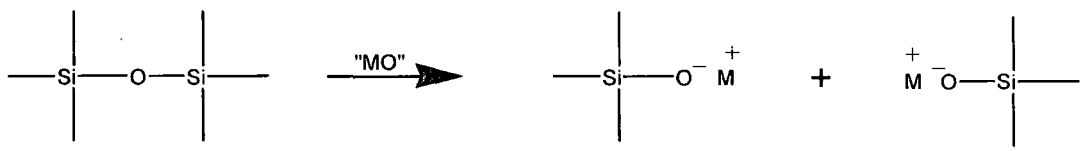

Figure 1.1 – The production of metal oxide (MO) induced terminal bonds.

Depending on the amount and type of metal oxide present in the glass, different "grades" of glass can be obtained. These have their own distinct properties, allowing them to be used for a variety of different applications.

Table 1.1 - Some of the different grades of glass.

Grade of Glass	Description
A	Glass containing aluminium, magnesium and calcium oxides.
C	Glass containing a greater proportion of boron oxide giving good chemical endurance.
D	Glass rich in silicon oxide with ~10% boron oxide. Provides improved chemical resistance in addition to enhanced dielectric properties.
E	Glass containing silicon, boron and aluminium oxides which provides improved electrical properties.
ECR	Glass contains silicon, calcium and aluminium oxide giving high chemical resistance, particularly with acids.
R	Glass contains silicon, aluminium, calcium and magnesium oxides. Has good resistance to thermal shock, moisture, ageing, corrosion and fatigue as well as its relatively high stiffness.
S	Glass contains silicon and aluminium oxides and ~10% magnesium oxide giving increased glass strength.

1.1.3 Production

Many different techniques exist to produce glass fibres, [4, 5] however they are all based around the same system and use the same apparatus with modifications to improve control throughout the system [6], see figure 1.2.

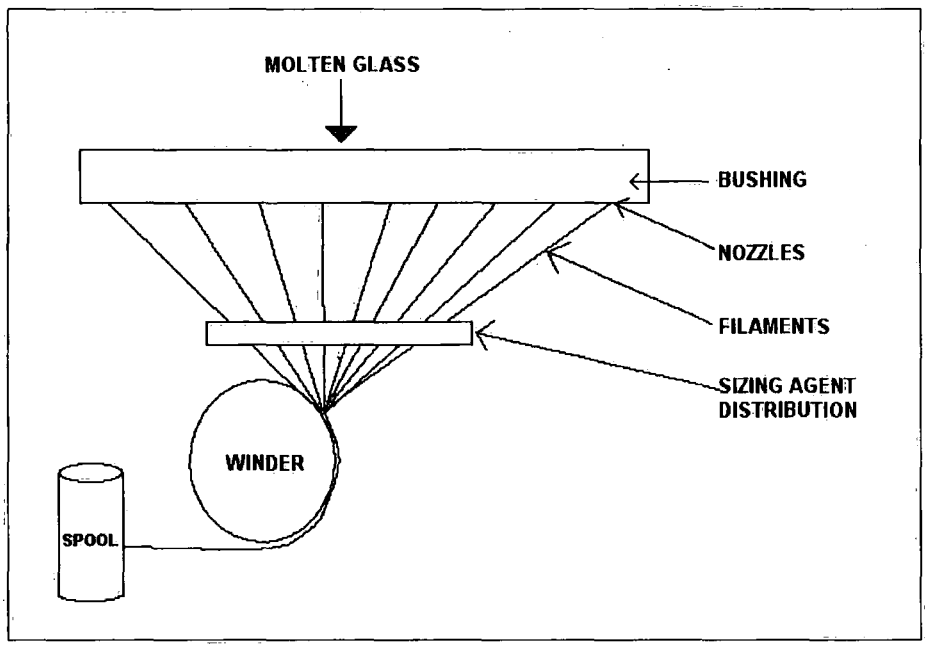

Figure 1.2 – Glass fibre production equipment.

To produce glass fibres, the glass must first be heated to 1250°C to melt it and make it malleable. The molten glass is then passed through a plate containing many apertures, which is called a bushing.[7] The bushing consists of a platinum-palladium alloy block with an array of holes (200-400), to each of which is attached a nozzle made from an alloy of gold and platinum. It has been observed [8] that different grades of glass require different ratios of gold to platinum in the alloy to produce strong glass fibres which do not break easily. The gold and platinum present in the alloy will not react with the glass; rather the difference in gold content will further reinforce the nozzle at the high temperatures to which they are subjected for each different grade of glass.

The molten glass will pass through the nozzles to produce filaments with a constant diameter of between 5-24 μm. The diameter of the filaments must be constant throughout to produce good quality fibres and this can be ensured by the control of a variety of procedures. After the filaments are drawn they are collected onto a winder and it has been found that the diameter of the fibre can be controlled effectively by controlling the speed of the winding.[9] If the speed of the winder is increased then the diameter of the filaments decreases due to the constant flow rate of the molten glass through the bushing. This can then be used to maintain a consistent diameter by increasing or decreasing the speed of the winder if the glass flow rate decreases or increases respectively. There is also mention of an additional plate fitted just above the bushing to control further the flow rate of the molten glass, to extend the control of the fibre diameter.[10] This plate is used as a precautionary measure to stop the molten glass passing too quickly through the bushing, producing filaments with variable diameter. To enhance the consistency of the flow of glass through the bushing a constant temperature is required throughout the entire system. This can be ensured using a recently developed technique, which employs a spaced pair of electric melters in the fully insulated system to ensure a constant temperature.[11]

Immediately after the filaments are drawn from the bushing but before they are wound onto the roller they are sprayed with a coating called a "size". The size is added to ensure cohesion between the fibres so they can be brought together to form a thicker strand and also to protect the fibres from abrasion. The concentration of the size on the glass is usually in the region of

2% by mass and the type of the size used depends on the intended application for the glass fibres.

For glass fibres intended for use in the reinforcement industry the size will contain a film-former, binding products, anti-static agents, plasticisers and coupling agents. These additives are included to ensure good compatibility between the polymer matrix and the fibres producing a composite. For glass fibres intended for use in the textile industry the size will also contain softening agents, additional bonding agents and lubricants.[12]

When the fibres are being used for reinforcement the roller collects all of the sized glass fibres and spools them together on a card roll to form a "cake". This results in the formation of a single strand of glass with a thickness of 2-3 cm. These cakes are then oven dried and used to produce rovings which are used in the fields of moulding and filament windings. The other product formed from the dried cakes is chopped strand mat which is used for reinforcing plastics.

If the fibres are to be used in the textile industry, they will be woven rather than spooled to strengthen the fibres and the size will be removed thermally.

1.1.4 Products & Applications

There are many different products which can be made from glass fibres in the textile, insulation and reinforcement areas.[7, 13]

Textile and volumised fibres are characterised by the amount of twists present in the fibre, the direction of these twists and the diameters of the filaments. Yarns are either single (one large twist) or plied (two or more twisted oppositely) and they can be used directly on industrial process machinery for weaving, braiding and covering. These fibres can be used to produce many useful compounds such as synthetic resins, bitumen, mica, paper and adhesives. The incorporation of support fibres into the glass fibres has produced much stronger yarns while remaining sufficiently flexible to allow it to be used as a textile material.[14] Volumised fibres are textile fibres which have had their volume increased mechanically; these tend to be mainly used to produce decorative fabrics.

Rovings are produced either directly from the bushing by the drawing of filaments (direct roving) or by assembling several strands in parallel with no twists (assembled roving). The characteristics of a roving depend on the conditions with which it will be used, i.e. equal tension of fibres (weaving), continuous impregnation (lubricity) or ease of cutting (choppability).[15]

A spun roving has extra transverse strength which occurs from the presence of extra loops perpendicular to the main direction of the roving. Pre-preg roving is also a strong roving since it has been impregnated with epoxy resin and is used in filament winding because of its good mechanical performance.

The problem of impregnating the fibres into a plastic is significant as the two components are often incompatible. One method of overcoming this, proposed by Gaymans et al. [16] employs direct rovings and polypropylene as the matrix. The rovings are etched using a sharp pin to create a site into which the polymer can diffuse, causing impregnation. It was also established that the number of pins used to produce the etchings on the glass fibres is directly proportional to the strength of the plastic. More pins produce more etching, which will lead to greater impregnation of polymer increasing the overall toughness.

Chopped strands are fibres which have been cut to lengths of 3-12 mm and are generally used as reinforcers for plastics, plaster, cement and paper due to their characteristic properties of integrity, flowability and compatibility. Chopped strand mats are chopped strands which have been brought together by a binder which is soluble in a monomer (such as styrene). [13]

Continuous filament mats are felts of continuous filaments distributed in uniform layers as they leave the bushing and are held together by a binder (the type and content of the binder is dependent on the application of the mat). They are used in moulding applications and in the production of continuous profiles such as circuit boards. [13]

Milled fibres are fibres which have been cut very finely to lengths of around 0.1mm and are mainly used for reinforcing thermoplastic resins and polyurethanes. [13]

1.1.5 Physical Properties

Glass fibres have many properties which are best exemplified when they are part of a composite material where they act as the reinforcer.[7] The most important properties are listed below.

Mechanical strength

Glass fibres have a greater specific resistance (tensile strength/volumetric mass) than that of steel. This makes them highly useful as reinforcing agents for plastics.[17, 18]

Electrical Characteristics

Glass fibres are an excellent electrical insulator even at low thicknesses. This has been exemplified by applications where glass fibre products have been used as both electrical and thermal insulators.[19-23]

Incombustibility

As a mineral material, glass fibres are incombustible and will not support or propagate a flame as well as not emit smoke or toxins when they are exposed to heat.[24, 25]

Dimensional stability

Glass fibres are insensitive to variations in humidity and temperature and also have a low coefficient of linear expansion.

Compatibility with organic compounds

Many different sizes can be attached to the glass surface as well as other mineral compounds (cement and plaster). There are also examples where rare earth elements have been introduced into glass fibres to produce

products with improved optical characteristics for the telecommunications industry.[26-28]

Non-rotting

Glass fibres do not deteriorate or rot. This makes them useful in long term applications where it is not possible to replace parts easily.[29]

Low thermal conductivity

This is a useful property in the building industry as glass fibre composites of cement and plaster eliminate thermal bridging, preventing heat flow.[30, 31]

Dielectric permeability

This is essential in applications such as electromagnetic windows.[32]

High resistance to chemical agents

When combined with appropriate resins, composites with this characteristic can be made from glass fibre.[33,34]

1.2 Glass Fibre Size

1.2.1 Introduction

Bare glass fibres do not remain bare for longer than a second when exposed to the atmosphere. Water is absorbed into the glass which causes the strength of the glass fibre to reduce by a factor of five, and the loss of strength further increases with longer exposure. To prevent this loss of strength the glass fibres are coated with a size to stop the atmospheric water from absorbing into the glass. As well as protecting the surface of the glass the size also aids the handling of the product. In order for a size to be successful, it must allow a bundle of filaments to be converted into a thicker strand. Furthermore the strands must be able to have good choppability, that is they must be able to be chopped cleanly producing shorter lengths of the strand without fraying of the fibres. It must also be resistant to abrasion, remain free from static electricity and remain intact as a single strand throughout. Finally the size must have a fast wet-out rate; this is the rate at which the size is removed from the strand reproducing the original glass fibre structure.

1.2.2 Compounds Present in the Size

1.2.2.1 Coupling Agents

A coupling agent, also known as a keying agent, is present to bind the glass fibres to the remainder of the size to produce a composite material. Coupling agents are a family of chemicals, characterised by their organo-silicon nature, which possess dual or multiple functionalities. It is known that each silicon atom has one or more functional groups which will react with the glass surface resulting in the removal of ethoxide (OEt) groups and the formation of oxide linkages to the glass surface and the production of ethanol. This proposal has yet to be proved beyond doubt and has been termed the chemical bond theory of coupling agents.[13] In most cases a further functional group on the silicon will be selected to allow it to co-react with the polymer creating a chemical bridge. To ensure this incorporation occurs the functional group on the coupling agent must have an affinity with the polymer thus making the chemical bridge sufficiently strong. A proposed scheme for the reaction between the glass and coupling agent is given below, figure 1.3.

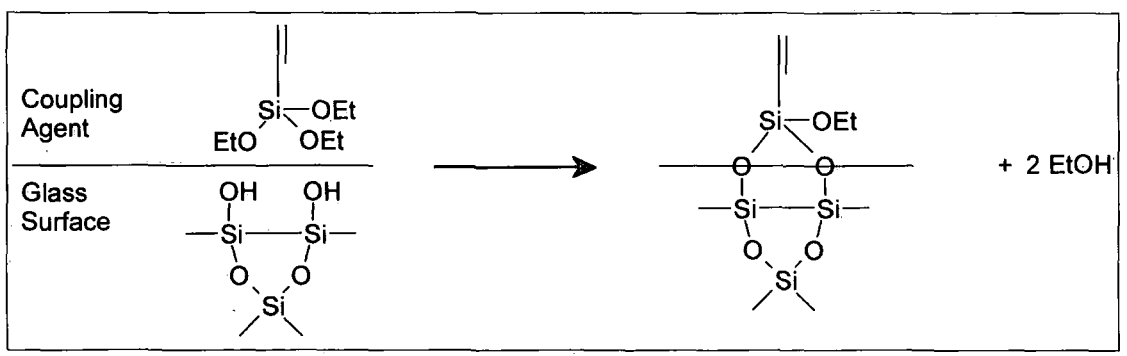

Figure 1.3 – Diagrammatic representation of the chemical bond theory of coupling agents.

Investigations of the validity of the chemical bond theory of coupling agents have been made previously. [35] Recently attempts have been made to

produce a universal coupling agent which will work equally well for all types of polymers. Unfortunately it has since been deemed that such coupling agents are counter-productive as any negative aspects (cost, complex chemistry and lack of market demand) far outweigh the benefits which they would provide. Instead a mixture of two or more different coupling agents are now used to promote the best possible adhesion between a polymer mixture and the glass surface.

Sjögren et al. [36] investigated whether the presence of a coupling agent in a glass fibre size affected the amount of transverse cracking found in a composite material made from these fibres. Poly(vinyl ester) / glass fibre composites incorporating two different sizes, one containing a strong silane-based coupling agent (CA) and the other containing a weak coupling agent based on polyvinyl alcohol (NoCA) were used for this study. Single fibre composite tests were used to study the strength of the two composites. From these tests it was found that the NoCA sized composite produced the first crack at a much weaker strain than the CA sized composite. Furthermore it was found that good wetting was a general prerequisite for good interfacial adhesion between the glass fibres and the polymer.[37] The explanation provided for these results is that the coupling agent produces a region of good ductility and adhesion between the interfaces giving a stronger composite.

Some typical coupling agents which are widely used are shown below. 3-Aminopropyltriethoxysilane (Union Carbide A-1100) and N-(2-Aminoethyl)-3-aminopropyltrimethoxy-silane (Union Carbide A-1120) are very popular coupling agents due to the wide variety of polymers with which they can couple to glass (epoxies, polyurethanes, polyvinyls, acrylics, nylons,

phenolics). However some coupling agents will only couple specifically to one type of polymer, for example vinyltriethoxysilane (polyesters) (Union Carbide A-151) and tris(2-methoxyethoxy)vinylsilane (polyolefins and polyesters) (Union Carbide A-172 & Dow Corning Z-6082).

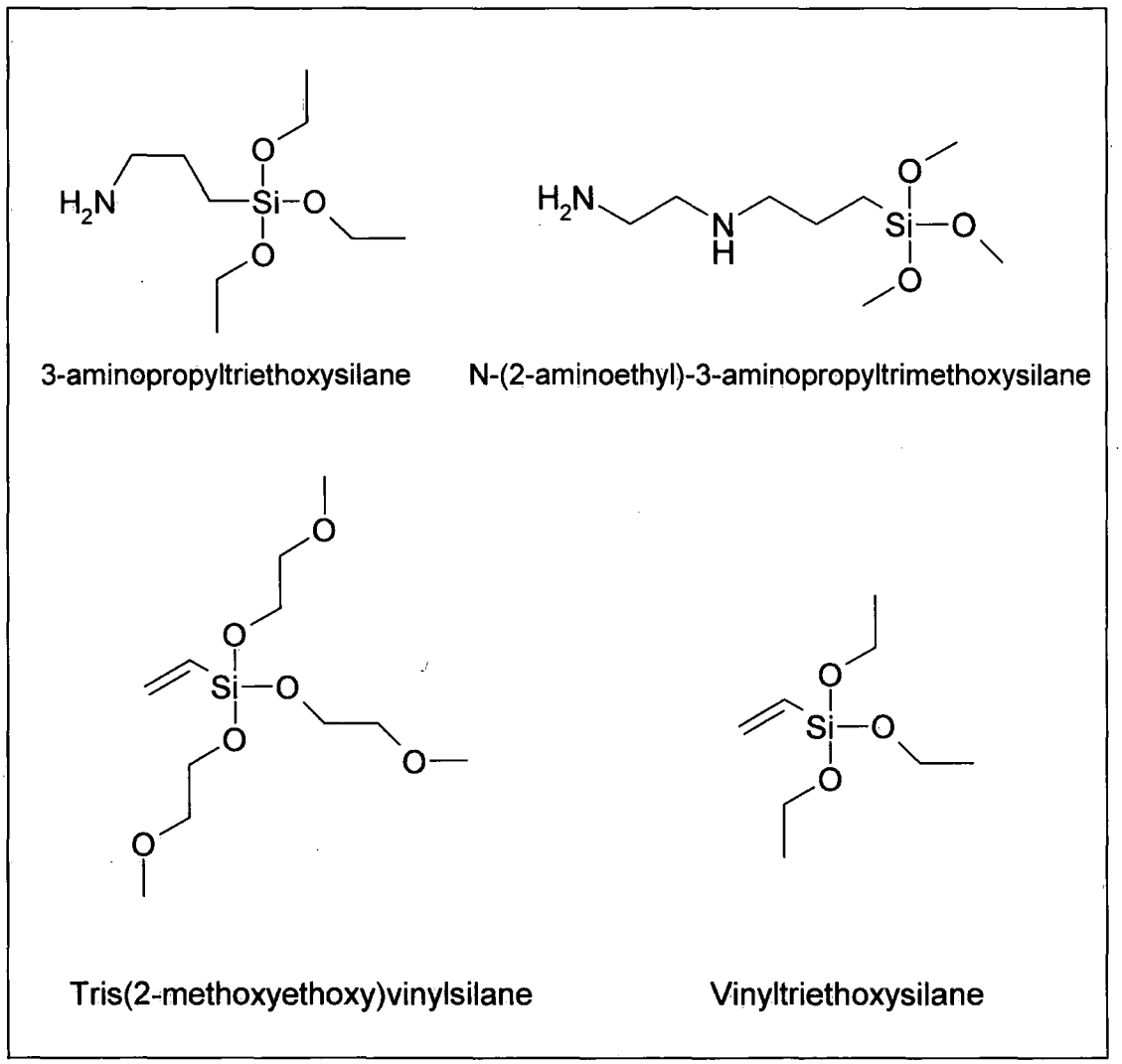

Figure 1.4 – Structures of selected glass fibre size coupling agents

1.2.2.2 Film-Former

The role of the film-former is to bind the fibres together as a strand to give specific handling characteristics and to protect the fibres and strand from damage. The majority of fibre sizes employ poly(vinyl acetate) (PVAc) as the film-former due to its low cost and the wide range of values of its properties which allows the production of many different materials with different uses (hard/soft strands, slow/medium/fast wet-out rates). There are other film-formers based on different polymers (polyesters and polyurethanes) and epoxy resins, which are used in certain circumstances where PVAc is unsuitable. [38-40]

It is widely accepted that the majority of film-formers will not produce a continuous film no matter how much is deposited onto the fibres or what temperature is used. Scanning electron microscopy (SEM) indicated that the film-former is deposited on the fibres as globules on the surface and in between the fibres, forming bridges that bind the fibres together, figure 1.5.

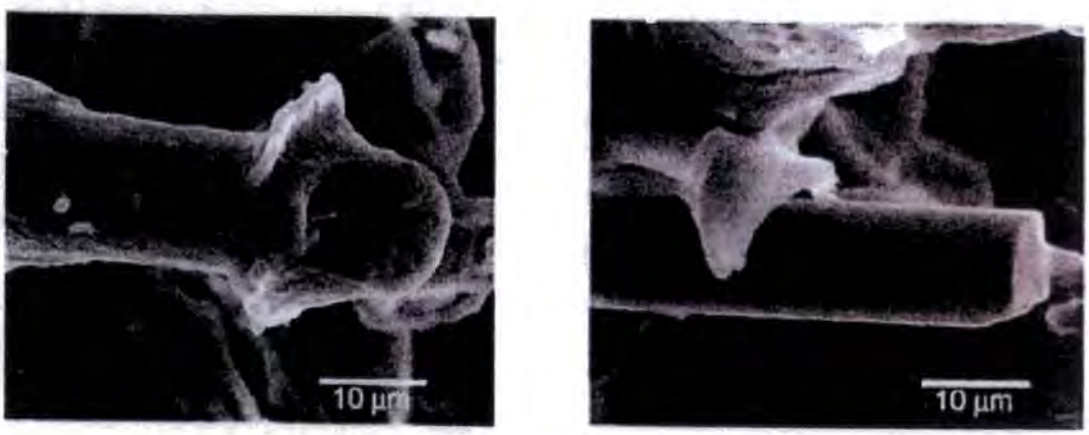

Figure 1.5 – SEM photomicrographs of sized glass fibres.

Left: size is based on anhydride silane; right: size is based on epoxy silane.[41]

(images taken direct from Paul DR et al., Polymer **2002,** *43*, 4673)

The PVAcs which are used as size components are formed using emulsion polymerisation, which results in the addition of further compounds to the size due to the requirement to stabilise the emulsion. These extra compounds therefore affect the physical properties of the glass fibres and any products made from the glass fibres. For example poly(vinyl alcohol) (PVA) is used as a stabiliser during emulsion polymerisation, but it will slow the wet-out rate of the size in the final matrix.[42]

In the production of glass fibres there is an enormous waste of size (about 70%) which occurs due to the excess being ejected from the fibres and lost during the sizing process. Attempts could be made to recover this by channelling the waste size into a vat and then delivering this back into the size storage medium. However it must be noted that the size has a limited life-time as some of the species present in it will degrade, so it must be re-distributed on the fibres quickly after it has been recollected.

In addition to PVAc many other types of film-former are being produced to increase the speed of the process and also to produce stronger composites. Generally the new film-formers which have been produced have resulted in improved compatibility and reduced wet-out times in polyester and epoxide resins, allowing them to be used in more demanding applications such as pressure vessels [43] and pipes. [44, 45]

1.2.2.3 Plasticisers

These are added to emulsions to increase the flexibility and thermoplasticity of the dried film. The physical properties can be varied by changing the concentration and type of plasticiser present. It is generally found that the choppability of the glass fibre strands improves as the concentration of plasticiser decreases. The two main types of plasticizers are given below.

Fugitive

These are mainly organic solvents (or water) that are used to promote film integration. They are lost by evaporation and as such are only temporary.

Permanent

These are characterised by their low volatility, low water solubility and high solubility in the film-former. The most common plasticisers of this type are dibutyl phthalate and poly(ethylene glycol) at various molecular weights (Carbowax 300/1000). These are shown below in figure 1.6.

The plasticiser content in PVAc latexes is between 0-20 wt % of the PVAc solid content.

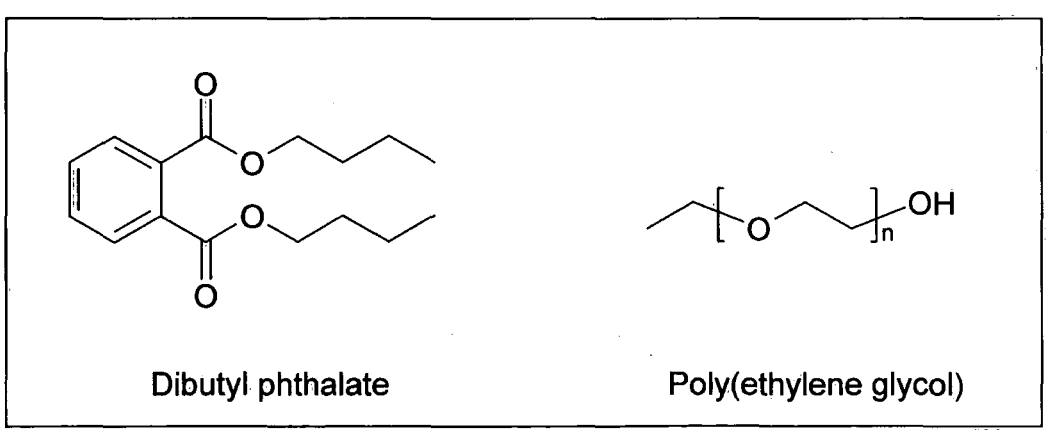

Dibutyl phthalate Poly(ethylene glycol)

Figure 1.6 – Structures of selected permanent glass fibre size plasticisers

1.2.2.4 Lubricants

Because glass surfaces are negatively charged, most lubricants tend to be positively charged cationic surface active agents, such as alkyltrimethyl ammonium chloride (Arquad S50). Another class of lubricant which is used widely in the glass fibre size industry consists of tetraethylenepentamine derivatives (Cirrasol 220). These lubricants are used in quantities between 0.2-2 wt % of the glass fibre size and they can be used in both cationic and anionic PVAc sizes.

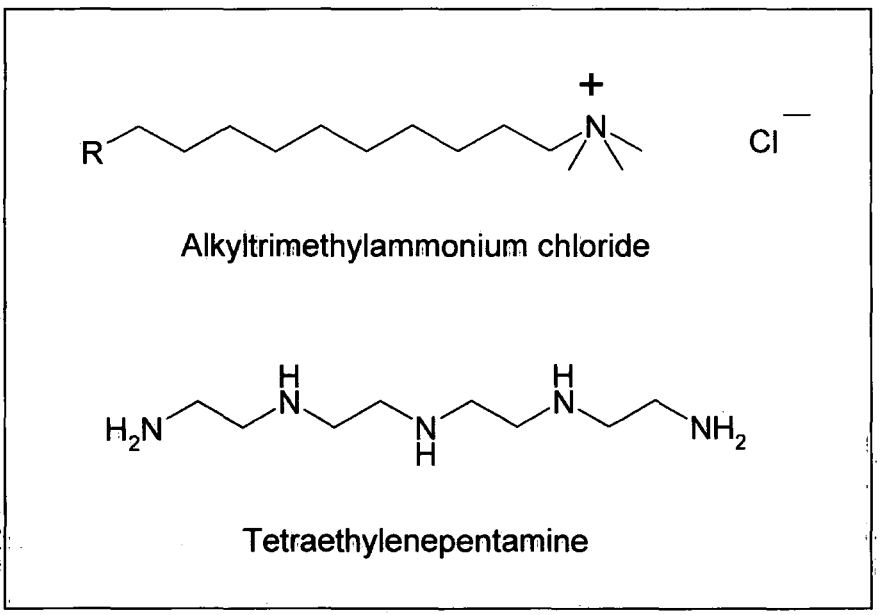

Figure 1.7 – Structures of selected glass fibre size lubricants

1.2.2.5 Anti-Static Agents

Glass fibres are generally made from E-glass, so a build up of static electricity can form on the glass surface. The static electricity is caused by friction and it may be conducted along the surface of the glass if it is sufficiently moist. Increasing the humidity of the surroundings (70-75%) to carry the electric charge away from the glass can solve this problem; however

this is not always a feasible option. Sometimes a chemical can be added to create an electrical path on the glass fibre; however it must not change the overall physical properties of the fibre. These chemicals must be able to form ions, which will create the electric path and also absorb water to allow this ionisation to take place. Some examples of such chemicals are LiCl, NH_4Cl, $MgCl_2$ and alkyltrimethylammonium chloride which is also used as a lubricant.

1.2.3 Formulations of the Size

There is no limit to the variations of the size that can be developed [46-54] although the proportions of the composition do have to be within certain limits.

Table 1.2 – General formulation of a size

Compound	Content in the size (wt %)
Coupling Agent	0.3 – 0.6
Film-Former & Plasticiser	3.5 - 15
Lubricants	0.1 – 0.3
Anti-Static Agents	0 - 0.3
Water	85 - 95

1.2.3.1 Selection of Coupling Agent

This is the first material to select because the choice of coupling agent is entirely dependent on the polymer being used in the film-former and the desired physical properties of the final composite. By using a mixture of coupling agents it is possible to produce a size which will perform better than just using a single coupling agent. This is especially useful for systems where the film-former consists of a co-polymer; a single coupling agent may only bind with one of the polymer units so a second would be added to bind with the other. As coupling of the size to the glass is restricted to the glass surface, it is found that only a small percentage of coupling agent is required within the size formulation (~0.5%).

Paul et al. [41] have proposed that the tensile modulus of a composite is relatively independent of the coupling agent present in the size. By studying composites of glass fibres and nylon-6 it was proposed that a weak interface between the two might produce a tougher composite material, although it was also stated that any increase in toughness would then be offset by a loss in the composite yield strength. The type of size used on the glass fibres had an effect on the weak axial properties where the most strongly bound interface would produce the highest yield strength but conversely the lowest toughness. It was found, using many different coupling agents, that the lowest yield strength came from the least polar coupling agent and the highest yield strength came from the most polar coupling agent.

1.2.3.2 Selection of Film-Former

The selection of a film-former is a more complex decision because of a number of reasons. One such reason is the compatibility between it and with the coupling agent previously selected. The stability of the size must also be considered both before and after it has been applied to the fibres. The handling properties of the strand after drying are also important as the strand must be relatively stiff so as not to produce breakages in the fibres while also ensuring cohesion throughout the strand preventing fraying of the individual fibres. The final product properties required must also be taken into account as the film-former is the major constituent of the size.

Due to the challenge of trying to select a film-former which will comply with all of the points above, it would be expected that the choice of film-former would be extremely difficult. However manufacturers aid the consumer by

supplying guidance when issuing their products. The type of film-former used can almost always be predicted by taking into account which polymer the glass fibres are intended to strengthen and the application of the final glass fibre products. Once the best film-former is selected some minor adjustments to the remaining additives need to be made to tailor the size for the intended application.

Since new materials appear on the market regularly, simple tests have been devised to determine the basic properties of the glass fibres. One of these tests is the rate of wet-out of film-former in the size. This involves determining the amount of time required for the size to be dissolved from the glass fibres; thus indicating the rate at which the strand will separate back into individual fibres. This method also indicates whether a particular plasticiser would be feasible as part of the size. However, it does not determine the quantity of film-former required for a specific amount of binding. To determine this, the wet-out test is repeated using different samples of sized glass fibres from different cakes. The quantity of the film-former incorporated into the size will depend on the end use of the glass fibre product and this can vary widely within these product types. This will depend on the molecular weight of the film-forming polymer and the amount of adhesion between the filaments or between the strands of the cake.

The properties of the film-former can be modified by changing the type and quantity of other additives present such as the plasticizer, coupling agents, lubricants, etc. For a wide range of fibre sizes a general picture is present which is dependent on the application of the fibres.

Sizes for chopped strands contain 4-8% film-former, 0.2-0.4% silane coupling agent and 0.05-0.08% lubricant, surfactants and anti-static agents. Strands which are sold as rovings for use in the compounding of thermoplastics are characterised by their high strand integrity and good wetting but also a slow dissolution into the thermoplastic resin. The size usually contains 5-12.5% film-former and 0.25-0.5% silane coupling agent. Strands used for dough moulding compounds generally have a high strand integrity and medium to slow wet-out rates. This is necessary to prevent excessive filamentisation during manufacture and to permit unhindered flow of the compound. Fibres which are chopped wet directly after formation and are used for roofing mat do not include a film-former. The size merely consists of surfactants, lubricants and emulsifiers in aqueous solution. Strands that are used in continuous lengths contain a higher size content than those for chopping and also have a film-former content of 4-13% while containing 0.8-1.2% by weight of size in the strand.

1.2.3.3 Selection of Lubricant

Lubricants are added to give lubricity to the strand, which reduces the amount of filament breakages. Generally ~0.2% of lubricant is sufficient to prevent any breakages occurring although; conversely, if too much lubricant is used then excessive filamentisation will occur as well as a reduction in the wet-out rate. Because of this it is better if the amount of lubricant added is kept to a minimum.

1.3 Polymers

1.3.1 Introduction

Ever since the early twentieth century, polymers have been widely accepted in the scientific community. [55] Before then only relatively small molecules were believed to exist as chemical entities and scientists were not keen to accept a long chain structure such as that in figure 1.8. An alternative suggestion, whereby small ring-like structures of low molecular weight would aggregate to produce a large macromolecular structure, was proposed to explain the behaviour of substances such as natural rubber. However, over time the scientific community as a whole started to accept the long linear chain theory.

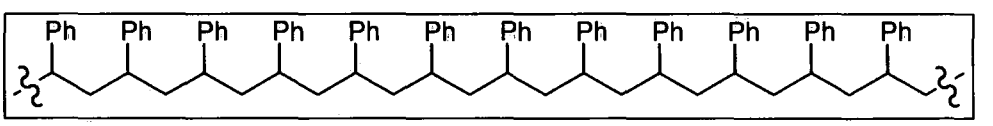

Figure 1.8 – Chain of Poly(styrene)

These long linear chains are actually made up of a single repeating unit called a monomer. These are known as the building blocks of polymers, which bind together via covalent bonds. Sometimes, as is the case for condensation polymerisation, these units are more appropriately called monomer residues because the covalent bond causes some atoms to be lost from the monomer unit. These monomer units can have many different types of functionality which allows the formation of many polymers with differing physical properties and uses.

1.3.2 Polymer Physical Properties

1.3.2.1 Molecular weight

The molecular weight of a polymer exists as a distribution of weights rather than one single weight. This occurs because not all of the polymer chains grow at the same rate during polymerisation. A typical molar mass distribution is shown below in figure 1.9.

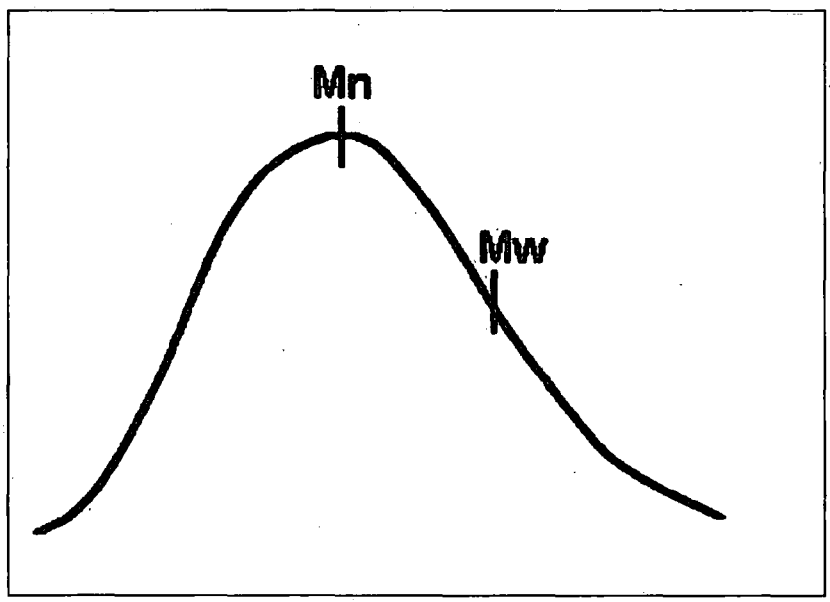

Figure 1.9 – Typical distribution of molar masses for a polymer [55]

The distribution is best described by a variety of different averages, the number average molecular weight, $\overline{M_n}$ (equation 1.1), and the weight average molecular weight, $\overline{M_w}$ (equation 1.2), being the two most common.

$$\bar{M}_n = \frac{\sum_i N_i M_i}{\sum_i N_i} \qquad 1.1$$

$$\bar{M}_w = \frac{\sum_i N_i M_i^2}{\sum_i N_i M_i} \qquad 1.2$$

Where: N_i = number of molecules of chain length *i* in the polymer sample and M_i = molecular mass of molecules of chain length *i* in the polymer sample.

The breadth of the molar mass distribution is known as the polydispersity; a value corresponding to the polydispersity can be calculated from the ratio of the two average molar masses shown in equation 1.3.

$$Polydispersity = \frac{\overline{M_w}}{\overline{M_n}} \qquad 1.3$$

For the narrowest distribution (a single peak) all of the polymer chains will have a uniform molecular weight and a polydispersity of exactly 1 due to $\overline{M_w}$ and $\overline{M_n}$ being the same; as the distribution increases so too will the polydispersity. Ideal polymerisation reactions tend to give quantifiable polydispersity values defined by the ideal nature. It is understood that an ideal step-growth polymerisation reaction will produce polymer chains with a polydispersity of exactly 2 and that an ideal living polymerisation will produce polymer chains with a polydispersity of exactly 1. Because emulsion polymerisation takes place in separated reaction sites due to compartmentalisation, then a wide range of molecular weight polymers will be produced. This causes the polydispersity of polymers made via this method to be larger generally with polydispersity values greater than 2.

1.3.2.2 Glass Transition Temperature

An amorphous polymer can exhibit five distinct states of mechanical behaviour which differ with temperature. [55] These can be displayed on a plot of elastic modulus against temperature (figure 1.10).

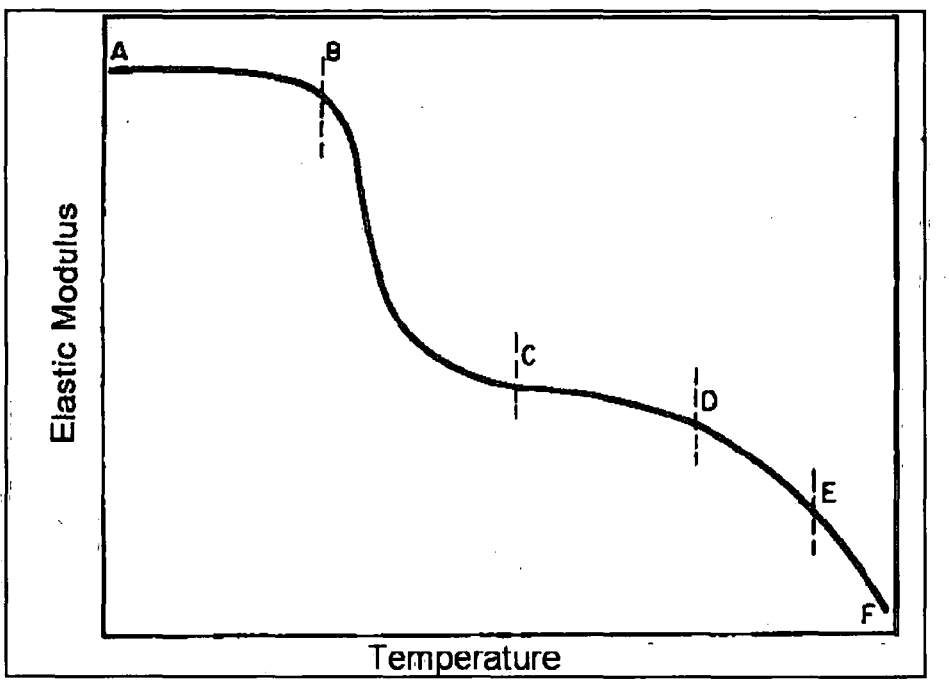

Figure 1.10 – Plot of elastic modulus against temperature for a polymer.

A-B This is the *glassy state*; here we find that the molecular motion of the polymer is frozen.

B-C This is the *retarded highly elastic state* and it is here that the glass transition region occurs. This is a region where molecular motion is allowed but is rather slow and gives rise to leathery properties existing in the polymer.

C-D This is the *rubbery state* where molecular motion is fully allowed but in a strained fashion. A reduction of force on the polymer at any point will cause the molecular motion to return to that of point C.

D-E This is called the *rubbery flow* region and it is where the effects of the applied force on the polymer will cause it not to return to its original orientation due to deformation.

E-F This is the *viscous state* where no elastic recovery in the polymer will occur and it will instead assume the characteristics of a viscous liquid.

All of these states are dependent on temperature; as heating causes motion in the chain to increase, cooling will produce a reduction. However this only occurs before point D because anything after this point has been deformed and, therefore, will not return to a previous state upon cooling.

The most important thermal property of a polymer is the glass transition temperature, T_g. It is at this point when a polymer's physical attributes, such as its hardness and elasticity, can alter dramatically. In molecular terms T_g is the point where a polymer will start to experience motion about the chain and below this point there is no motion. The glass transition is not only restricted to linear polymers, any substance which can be cooled below its melt temperature by a sufficient amount without crystallisation occurring will form a glass. [56]

The value of T_g largely depends on the amount of thermal energy required to keep the polymer chains moving; factors that affect the rotation along the chain links will also affect T_g. [55] The main variation between values of T_g arise from the polymers number average molecular weight, $\overline{M_n}$. This relationship between $\overline{M_n}$ and T_g has been studied to produce equation 1.4 which was then simplified to equation 1.5:

$$T_g = T_{g_\infty} - \left(\frac{2\rho\theta_A}{\alpha}\right)\left(\frac{1}{\overline{M_n}}\right) \qquad 1.4$$

$$T_g = T_{g_\infty} - \frac{K}{\overline{M_n}} \qquad 1.5$$

where: $\overline{M_n}$ = number average molecular weight, $T_{g\infty}$ = T_g at infinite molecular weight, ρ = density of the polymer, N_A = Avogadro's number, θ = free volume per chain end, α = free volume expansion coefficient, the integer 2 = number of chain ends and where K is a constant.

Other factors which influence the T_g are described below.

Chain flexibility

The flexibility of the chain is an important factor which influences the T_g. A polymer which is of sufficient flexibility will produce rotations about the chain backbone and will give a lower value for the T_g, whereas a rigid polymer chain will give a higher value for the T_g. A linear polymer with groups embedded in it that impede rotation about the chain will also cause an increase in the T_g.

Steric effects

If large, bulky pendant groups are present on the polymer chain rotation of the polymer is hindered which causes the value of T_g to increase. We can make this effect even greater by increasing the size of the side group as the bulkiness is directly linked to the T_g value. Polar groups are also thought to produce a higher value of T_g due to an increase in lateral forces occurring because of the polarity.

Configurational effects

Cis–trans isomerism and tacticity variations in certain α-methyl systems will produce a shift in the T_g.

Crosslinking

When crosslinks are introduced into a polymer the density increases proportionally, this restricts the molecular motion in the polymer and the T_g increases.

1.3.3 Free Radical Polymerisation

1.3.3.1 Mechanism of polymerisation

Long chain polymers can be produced from bi-functional units such as carbon-carbon double bonds due to the special reactivity of the π-bonds. These can undergo rearrangements if activated by free radical species and can react with further single monomer units propagating a chain. The propagation will only be stopped if the active site of growth is stopped by a further reaction with another free radical species. This whole reaction scheme, known as a chain growth polymerisation, can be split up into three distinct stages. The first stage is *initiation* where the active site is formed to begin chain growth. The second stage is *propagation* where the chain grows one unit at a time due to repeated reactions with further monomer units. The third stage is *termination* where the growth of the chain is brought to a halt by neutralisation with another free radical species.

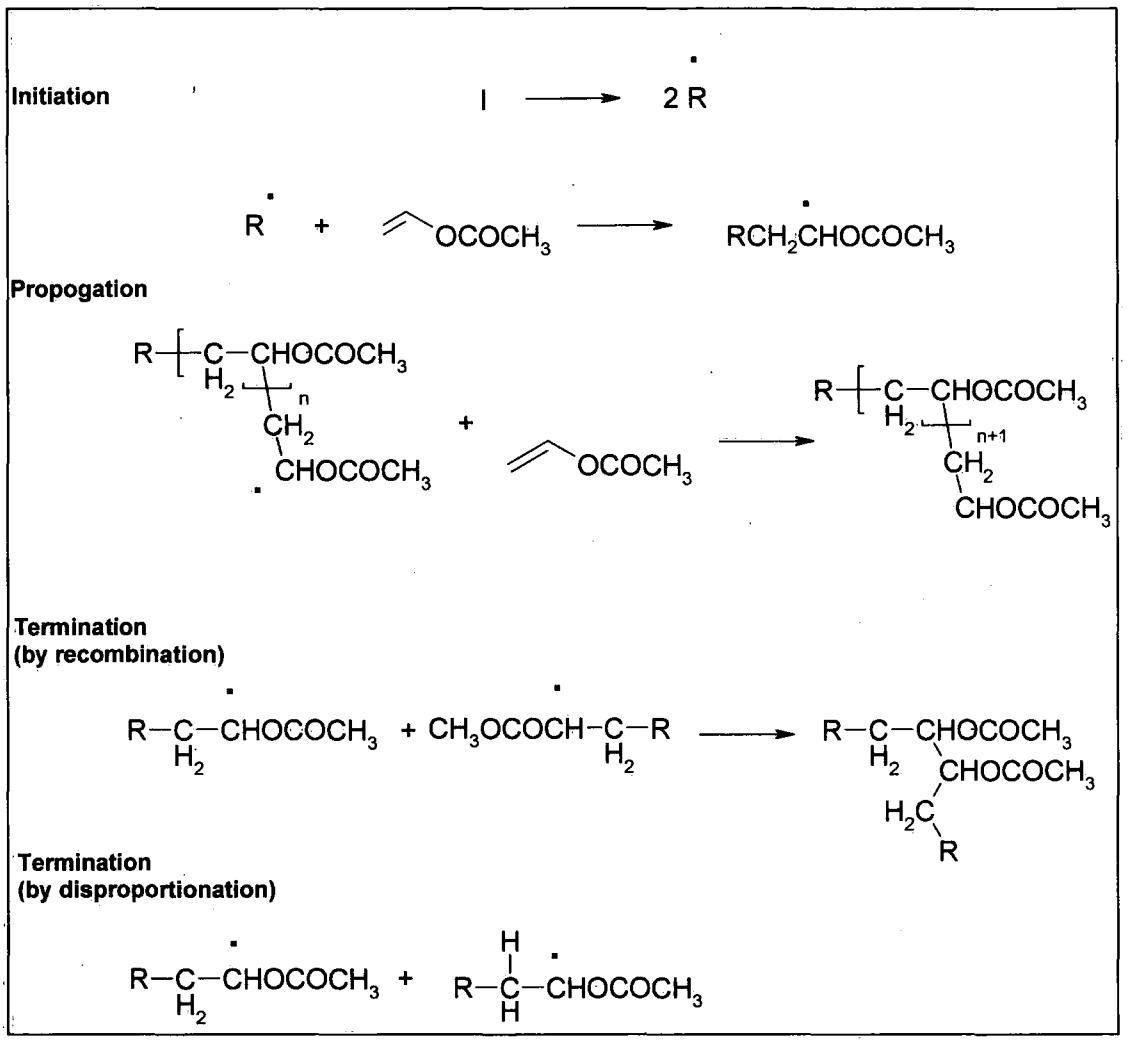

Scheme 1.11 – Mechanism of free radical polymerisation of vinyl acetate

1.3.3.2 Methods of free radical initiation

An effective initiator is a molecule which will produce relatively stable radicals, upon exposure to heat, radiation or a chemical which induces a reaction, with a greater reactivity than the resulting monomer radical. There are many different types of initiation reactions which can be used to produce free radicals to start the polymerisation reaction. [55]

Thermal decomposition

Weak bonds present in peroxide or azo compounds can decompose when exposed to heat, to produce radicals. Benzoyl peroxide when heated produces two phenyl radicals with the loss of CO_2.

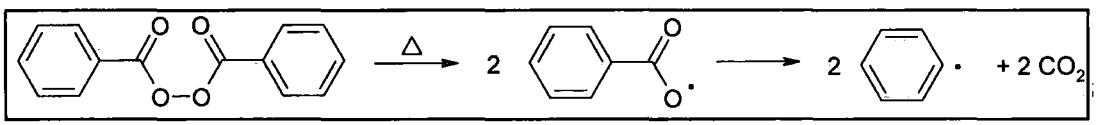

Scheme 1.12 – Thermal decomposition of benzoyl peroxide

Photolysis

Metal iodides, metal alkyls and azo compounds are decomposed by radiation with a specific wavelength. Azobisisobutyronitrile (AIBN) decomposes in UV radiation.

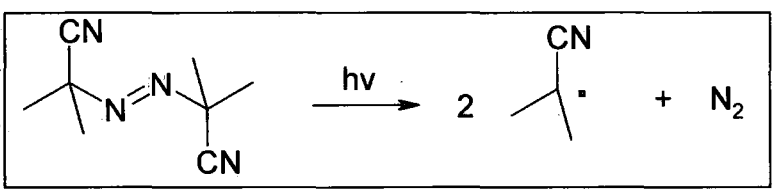

Scheme 1.13 – Photolysis of AIBN

Redox reactions

A variable oxidation state transition metal ion and hydrogen peroxide react together to produce hydroxyl radicals. Iron is often used as the transition metal.

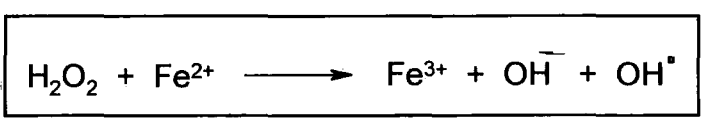

Scheme 1.14 – Redox reaction of ferrous ion and hydrogen peroxide

Persulfates

These are mostly used in emulsion polymerisation where decomposition occurs in the aqueous phase. The radical will diffuse into the micelles which contain monomer and polymerisation ensues.

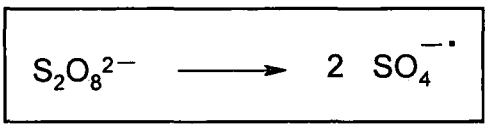

Scheme 1.15 – Persulfate decomposition

Ionising radiation

Alpha, beta and gamma radiation or X-rays can be used to initiate a polymerisation. They cause ejection of an electron from a molecule which is followed by dissociation and electron capture to produce a radical.

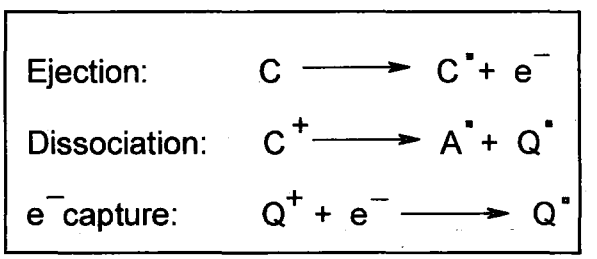

Scheme 1.16 – Radical production by ionising radiation

Not all radicals generated go on to cause chain initiation to start the polymerisation reaction. Side reactions can occur which reduce the efficiency of the initiator as shown below. [55]

Primary Recombination

This occurs if the movement of radical fragments in solution is reduced; this produces a cage-effect around the fragments.

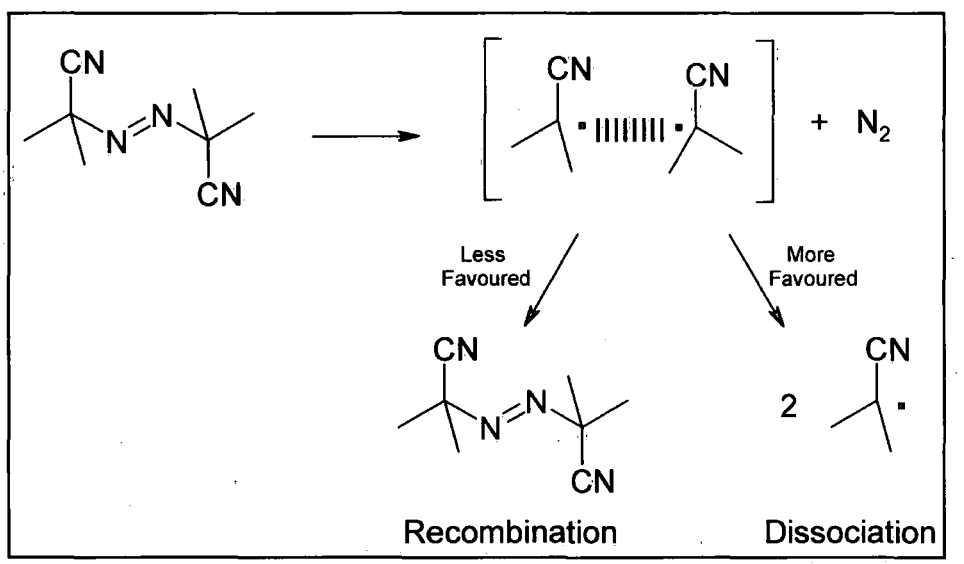

Scheme 1.17 – Primary recombination of initiator [55]

Induced Decomposition

This occurs when a radical reacts with the initiator before decomposition has occurred. It results in only one radical being formed instead of three.

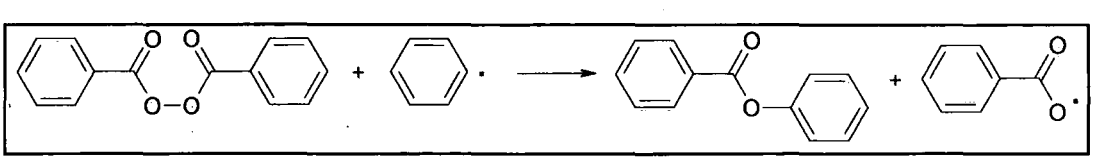

Scheme 1.18 – Induced decomposition of initiator [55]

1.3.4 Emulsion Polymerisation

1.3.4.1 Introduction

The process of emulsion polymerisation has been widely used as a method of production of synthetic latexes since the 1930's. Many of the major developments in emulsion polymerisation have occurred as a result of collaboration between government, industry and academics during the Second World War. These efforts resulted in the first viable processes for large scale manufacture of latex products, such as rubber, which were in large demand at the time. [57]

During the 1950's these methods of producing latexes were continued to produce many different products with their own uses such as latex paints, adhesives, sealants, paper coatings and high-impact polymers. Latexes are now also produced for more speciality applications such as, diagnostic tests, biological cell labelling, size calibration standards, drug delivery systems and chromatography separations.

1.3.4.2 Process Techniques

The emulsion polymerisation process is a free-radical initiated polymerisation which occurs in a heterogeneous dispersion producing latex polymer products.[58]

There are many different types of emulsion polymerisation possible, the type depends on the type of dispersion, particle size, surfactant present, the method of polymerisation and the monomer feed regime.

On discussing the type of dispersion, usually an oil-in-water system is referred to where the oil is generally monomer with a molecular weight in the region of 60-200 Daltons. Some examples of the monomers typically used in such systems are styrene, butadiene, vinyl chloride and vinyl acetate. Copolymerisation of two or more of these monomers can be undertaken to produce polymers with an even wider variety of properties.

The feed regime mentioned is the method of addition of the ingredients during the polymerisation reaction. Batch polymerisation is the addition of all of the ingredients at the beginning of the process, semi-batch polymerisation is where one (or more) of the ingredients is added continuously during the process and continuous is where all of the ingredients are added during the process.

The main contents of an emulsion polymerisation are, the monomer, dispersion medium, emulsifying agent, protective colloids, buffers and an initiator.

The dispersion medium used is generally water because it maintains a low viscosity and provides good heat transfer. It also isolates the polymerisation loci meaning that many different polymerisation reactions can occur at the same time – this is often termed compartmentalisation.

The emulsifying agent performs the dual role of providing a site for nucleation and providing colloidal stability to the growing particles. Generally anionic surfactants are used in emulsion polymerisations although cationic and non-ionic surfactants can also be used in special circumstances.

Water soluble colloids are added to the system to provide stability for the suspended polymer particles. These colloids are either non-ionic or

anionic in character. Poly(vinyl alcohol) is a typical example of a popular colloid used in such systems. A buffer is added to control the pH of the system.

The initiator, which results in the formation of free radicals, ideally must be water soluble and function at temperatures less than 100°C.[59] The initiator that is mainly used is a persulfate salt, although peroxides are also used.

Emulsion polymerisation is a very useful method of making polymers for manufacturers because no solvent is required meaning the reaction is environmentally friendly. A high extent of monomer conversion is achieved which again is environmentally friendly while reducing the cost. The water present will act as a heat sink to remove any of the excess heat meaning that the reaction is carried out in a controlled manner and high molecular weights can be readily achieved.

1.3.4.3 Method of Polymerisation

The method of emulsion polymerisation can be described best as a series of steps as shown below. [57]

Addition of emulsifier to the water

When the emulsifier is added micelles will form beyond the critical micelle concentration (cmc) point. Below the cmc no micelles exist but above this point the number of micelles increases with an increasing surfactant concentration.

Addition of a water insoluble monomer

Monomer is added to the emulsified water which is then distributed throughout the system. A small amount of the monomer dissolves in the water and in the micelles but the majority is dispersed as small monomer droplets throughout the aqueous phase. This occurs due to some emulsifier stabilising the monomer droplets by absorbing to the droplet surface keeping the particle intact.

Addition of initiator

Radicals formed from the decomposition of the initiator react with the monomer dissolved in the aqueous phase eventually to form a surface active oligomeric monomer radical. The polymerisation will continue in the water for several steps before the oligomer becomes too hydrophobic to remain in the aqueous phase and it enters the micelles. Polymerisation occurs in the micelles because these are more likely to capture a free radical than the monomer droplets due to their much larger surface area. The polymer chain then grows in the micelles by the diffusion of more monomer units from the droplets.

Micelle stabilisation by emulsifier absorption

Stabilisation of the micelles occur at the water-polymer interface by absorption of emulsifier from uninitiated micelles. As only a small quantity of the micelles will produce polymer particles the remainder begin to disintegrate at a 10-20% conversion. The emulsifier from these micelles dissolves into the aqueous phase and the monomer is released to continue propagation. The monomer droplets disappear at roughly 60-80% conversion meaning the

polymerisation continues after this point using monomer from the two remaining sources. The polymer will only stop growing when there is no further monomer remaining to polymerise.

Typically in emulsion polymerisation you can only achieve 99% conversion since the remaining monomer can no longer reach the reactive centre. Further polymerisation occurs in preference to termination because the radicals will react with a monomer unit much faster than they will with one another. Because of this each micelle must contain either one growing chain or none at all.

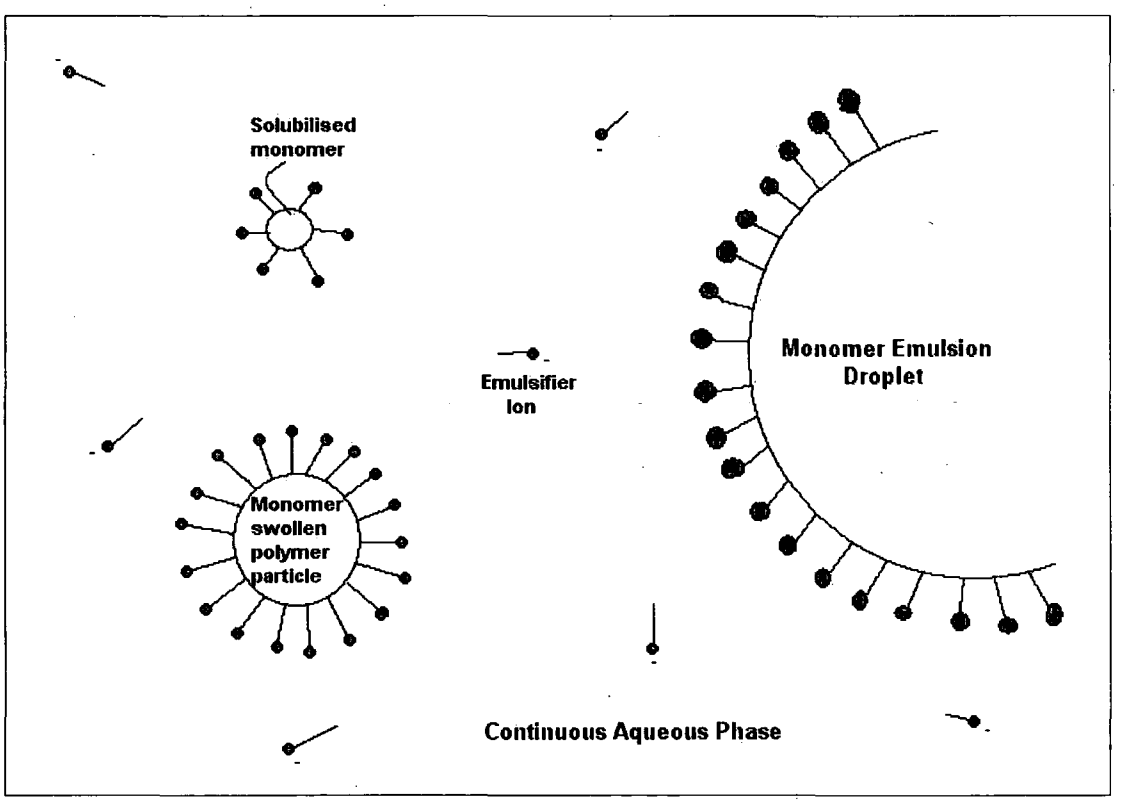

Figure 1.19 – Schematic diagram of the emulsion polymerisation process

(some monomer is also dissolved in the aqueous phase – not shown)

The kinetics of emulsion polymerisation is discussed in great detail by Smith and Ewart [60] and the results of their findings are described below, see equations 1.6 & 1.7.

$$R_P = \frac{Nk_P[M]}{2N_A} \qquad 1.6$$

$$DP_N = \frac{k_P N[M]}{\rho} \qquad 1.7$$

where: R_p = rate of polymerisation, DP_N = degree of polymerisation, k_p = rate constant for propagation, [M] = monomer concentration, N_A = Avogadro's number, N = number of polymer particles in a cubic centimetre of the aqueous phase and ρ = rate of generation of radicals from the initiator (this assumes that the monomer is water insoluble and that all of the radicals present will initiate the polymerisation process, however in practice only a fraction do).

In equation 1.6, R_p relates to the overall rate of polymerisation per unit volume of water and k_p is the rate constant for the propagation reaction, during which the polymer grows by another monomer unit. The reaction to which k_p relates, with reference to the polymerisation of styrene is shown in figure 1.20.

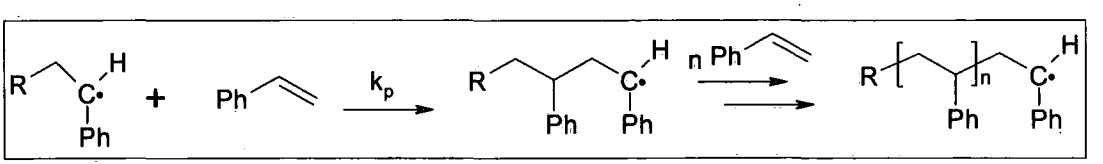

Figure 1.20 – Reaction scheme for the polymerisation of styrene

k_p can be determined from equation 1.6 because we can calculate R_p, N and [M] experimentally and N_A is constant. The factor of two in the denominator of equation 1.6 is because it is presumed that only half of the polymer particles will contain a growing radical and the other half will contain none. [61]

In equation 1.7, DP_N is the degree of polymerisation which corresponds to the ratio of the rate of growth of a chain (i.e. k_p and [M]) to the frequency of radical capture by the polymer chain (ρ/N). Each primary radical is thought to produce a new polymer chain up to the point when it is terminated; the final size this chain achieves before termination is dictated by the degree of polymerisation. Both equations 1.6 and 1.7 vary directly on the number of particles present, N; however the degree of polymerisation also depends on rate of radical generation, ρ.

1.3.4.4 Vinyl Acetate Emulsion Polymerisation

The production of vinyl acetate (VAc) was first patented by Klatte [62] in 1914, and it was polymerised shortly afterwards. In 1926 the first major industrial use of PVAc was developed. It was found that poly(vinyl alcohol) (PVA), which was used as a textile size, could be synthesised from PVAc. Nowadays around 3 million tons of vinyl acetate are manufactured worldwide every year; the method of production is mainly by the oxidative addition of acetic acid to ethylene in the presence of a palladium catalyst. [63]

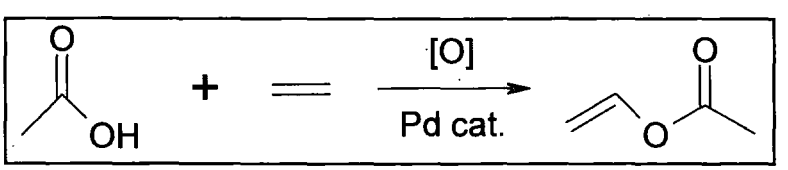

Figure 1.21 – Reaction scheme for the production of vinyl acetate

When high molecular weight PVAc is required, generally for use in the adhesive and surface coating industries, it is produced by emulsion polymerisation. Its low cost and good performance as well as its ability to copolymerise with acrylates and other vinyl esters has ensured its continued use in the field of emulsion polymerisation.[64-69]

PVAc is often considered the extreme case for emulsion polymerisations because of the polarity of the monomer, which means that it is relatively highly soluble in water (2%). Because of this polarity the propagation rate of the polymerisation is very high, as is its rate coefficient for transfer when compared to other monomers. It also induces accelerated decomposition of the persulfate initiator to produce radicals at a much quicker rate than for any of the other common monomers. As well as this, it also gives highly unfavourable reactivity ratios for inclusion of vinyl acetate monomers in copolymer chains.

The distribution of molecular weights of poly(vinyl acetate) emulsion polymers has been investigated by Lee et al.[70] They found higher molar concentrations of low molecular weight chains occurring at high surfactant concentrations. They also found that molecular branching occurs in most cases, due to multiple propagations and radical transfers which cause a rapid increase in higher molecular weight fractions.

There have been many different types of initiators devised to produce PVAc using both the thermal and redox methods of radical production. Thermal decomposition of potassium persulfate is a method frequently used by chemists to produce radicals. Sarker et al. [71] found that the rate of

decomposition of potassium persulfate to produce radicals did not depend on the presence of PVAc. Lepizzera et al. [72] found that the addition of PVA to produce a copolymer with PVAc increased the rate of decomposition of the persulfate initiator; they also found that the high molar mass PVA materials promote decomposition of the persulfate even quicker.

The properties of PVAc latexes can be enhanced further through copolymerisation with other monomers, as is the case with many types of latex. Makgawinata et al. [73] have discussed one such copolymer which is the vinyl acetate/*n*-butyl acrylate (VAc/BA) copolymer latex. They found that the feed rate of the monomer mixture has an effect on the final properties of the latex and concluded that semi-batch polymerisations provide better control over compositional heterogeneity than batch polymerisations.

The stabilisation of polymer colloids has been well studied and it has been found that the choice of surfactant is the main criterion. This is especially the case when producing latexes because the stability of the polymer-water interface is essential to create a stable dispersion. Urquiola et al. [74, 75] used sodium dodecylallylsulfosuccinate (SDAS) as the stabilising surfactant for PVAc emulsions, and found that it played a significant role in the rate of polymerisation as well as in the physical properties of the latex. It was found that SDAS decreased the rate of polymerisation by congregating predominantly at the polymer-water interface, leading to a more efficient termination step which resulted in a decrease in the total number of radicals.

PVAc emulsions are used as film-formers in the coatings industry to coat many different structures. The main reasons for using PVAc are discussed more thoroughly in the following section.

1.4 Latex Film Formation

1.4.1 Introduction

The oil-in-water product obtained from emulsion polymerisation is generally known as a latex. Initially these were only found to occur naturally in the form of sap from the para-rubber tree (*Hevea brasiliensis*) but the discovery of synthetic latex during the 1940's allowed many different variations to be produced using different polymer systems. The main use of latexes is as synthetic rubbers, which are themselves used in many different applications. They are useful because they produce compounds which are both flexible and impermeable whilst retaining good mechanical strength. This has led to their use in many different areas such as sealants, coatings and other flexible compounds.

Films can be made readily from the latex emulsion by drying down the water phase, leaving a continuous film. Due to their ability to form films readily as well as the physical properties associated with latexes, these are used as the bulk polymer binder (film-former) in glass fibre size formulations.

1.4.2 Film Formation Mechanism

The method of latex film formation has been investigated in depth using many different analytical techniques such as electron microscopy, [76] atomic force microscopy, [77, 78] neutron scattering [79] and dynamic mechanical analysis. [80]

The mechanism of film formation can be split into four distinct stages:[81]

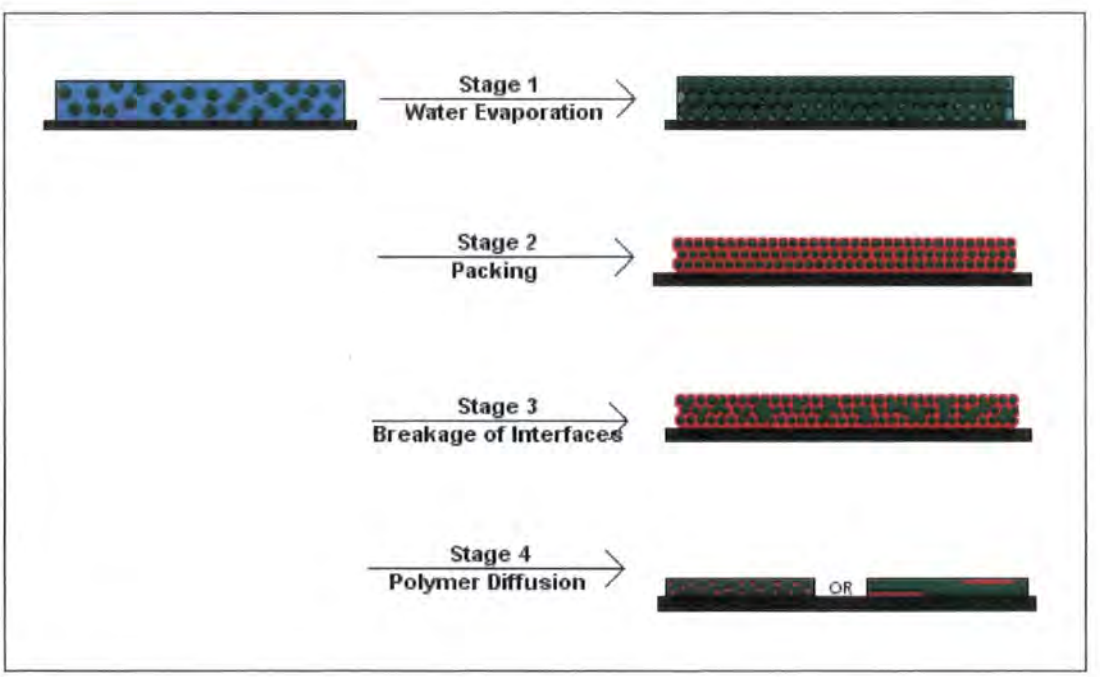

Figure 1.22 – Schematic diagram showing the process of latex film formation

Water Evaporation

The water present in the emulsion evaporates, leaving the polymer particles which pack together densely. The rate of evaporation of water was found to be constant over time, initially it was even found that the rate was similar to that of water due to the dilution being so high. Eventually, though, as

the water content decreases there is some slowing of the rate of evaporation.[83]

Packing of polymer particles

If the temperature is above the minimum film forming temperature (MFFT), [84] the particles will deform to pack together more efficiently. The MFFT is generally close to the T_g, but not always.[85, 86] Problems occur when the latex is dried at a temperature lower than the MFFT as this creates a discontinuous film with voids present, making the film appear opaque promoting scattering of light. Conversely, if the diffusion of the polymer in the particles is too great a stable dried film will not form, instead creating a tacky glue-like substance which may be used as an adhesive. [87] It has been postulated that the MFFT can be related to the polymer particle size. [88] However, this effect is dependent on particle size since a large increase from 150 to 1200nm only increases the MFFT temperature only slightly.[85]

Breakage of interfacial barriers

After sufficient time the hydrophilic interfacial barriers between the particles will break allowing free movement of the polymer chains which will aid diffusion.

Polymer diffusion

If the temperature is above the T_g, the polymer chains will diffuse together, increasing the mechanical properties of the film which allows a stable film to form. [89-91] Depending on the film formation conditions, the

hydrophilic material either will be dispersed throughout the film or will congregate at an interface.

It was found that, on ageing, further coalescence occurs between the polymer particles, which removes any of the residual particle-like structure from the film (a small amount of particle structure generally remains due to the continued presence of hydrophilic species in the film). This occurs due to the hydrophilic species migrating to the interface of the film.[92] However, Bradford et al. [93] discovered this was not the case for PVAc as they recorded a faint particle like structure remaining in the film even after 280 days. They attributed this to the surface hydrolysis of a small amount of PVAc which created PVA. This then formed a continuous network throughout the film separating the PVAc particles and hence ensuring the faint particle-like structure remained.

Models of the film formation process have been postulated to rationalise the experimental results, [94, 95] however there are some minor problems with these models. One such problem is that the evaporation of water from the emulsion is non-uniform meaning that different areas of film dry at different rates. This necessitates the use of estimates in the simulation, which reduces accuracy.

1.5 Conclusions

There are many different aspects to the chemistry related to glass fibre sizes which can be investigated. It has been shown that glass fibres can be used in a variety of different areas due to their attractive physical properties. It has also been shown that the size which binds the individual glass fibres together plays a major role in maintaining their usefulness. The size has been shown to consist primarily of a latex based film-former with a number of additives which tailor the compound to the specific area in which it will be used. Due to its latex nature, a continuous film should form so long as it is dried under certain conditions.

It is very surprising that, despite the widespread use of glass fibre sizes, a complete investigation of the performance of a glass fibre size has never been undertaken. Even the structure of a fibre size has never been published in any great detail.

The aim of this thesis is to rectify this anomaly by characterising fully the structure of a common glass fibre size as well as determining the effect of the size composition on its performance. The performance is to be split into three different sections: clarity; glass protection; and strand integrity, each of which are required to produce a fully functional glass fibre size. The physical properties of a common film-former will also be altered to produce a range of molecular weights and average latex particle sizes to determine how they too will affect the performance. This work has been carried out in collaboration with Celanese Emulsions, who are based in the Netherlands, and with St. Gobain Vetrotex, who are based in France.

Chapter 2

Experimental Technique

Theory

2.1 Introduction

The aim of this project is to determine the performance properties of a variety of glass fibre sizes. To achieve this, a wide variety of techniques must be employed to investigate the wide range of performance criteria which have been detailed previously in section 1.5.

Initial investigations into the physical properties of the film-former must be undertaken using analytical techniques specific to polymers (such as gel permeation chromatography and particle size analysis) to determine the range available. When these are known the actual structure of films of the dried size will be investigated using microscopic and chemical & elemental analysis techniques. This should produce an accurate representation of the size where the different components present are mapped to different areas of the film. This work will then be followed by further investigations into the performance of the films for use as industrial glass fibre sizes. Evidence of trends will be explored using the different physical property based sizes as well as sizes which contain varying concentration levels of additives.

The performance investigation has been split into three distinct areas: clarity; glass protection; strand integrity, with each requiring different pieces of instrumentation.

The investigation into the clarity of the dried films will focus on absorption spectroscopy. Microscopy will also be used to investigate the homogeneity of the film as this can affect the clarity. The wetting ability of the size will also affect its clarity so goniometry and wet-out testing will also be required.

Glass protection will be investigated primarily using microscopy in an effort to determine whether any differences in film formation occur during the drying process for all of the different variations of the size.

The strand integrity property to be measured primarily involves the determination of the physical strength of the dried films. This will be investigated using a range of tensile testing instruments including dynamic mechanical analysis.

2.2 Experimental Technique Theory

2.2.1 Gel Permeation Chromatography

The most common method of determining the molecular weight and polydispersity of a polymer is by using a specialised form of liquid chromatography called gel permeation chromatography (GPC), also known as size exclusion chromatography (SEC). Polymer is injected into the GPC as a dilute solution and is forced through a column packed with cross-linked polymer particles at a very high pressure. It is essential that the polymer is dissolved fully as all remnants must pass through the instrument. If any polymer is left behind then future samples would be contaminated. The polymer sample then passes through a matrix of cross-linked particles present within a column which separates the molecules accordingly hydrodynamic radius (R_h). It is found that the lower R_h species present in the sample undergo more interactions with the matrix, producing a longer retention time within the column. Since R_h is related to molecular weight, this provides a means of separation based on molecular weight. The larger molecular weight species will therefore have a smaller retention time and a full analysis of the molecular weights present can be determined.

A refractive index detector is used to identify the polymer sample as it passes off the column. Due to interactions within the column the sample passes off according to molecular weight and the detector measures how much of the sample is eluted from the column at a given time. A plot of relative response from the detector against time (which starts at zero when

the sample is injected) is produced and a computer calculates the molecular weight of each peak on the graph. A calibration curve plotted from the data produced from a range of standard samples of known molecular weights are used to correlate the retention time of the column to a range of molecular weights.

2.2.2 Photon Correlation Spectroscopy

Particle size analysis can be performed using a photon correlation spectrometer. This technique calculates the particle or molecular size distribution in a sample from direct measurement of diffusion coefficients. The instrument contains a laser light source coupled with an optical adjuster to focus the incident beam. As the particles in the sample undergo Brownian motion (due to thermal agitation) they are detected and analysed by illumination with a laser and measurement of the scattered light with a photomultiplier. The scattered light at any instant in time will produce an interference pattern, which is dependent upon the pattern of particles illuminated by the laser beam. As the particles diffuse their relative positions change thus causing a constantly fluctuating interference pattern. This varies the light intensity at the detector which is positioned at 90° to the incident beam. These intensity distributions are random and occur on a time scale of micro to milli-seconds. Large particles move more slowly than small particles, meaning they will change positions more slowly creating slower intensity fluctuations at the detector. Conversely smaller particles move faster and produce rapid intensity fluctuations. Photon correlation spectroscopy is based on measuring the fluctuations in the numbers of scattered light photons and determines the particle size of a sample by characterising the timescale of the fluctuations.

For a solution of given viscosity, at a constant temperature, the rate of diffusion or the diffusion coefficient (D) is inversely related to particle size according to the Stokes-Einstein equation (equation 2.1):

$$D = \frac{kT}{3d\pi\eta}$$ Equation 2.1

Where: k is the Boltzmann constant, T is the temperature in Kelvin, d is the spherical hydrodynamic diameter and η is the viscosity of the diluent.

This type of instrument can also calculate the mean size distribution, which indicates the polydispersity of the sample, and the presence of more than one mean particle size.

2.2.3 Scanning Electron Microscopy

Scanning electron microscopy (SEM) works in a very similar manner to optical microscopy, using electrons instead of light waves to observe the structure of a sample. Electrons are accelerated from the cathode electron gun by positioning a positively charged anode beneath it. Electromagnets are then used to bend the electron beam to focus the image much like lenses are used in an optical microscope. This allows greater accuracy in producing clearer images with a much greater range and control of magnification. The image is produced by the conversion of backscattered or secondary electrons emitted from the sample by the electron beam into a signal, constructed by computer software, which produces a live picture on a screen. As the number of secondary electrons emitted changes, so too will the amplification of the signal received, as one increases so will the other. Similarly, the signal alters as the number of electrons emitted alters, i.e. increase in electrons emitted produces an increase in the signal, it is this difference in signal which produces an image of the sample with varying contrasts identifying regions in the sample emitting different levels of secondary electrons.

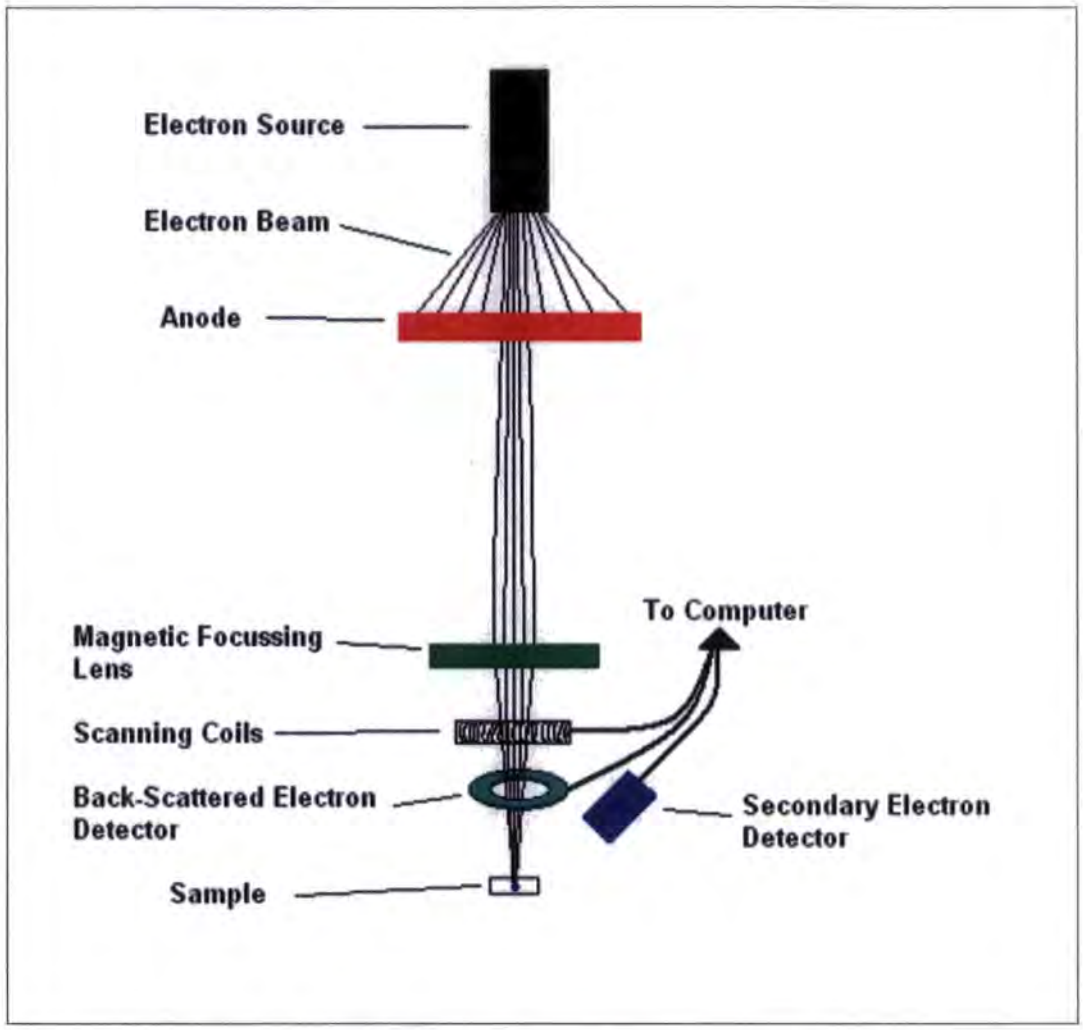

Figure 2.1 – Schematic diagram of the electron beam path in a SEM

Individual points are scanned by the electron beam to produce a matrix which is transferred to the screen and arranged in order. Magnification is produced on the screen by changing the size of the scanned area while the screen size remains constant. For SEM to produce a clear image, the sample chamber must be kept under vacuum; if any gases are present then any interactions they undertake with the electron beam will produce an obscured image. SEM can produce suitably clear images at magnifications of six million.

For samples which are poor conductors a build up of charge on the sample surface can accumulate due to the bombardment of the electron beam with the sample. This can also damage the surface of the sample by burning the actual sample due to the high energy of the beam. An excessive amount of electrons accumulate due to the poor conducting ability of the sample leading to a blurred image being produced. This is overcome by coating the surface of the sample with a thin layer of conducting material such as gold. It is essential that this coating is thin to ensure that the topology of the sample is not masked by the extra material deposited on the surface. It should be noted that the SEM detects topographical details of the sample by measuring the amount of back-scattered electrons from the electron beam at any given point by line-of-sight. If the coated material was applied excessively then the possibility of the contours of the sample surface being modified would increase. This would cause the image displayed to appear more uniform due to more electrons being in the field of sight of the detector producing an inaccurate image of the actual sample.

Over time the electron beam will begin to damage the surface of the sample due to the

2.2.4 Environmental Scanning Electron Microscopy

Environmental scanning electron microscopy (ESEM) is an analytical technique used to observe samples in their natural state or under different environmental conditions. By incorporating an atmosphere within the ESEM chamber a sample need not be conductive and therefore this erases the need for the sample to be coated with a conductive material. SEM works by detecting all of the backscattered electrons within range of the detector and producing an image from these results. A vacuum is required to prevent any of the electrons released from the sample from not reaching the detector which would reduce the clarity of the image. ESEM avoids the need for such a vacuum by relying on interactions between the backscattered electrons and that of other molecules (typically water) which will themselves release an electron for detection. Due to these interactions coupled with the fact that fewer electrons are being detected the images produced for ESEM are not as clear and sharp as those for SEM. This indicates that the levels of magnification achieved and the clarity of the image produced are not as great for ESEM as they are for SEM.

The electron beam present in the microscope is focussed on the sample which results in the emission of secondary electrons. These electrons are attracted to the positively charged detector electrode present above the sample and, as they travel through the gaseous environment, collisions occur.[96] The electrons collide with the vapour particles producing further electrons and promoting ionisation of the vapour. This increase in the amount of electrons amplifies the original secondary electron signal whilst the

positively charged ions are attracted to the negatively charged specimen to counterbalance the overall charge.

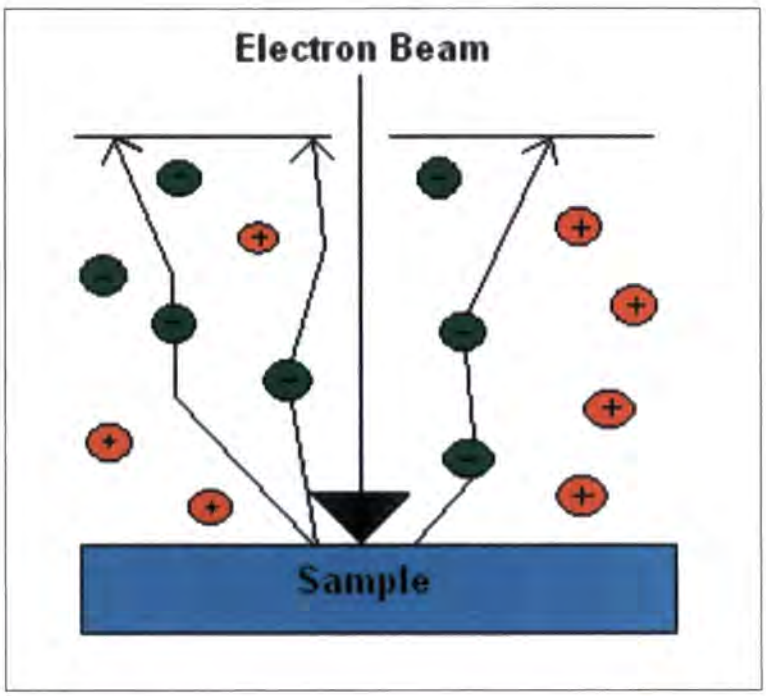

Figure 2.2 – Schematic representation of how an ESEM image is resolved

It is possible to obtain resolutions of 100 Å and variable magnifications up to 80000 by varying the electron beam whilst not harming the sample.

Because of the nature of this technique, sample preparation is minimal which ensures that any errors that may arise due to this are avoided and allows fast and accurate analysis. As discussed in the previous section the coating of a sample in a conducting material can alter the topography of the surface, ESEM doesn't require this, hence, producing a much more accurate image of the sample.

2.2.5 ESEM-Energy Dispersive X-Ray Analysis

This is a specialised variation of environmental scanning electron microscopy (ESEM) which employs an energy dispersive X-ray detector (EDX) in conjunction with secondary and backscattering detectors. This allows the identification and quantification of elements present in the sample and also the calculation of the sample's empirical formula. Initially the sample is viewed exactly as stated previously for a typical ESEM and any sites of interest will then be investigated using EDX. As the electron beam penetrates the sample, secondary electrons are emitted to produce the ESEM image. This causes the presence of electron emission holes to be present in the electron shell. If the holes present occur in the inner electron shells then outer shell electrons will undergo relaxation into the vacant inner voids to increase the stability of the atom. As the energy of an outer shell electron is greater than that of an inner shell electron, relaxation energy is released in the form of X-rays. The precise energy released corresponds to an individual element and the type of relaxation occurring.[97]

The X-ray spectrum obtained from this technique contains peaks which correspond to specific elements which can be mapped using image processing software. Various integration routines allow the amount of each element to be identified as a proportion of the whole sample; this can also be achieved simply by comparing the heights of the peaks, however this is also less accurate. EDX scans can be undertaken over various ranges of areas including point locations, which can eliminate readings from regions around the site of interest.

2.2.6 Attenuated Total Reflectance – Fourier Transform IR Spectroscopy

Attenuated total reflectance - Fourier transform infra-red spectroscopy (ATR-FTIR) is a non-destructive technique which can determine specific bonds present in a sample. Samples typically investigated using this technique are solids and liquids which don't have to be further treated as is the case for normal FTIR. ATR spectroscopy is also particularly useful for measuring specific areas of a sample as the area of investigation can be accurately selected by changing the angle of incidence of the IR beam. This allows different depths of sample to be investigated and thus make it possible for a depth profile of a sample to be determined. This is very different from standard FTIR spectroscopy which can only investigate the whole sample.

Mid-IR spectra of a sample are obtained by passing an IR beam through an internal reflection element (IRE) and the sample. The IR beam is internally reflected through the IRE and passes a short distance into the sample (see figure 2.3). The penetration of the beam into the sample causes the functional groups present to be excited at specific wavelengths of the beam. Therefore any functional groups present can be determined by the loss of intensity at certain wavelengths which correspond to specific bonds.

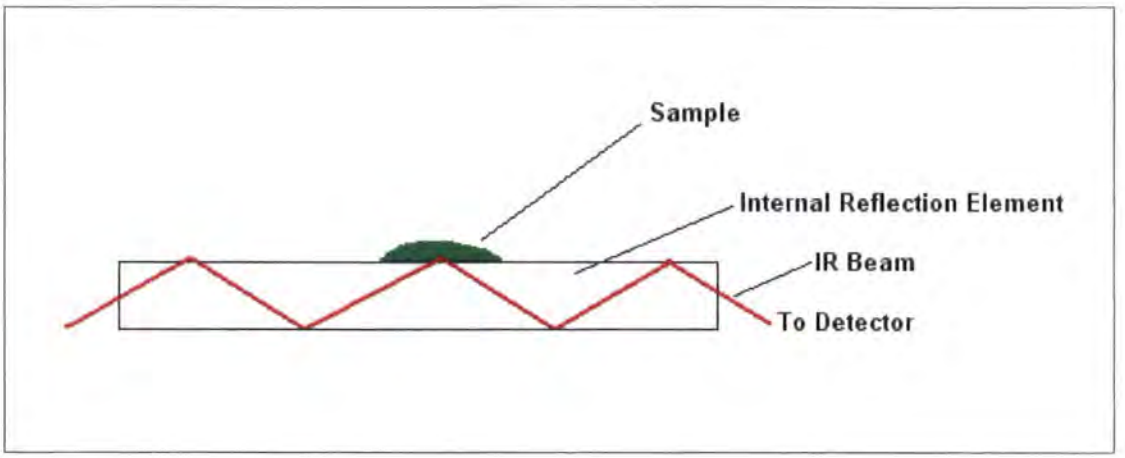

Figure 2.3 – IR radiation passing through the internal reflection element producing total internal reflection (TIR)

2.2.7 Ion Beam Analysis

Ion beam analysis (IBA) utilises high energy ion beams to probe the elemental composition of a sample as a function of depth, this can be determined to a range of several microns with a resolution of 100 Å. The depth of an element can be calculated using the energy distribution of backscattered ions released from the sample. Distinctive X-rays emitted from the different target elements upon beam bombardment ensure accurate identification of similar mass elements. γ-rays emitted from beam-induced nuclear reactions provide excellent sensitivity (in the parts per million range) and depth resolution (around 50 Å) for certain light isotopes such as ^{1}H, ^{15}N and ^{19}F.

This technique is fast and does not require calibration using standard samples while producing atomic ratios for samples which are insensitive to their chemical environments. It is also possible to determine the film thickness and density of a sample as well as the presence of any structural disorders in a single crystal of the sample.

IBA is a broad term that involves several specific techniques:

- Rutherford Back Scattering (RBS)
- Induced Luminescence (IL)
- Scanning Transmission Ion Microscopy (STIM)
- Secondary Electron emission analysis (SEI)
- Particle Induced X-ray Emission analysis (PIXE)
- Particle Induced γ-ray Emission analysis (PIGE)
- Nuclear Reaction Analysis (NRA)

Some of these techniques are depicted below in figure 2.4 which shows the different interaction mechanisms between the ions produced by the instrument and the nuclei present in the sample.

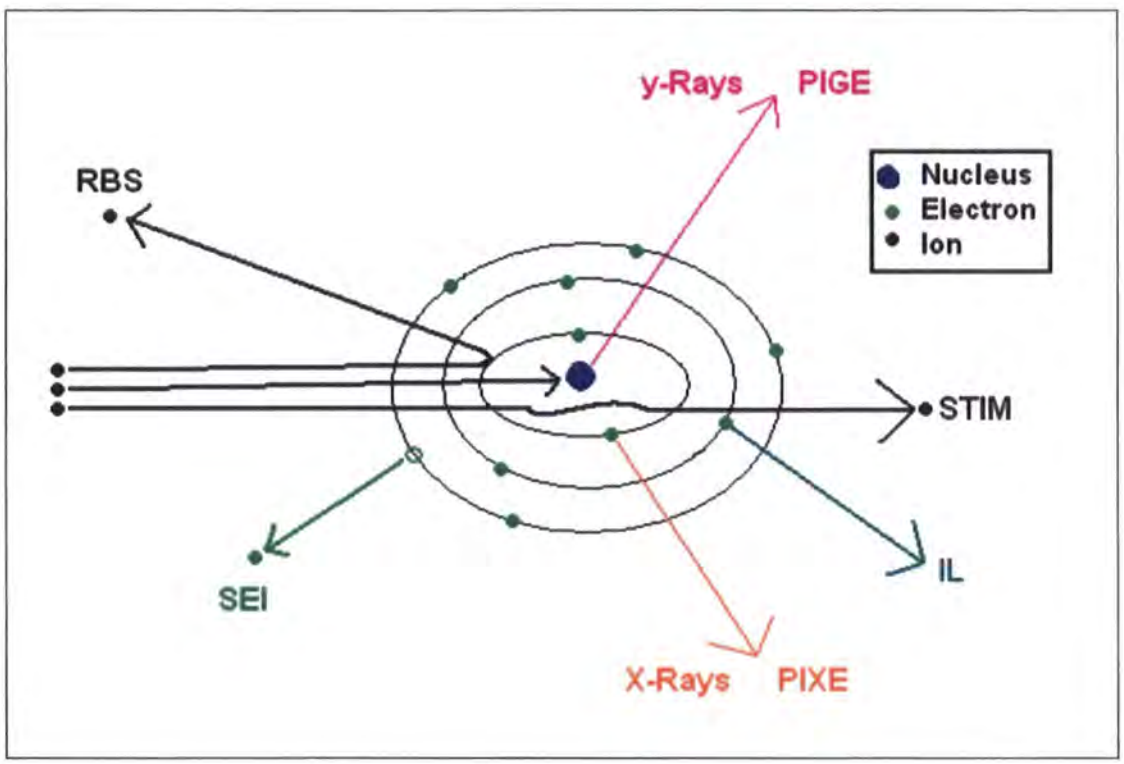

Figure 2.4 – IBA Schematic diagram showing different interaction mechanisms possible

2.2.8 Dynamic Mechanical Analysis

Dynamic mechanical analysis (DMA) is a technique used to measure the mechanical properties of materials while they are subjected to a stress force. When a material is subjected to a force it may behave in a variety of ways. Brittle materials will deform reversibly upon the application of a small amount of force before fracturing. A ductile material will also deform reversibly initially under force, however rather than fracture it tends to yield and begin to flow under the continuous application of force until it eventually hardens and fails. Up to the elastic limit the material will return to its former shape and size when the force is removed, however beyond this point deformation is irreversible and creep has occurred.

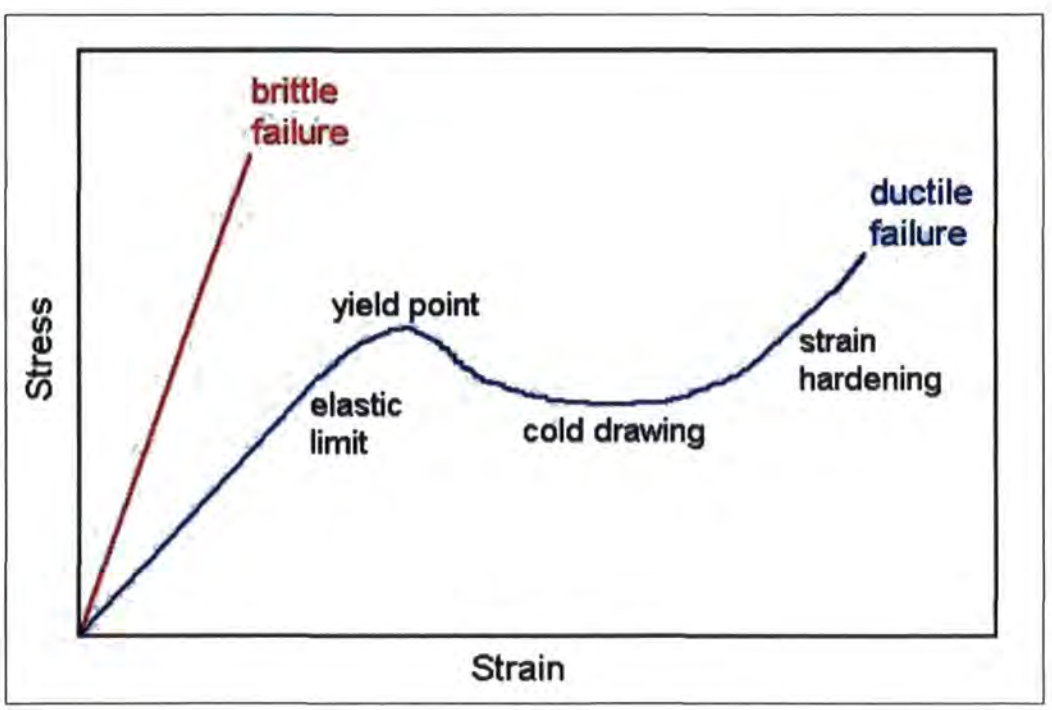

Figure 2.5 – Typical stress / strain curve

The stiffness of a material can be expressed as the ratio of change of stress with strain. This ratio is commonly known as the Young's modulus of a sample and is expressed in equation 2.2.

$$Y = \frac{\text{Tensile Stress}}{\text{Tensile Strain}} = \frac{\sigma}{\varepsilon} = \frac{Fl_0}{A_0 \Delta L}$$ Equation 2.2

Where: Y = Young's modulus (measured in Pa), F = force applied to the object, A_0 = initial cross-sectional area through which the force is applied, ΔL = change in length of the sample; l_0 = initial length of the object.

DMA can be used to calculate the Young's modulus of a sample from the gradient of a plot of stress against strain.

2.2.9 Adhesion

Adhesion is defined as the molecular attraction exerted between two un-like bodies in contact. An example of this is the interaction of a water droplet on a glass window, it can be observed that the water will adhere to the surface of the window and the water droplet will run down the window whilst remaining in contact with it, see figure 2.6.

Figure 2.6 – Water droplets adhering to a glass window

The strength of adhesion can be determined by measuring the force required to fully separate the two adhering species. The adhesion between the dried size and the glass surface is an important property to investigate as it indicates the ability of the size to bind to the glass fibre. A size which does bind strongly to the glass surface will provide improved protection although this will also decrease the processability of the size. This means that it is increasingly difficult to remove when it is no longer required.

2.2.10 Cohesion

Cohesion is defined as the molecular attraction of like molecules present within a species. The cohesive strength of a species is the amount of force required to break the bonding within the molecular structure.

The strength of cohesion of a size can be determined by measuring the force required to separate the two surfaces which have been bound together by it. Therefore, in our system, the cohesive strength of the size can be determined by measuring the force required to separate two glass surfaces held together by the size. In reality, the size binds together at the same time more than two glass surfaces. Nonetheless this measurement should provide a simplified value for the cohesive strength, which should allow comparison between different sizes. This test is only valid if evidence of the size is present on both of the glass surfaces after separation has occurred. If the size is only present on only one of the glass surfaces then the strength determined has been that of adhesion rather than that of cohesion.

2.2.11 Contact Angle Measurements

One major factor which determines the effectiveness of a glass fibre size is how the wet size binds to the glass surface. Generally, a size is required to coat completely the exposed glass surface, resulting in an increased fibre strength. This will promote cohesion between the individual fibres and produce a well bound glass strand. However, the size must also be easily removed from the glass surface when it is no longer required, such as when the glass fibres are impregnated into the resin matrix. The balance of these two requirements is one of the key objectives to consider when designing a successful size formulation.

The most common method of investigating the wetting properties of surfaces is by determining their contact angle, which is the angle of contact produced by a liquid on a surface.[98] This angle indicates the nature of wetting and adhesion exhibited by the surface; in our case it determines the suitability of the different polymer films as a size.

The contact angle is produced by the three different surface tensions that surround the sample at equilibrium. These surface tensions correspond to the vapour-sample, vapour-liquid and sample-liquid interfaces, figure 2.8.

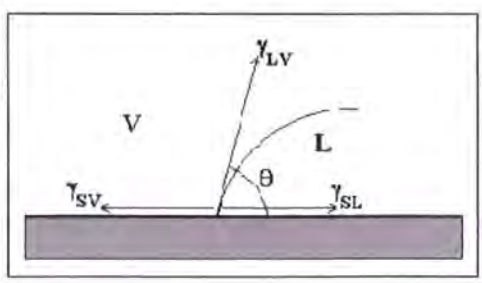

Figure 2.7 – Diagrammatic representation of the equilibrium between the solid (S), liquid (L) & vapour (V) phases, their subsequent surface tensions (γ) and the resulting contact angle (θ)

The contact angle, Θ, is related to these three surface tensions through Young's equation (equation 2.3).

$$\cos\theta = \frac{(\gamma_{SV} - \gamma_{SL})}{\gamma_{LV}}$$ Equation 2.3

Where: θ = contact angle and γ = surface tension (units N m^{-1}) of various boundaries, SV = solid-vapour, SL = solid-liquid; LV = liquid-vapour.

The contact angle provides a quantifiable description of the wetting ability of surfaces. At low contact angle values (< 45°) the surface favours wetting, causing the liquid to spread out, and the surface is characterised hydrophilic. Conversely, at high contact angle values (> 45°) the surface repels the liquid, causing it to bead up. Surfaces showing this behaviour are known as hydrophobic. It is also possible to encounter surfaces which disfavour wetting very strongly (contact angle > 90°), which cause the liquid droplet to remain almost spherical in nature when applied to the surface. Such surfaces are termed superhydrophobic, see figure 2.8.

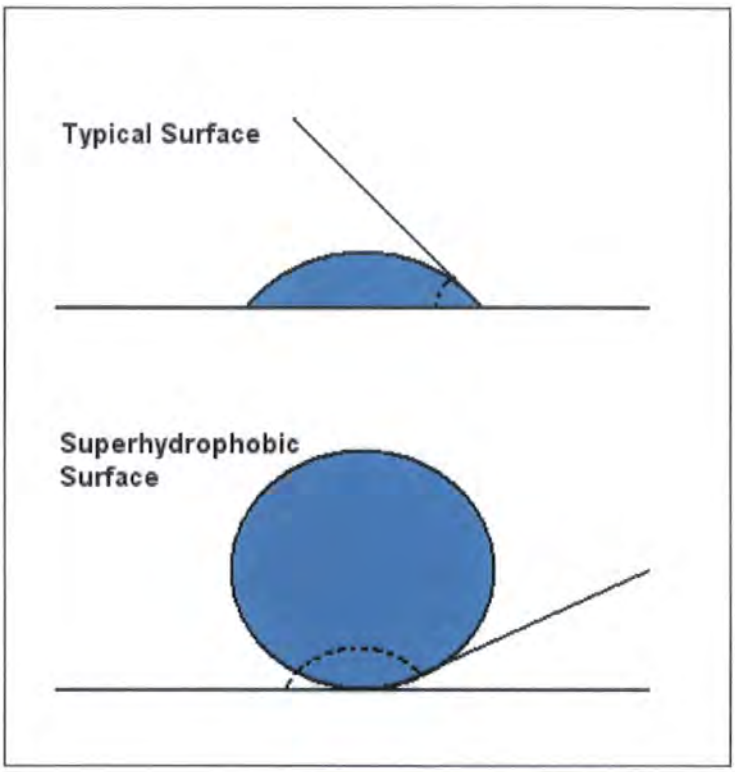

Figure 2.8 – a). a typical interaction between a liquid and surface; b). another liquid interacting with a very hydrophobic surface producing a large contact angle.

2.2.12 Wet-out Rate

The wet-out rate provides an indication of how easily a coating can be removed by a secondary species, i.e. the speed at which it can be dissolved. For glass fibre sizes the wet out rate is an especially useful quantity as it indicates the ease at which the size can be removed from the glass fibres by a dissolving solution system. This process is analogous to that of impregnation of the sized fibres in a resin to produce a toughened composite material.

The wet-out rate can be accurately calculated using a special instrument designed by Celanese. The instrument consists of an LED light source, used to prevent excessive heat which would promote evaporation of the resin, a phototransistor sensor, used as the detector, and software on a computer which interprets the data received from the sensor.

The light source, positioned above the sample, passes through a glass window upon which is placed a chopped strand mat (csm) of the sized glass fibres. The mat is then held in place with a metal plate which has been cut to leave a circle of the sample exposed. The exposed area is treated with the resin, which acts to dissolve the size from the fibres, and the detector is placed below. As the size dissolves from the fibres the mat will begin to open up which increases the amount of light being transmitted through the sample to the sensor below, see figure 2.9. The time taken for the size to dissolve from the glass surface can then be calculated for all samples if a uniform final intensity threshold is used throughout.

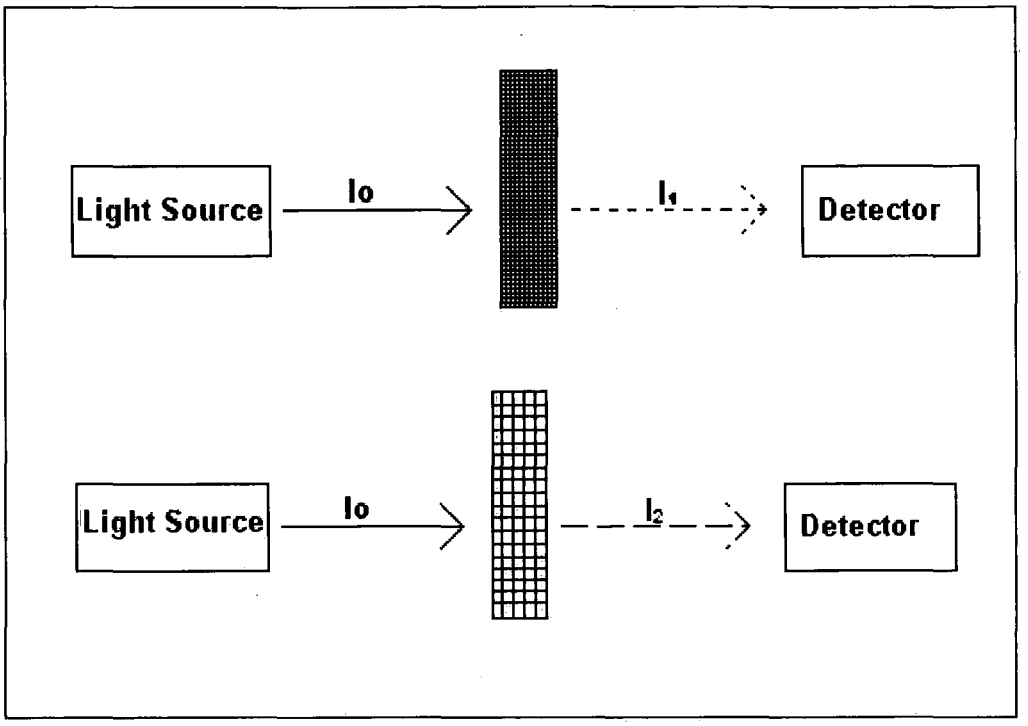

Figure 2.9 – Sized cloth before (top) and after (bottom) immersion in styrene ($I_2 > I_1$)

Chapter 3

Experimental

3.1 Materials

The bulk of the materials used during this investigation were supplied by the sponsors of the project. The base materials used to create the different variations of the vinyl acetate based film-former were supplied by Celanese who have requested that the polymerisation procedure and the materials used remain confidential. St. Gobain Vetrotex supplied the additives which are added to the film-former to create the size, however they have only supplied ambiguous names rather than detailed information regarding the components present in each additive.

Deionised water was used throughout the investigation. Acetic acid was used to buffer the size solution during synthesis and this was supplied by Aldrich. Styrene was used as a wetting liquid during the contact angle determination and this was supplied by Fluka. A granulated sample of PVAc was used to produce an ATR-FTIR spectrum against which the dried size films could be compared against, this was supplied by Aldrich ($\overline{M_n}$ = 74 kDa).

Glass slides (consisting of E glass), which were used to create thin films of the dried size, were supplied by Fisher. Glass fibres, which were used during the wetting investigation, were supplied by St. Gobain Vetrotex.

3.2 Sample preparation

3.2.1 Introduction

The general aim of this project was to determine how the glass fibre size formulation and physical properties affect the performance of the sized fibre. To carry this out, a range of film-former latexes with different physical properties were created for use throughout the project. Initial testing was performed to determine the physical properties of the film-former latexes prior to size preparation. All of the sizes were synthesised in the Chemistry Department laboratories at Durham University using standard laboratory glassware.

Due to restricted access to fibrising facilities and small scale measurement apparatus, used to measure accurately properties of thin films on fibres, the majority of testing was undertaken on size films created on flat microscope glass slides. As these samples are different from those produced in industry it must be understood that the results obtained will likely be different from those relating to actual glass fibres. Such differences attributable to the low surface area of the glass interface should exist such as the adhesive strength. However, it is assumed that any trends exhibited by the different sizes on flat surfaces should also be present on curved systems. It is these trends rather than the actual values obtained which will form the basis of the discussion and conclusions.

3.2.2 Film-former preparation

The film-former is a complex emulsion-based polymer system which contains surfactants and additives to impart specific properties. Small amounts of monomer and initiator are added initially to start the reaction and this is maintained by the further addition of both in a semi-batch process.

The preparation procedure of the PVAc based film-former which was followed is detailed below in Table 3.1. The equipment used and the names and amounts of the substances have not been included at the request of Celanese due to privacy issues. All of the variations of the film-formers produced using this procedure were created by myself at Celanese's laboratories and were not interfered with by anyone else to ensure the validity of both the results and the conclusions hence drawn.

Table 3.1 – General film-former emulsion preparation procedure

Stage	**Comment**
1	PVA stabilised aqueous solution produced
2	Buffer solution added
3	First stage monomer added and solution heated
4	First stage initiator added
5	Continuous additions of: • Reducing agent (sodium thiosulfate / bicarbonate mixture) • Oxidising agent (hydrogen peroxide) • Monomer (VAc)
6	Final stage initiator added
7	Solution cooled and anti-bacterial agent added

The formulation of the film-former was altered to produce a range of molecular weights and particle sizes. This produced a range of physical property differences in the size which could be investigated to determine how each property affects the performance. It is known that the molecular weight can be altered by changing the concentration of initiator used and that the particle size can be altered by changing the concentration of first stage monomer.[63] The standard formulation of the film-former uses a 100% concentration of initiator and 5% first stage monomer, so by altering the concentrations of both (12.5-150% initiator concentration; 0–25% first stage monomer) a range of molecular weights and particle sizes could be produced. Each film-former emulsion was produced as a 2.5 litre batch and has a stated shelf life of over three years.

3.2.3 Size preparation

Sizes were created from a standard formulation supplied by St. Gobain–Vetrotex using the film-formers created in the previous section. All of the variations of the sizes produced using this procedure were created by myself and were not interfered with by anyone else to ensure the validity of both the results and the conclusions hence drawn. The formulation used is detailed below:

400 g of deionised water was charged to a 2 litre conical flask and acidified using 0.1 g of acetic acid. 3.5 g of coupling agent was added to the reaction dropwise over 10 minutes under stirring and the reaction was allowed to stir out for a further 30 minutes.

45 g of film-former was charged to a 250 ml conical flask and diluted with 10g of deionised water under stirring. 4.5g of plasticiser was added to the reaction dropwise over 15 minutes and the reaction was allowed to stir out for a further 30 minutes.

5 g of lubricant was charged to a 100 ml conical flask. 50 g of deionised water which had been heated to 35°C was charged to the reaction under stirring.

2.5 g of anti-static agent was charged to a 100 ml conical flask. 50 g of deionised water which had been heated to 35°C was charged to the reaction under stirring. 50 g of cold deionised water was then added and the reaction was allowed to cool to room temperature.

Combine all four solutions into one pot and charge 379.4 g of deionised water to the reaction under stirring.

Table 3.2 – Weight composition of standard size formulation

Constituent	**Weight (g) for 1 litre of size**
Acetic acid	0.2
Coupling agent	3.5
Film-former	45
Plasticizer	4.5
Lubricant	5.0
Antistatic agent	2.5
Deionized water	939.3
Total	**1000 g**

From this composition we can observe that the solid content of the sizes produced will amount to only 6%, due to the large quantity of water present in the size. However, film-former emulsions tend to have only a solid content in the region of 55% meaning that the overall solids content of the size is actually only about 4%. This value is in the region stipulated by Lowenstein at which a size will be most effective. [13]

3.2.4 Size film preparation

Due to the size having a very low solid content, a large amount is required to produce a film which can be handled. Obviously spin coating is only useful for very thin films under these circumstances so a direct application of the liquid size onto the glass surface is required. To obtain films with similar dimensions it was decided that they should be coated on identical 75 x 25 mm flat glass microscope slides. The glass was washed with acetone prior to use to remove any possible residues which could contaminate the films and they were dried using clean tissue paper. These slides were then placed inside glass Petri dishes and completely immersed in an excess of size. After the sample had been dried in an oven the coated slides were then cut from the Petri dish using a clean scalpel and any excess film overlapping the edge of the flat glass surface was cut away. By testing a range of solution quantities it was found that 30 ml of liquid size produced a film with a thickness of around 50 μm which could be handled relatively easily without deformation of the film. The reverse side of each slide was cleaned with acetone to produce slides with size only on one side.

There are two main methods of drying the size to produce uniform films, vacuum drying and heat drying (or a combination of the two). It was found that when the liquid size was placed under a vacuum, bubbling occurred which produced non-uniform films. This occurred due to trapped air in the size solution due to the large amount of stirring used to mix the solution. Because of this problem, heating alone was used to dry the solution and produce uniform films.

A preliminary investigation was undertaken to determine the standard drying temperature to be used. Four samples were created from the same batch of size and each of the samples was dried at a different temperature in an oven. The point at which no liquid size remained was used to determine the time to complete drying. Since the point at which the sample was fully dried is fairly ambiguous, the actual drying times were only recorded to the nearest hour. The resulting drying curve plot is shown below in figure 3.1.

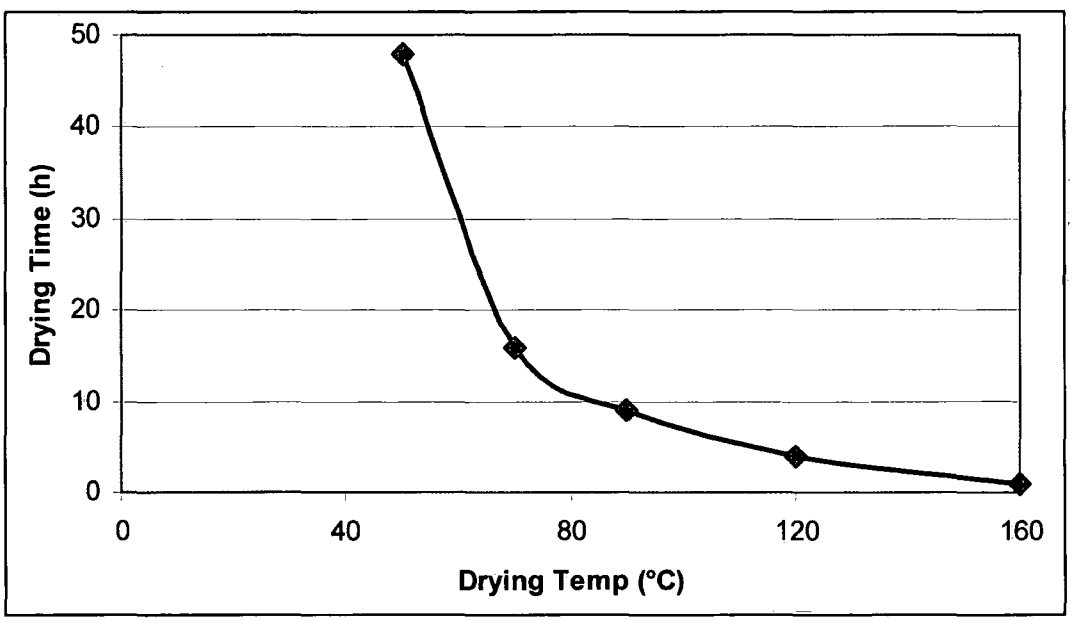

Figure 3.1 – Size drying curve for the standard formulation at different temperatures

It can be observed that as the drying temperature approaches the boiling point of water (100°C) the drying time decreases rapidly. Above 100°C the drying time decreases even faster and at a temperature of 160°C the drying time of the film is only one hour. Although it could be concluded that a very high drying temperature is beneficial, it was found that the film begins to degrade and becomes coloured and opaque at high temperatures. Also there is the likelihood that the size will not have bonded chemically to the glass

surface due to the fast nature of the drying, and the latex particles would not have coalesced properly to produce a continuous film. Because of these factors the drying was decided to be undertaken at a temperature of 70°C which takes approximately 16 hours to produce a dry film.

3.3 Experimental Techniques

3.3.1 Gel Permeation Chromatography

Gel permeation chromatography (GPC) was used to determine the molecular weight of the different batches of film-formers produced. The molecular weight determination was carried out on freeze dried samples of the film former rather than the size so as to minimise contamination of the results. Low molecular weight species not originating from the PVAc may arise from other additives present in the final size.

A Viscotek TDA 302 SEC apparatus fitted with two PLgel mixed C 300 x 7.5 mm columns, running at 30°C with a THF flow rate of 1ml min^{-1} with a refractive index detector was used to determine the molecular weight data for the samples. Chromatography grade (>99.9% pure) THF was used as the solvent throughout. The refractive index detector was calibrated using a poly(vinyl acetate) standard (M_n 71.5 kDa).

4 mg of dried film-former was dissolved in 4ml of THF to produce a solution with a polymer concentration of 1mg / ml. This whole sequence was repeated to ensure reproducible molecular weight values could be obtained.

3.3.2 Photon Correlation Spectroscopy

A Malvern Mastersizer 2000S instrument was used to determine the size distribution of the polymer particles present in the film-former emulsion. 2 ml of liquid film-former was diluted in 50 ml of deionised water to reduce the concentration of particles present in the sample. This is required as a high concentration of particles will affect the scattering and mask the actual particle size distribution. The dispersion medium used in the Mastersizer was purified water and red and blue lasers of defined wavelengths (633 nm & 466 nm respectively) were used to produce the light. A mechanical stirrer set at 1700 rpm was used to pump the size solution through the Mastersizer.

The distribution was determined three times for each run with a gap time of ten seconds between each determination. The particle size distribution data were collected and averages of the distribution from three repeats were produced.

This whole sequence was repeated to ensure reproducible particle size distributions and values could be obtained.

3.3.3 Scanning Electron Microscopy

Samples were dried onto 5 x 5 mm square silica stubs in an oven at 70°C for 16 hours. The samples were then coated with a thin film of chromium particles using a Cressington 308R coater to improve the image quality by reducing the effect of charging of the sample by the electron beam. The sample was mounted in a S5000 Mesh holder and placed in a Hitachi S5200 field emission scanning electron microscope. The sample was held in the microscope chamber under vacuum at $1x10^{-8}$ Pa for 2 minutes prior to the electron beam being switched on. A beam voltage of 1.5 keV was used throughout for all samples and a secondary electron detector was used to produce the image. Various magnifications were used to obtain images to investigate the samples fully.

Imaging of the polymer particles was possible using this instrument coupled with a fast drying technique. This involved applying a vacuum to silica squares coated with the wet size; due to the rapid evaporation of the water under vacuum, the particle-like structure could be trapped as a film without coalescence of the PVAc particles occurring. The samples were then placed in the mesh holder and inserted into the scanning electron microscope (SEM) and investigated using the method already discussed. Measurements were then taken of the resulting particle diameters using the measurement tool in the SEM software.

Both of these sequences were repeated to ensure reproducible images; particle size measurements could be obtained from the SEM with a reasonable degree of accuracy.

3.3.4 Environmental Scanning Electron Microscopy

An FEI/Philips XL30 environmental scanning electron microscope (ESEM) was used to investigate the surface of films of the dried sizes. The films were created on glass slides as described previously. The samples were frozen by immersion in liquid nitrogen to adhere them fully to the glass slide prior to cutting; this ensured that the film would not be deformed during the cutting of the sample. This was undertaken to produce a smaller sample with dimensions 10 x 10 mm which would fit inside the ESEM chamber. A diamond-tipped pen was used to cut the sample to the required size and this was then attached to an ESEM stub using carbon tape, with the film pointing towards the detector. The sample was then left for ten minutes at room temperature to thaw before the electron beam was switched on and the investigation was begun.

Samples were also mounted perpendicular to the detector to produce images of the cross-section of the dried film on the glass. A screw stub, which consists of a perpendicular groove through the stub where the sample stands and a screw which tightens onto the sample to keep it in place, was used to achieve this orientation. The stub fitted directly into the ESEM stage without the need for carbon tape to keep it in place.

For these experiments the images were acquired using a back-scattered electron detector at a range of voltages between 5 – 25 kV and at a water vapour pressure of 70 Pa. The samples were imaged at varying magnifications with varying brightness and contrast to obtain the best images possible.

Wetting images of the size drying down on bare glass fibres were also obtained using the ESEM. Fibres provided by Vetrotex were heated up to 700°C in a Carbolite CWF-1200 furnace at a rate of 5°C per minute from room temperature and held as an isotherm for 8 hours to burn off the original size. The furnace was then allowed to cool to 120°C at a rate of 10°C per minute for a further 5 hours to stop any water from the atmosphere condensing on the fibres and weakening them. The fibres were then removed from the furnace and placed into a dessicator over phosphorus pentoxide to minimise their interaction with water in the atmosphere.

A small quantity of the fibres was placed into the bottom of a stub with a small amount of the surface ground away to produce a concave bowl-like surface with a depth of 5 mm. The fibres were then fully covered with an excess of wet size and placed within a cooling stage inside the ESEM. The temperature of this stage is controlled externally using a refrigerated water supply which alters the temperature of the sample accurately to within 0.1°C. As the pressure in the ESEM decreases the water present in the size evaporates and the solid PVAc size mixture coats the glass fibres. The rate of water evaporation is controlled by the sample temperature and the environmental pressure within the ESEM chamber. As these variables can be both increased and decreased, precipitation of water on the surface of the fibres is also possible.

For these wetting experiments the images were acquired using the gaseous secondary electron detector at a range of voltages between 5 – 25 kV and at vapour pressures between 200 – 900 Pa. A standard sample temperature of 4.0°C was used throughout for all of the different batches of

size. The samples were imaged at varying magnifications with varying brightness and contrast to obtain the best images possible.

All of these different techniques using the ESEM were repeated to ensure that reproducible images could be obtained for all of the tests with a reasonable degree of accuracy.

3.3.5 ESEM-Energy Dispersive X-ray Analysis

An FEI/Philips XL30 ESEM with a Roentec Quantax energy dispersive X-ray analyser (EDX) attachment based at Newcastle University was used to investigate the elemental composition of specific areas of a film-coated glass slide sample. Films of the sizes were created on glass slides as described previously; these were then frozen in liquid nitrogen to prevent the film from moving and cut using a diamond tipped pen. The samples were mounted perpendicularly into the ESEM using a screw-stub as described previously.

Individual points on the sample were investigated using X-ray analysis via the EDX to determine the elemental composition. Larger areas were also investigated in the form of a line scan which produces an elemental composition graph showing the change in elemental abundance in different parts of the scanned area. For the individual point investigation an analysis time of 60 seconds was used to obtain a sufficiently large amount of data which could be converted into a composition map of the sample. For the line scan investigation this analysis time was increased to 300 seconds to account for the larger area being investigated.

For these experiments the images were acquired using a back scattered electron detector at a range of voltages between 10 – 25 kV and at a constant water vapour pressure of 70 Pa. The samples were imaged at varying magnifications with appropriate brightness and contrast settings to obtain the best images possible.

This whole sequence was repeated to ensure reproducible elemental composition data could be obtained with a reasonable degree of accuracy.

3.3.6 Attenuated Total Reflection – Fourier Transform Infra-Red Spectroscopy

A Nicolet Nexus attenuated total reflection-Fourier transform infra-red (ATR-FTIR) spectrometer was used to investigate the difference in the chemical group concentrations at the two interfaces of the dried size film (the air and the glass interfaces). The films were created on glass slides as described previously and were peeled from the slide carefully so as not to cause deformation of the film. A reference spectrum of pure PVAc was produced using a standard sample of granulated PVAc supplied by Aldrich ($\overline{M_n}$ = 74 kDa). The granules were ground to produce a fine powder using a pestle and mortar and a small sample of this was used to produce the comparative IR spectrum.

The instrument was pre-cooled using liquid nitrogen and a cycle of 32 repeating steps was used for the collection of both the background and the sample spectra. The top (size-air interface) and the bottom (size-glass interface) of the film were investigated and the resulting spectra were compared to determine whether differences could be observed.

This whole sequence was repeated to ensure reproducible IR spectra could be obtained with a reasonable degree of accuracy.

3.3.7 UV-Visual Absorption Spectroscopy

An ATI Unicam UV-2 spectrophotometer was used to determine the optical absorption properties of glass coated films of the sizes. The size films were created on glass slides as described previously. To ensure accurate absorbance results the thickness of the sample films have to be the same for all of the samples investigated. This is because the amount of light scattered is proportional to the amount of particles present in the sample and the amount of particles will increase with thickness. To ensure films with uniform thicknesses were produced, many films of each size were created on glass slides with known thicknesses. The thickness of the film could then be determined accurately by subtracting the thickness of the glass slide from the overall thickness of the sample; all of the measurements for this were performed using a digital micrometer. Only films with a set thickness of 50±2 μm were used for this investigation.

The absorbance measurements were undertaken on the complete samples; this means that the absorbance data obtained also include that of the glass slide. However, by recording the absorption spectrum of the bare glass slide and subtracting this from the spectrum of the whole sample, the trace for the film alone could be obtained. This whole sequence was repeated to ensure reproducible absorbance spectra of the films alone could be obtained with a reasonable degree of accuracy.

3.3.8 Ion Beam Analysis

The films were created on glass slides as described previously. The samples were frozen by immersion in liquid nitrogen to adhere them fully to the glass slide prior to cutting; this ensured that the film would not be deformed during the cutting of the sample. This was undertaken to produce a smaller sample with dimensions 25 x 10 mm which would fit inside the ion beam chamber. A diamond tipped pen was used to cut the sample to size and this was then attached to a rectangular stub with carbon tape. The stub was then inserted into the chamber and ten minutes were allowed for the sample to thaw before the ion beam was switched on and the investigation was begun.

Prior to this, initial testing had taken place on spin coated films, however these films were found to be too thin due to the low solid content of the size. The ion beam burned through the films at even the lowest possible beam energies and analysis of the sample could not be undertaken.

The near-surface elemental distribution was analysed using $^{4}He^{+}$ ion beam analysis, with a beam energy of 3.2 MeV. Backscattered $^{4}He^{+}$ ions were detected with a passivated implanted planar silicon detector at 170° to the direction of the incident beam. Rutherford back-scattering data were collected by the detector and the spectra obtained contained information about both the elemental composition and the depth distribution of the elements present in the sample. In order to decouple the elemental information from the depth distribution it was necessary to compare spectra measured at multiple angles

of incidence. To achieve this, analyses were performed with the sample aligned at 65°, 75° and 80° to the incident beam.

By using data fitting software it was possible to produce a realistic simulation of the depth profile of certain elements present in the sample. The IBA instrument used was a NEC 5SDH Pelletron device and the data fitting was undertaken using Surrey University's Datafurnace software. This whole sequence was repeated to ensure reproducible elemental analysis and depth profile data could be obtained with a reasonable degree of accuracy.

Figure 3.2 – IBA instrument used for investigation

3.3.9 Dynamic Mechanical Analysis

Dynamic mechanical analysis (DMA) was used to determine the Young's modulus of films produced from the sizes. Unlike previous samples, the films produced for this technique were not coated onto flat glass slides. Instead, 30 ml of wet size was poured into a glass Petri dish, which was dried in an oven at 70°C for 16 hours to produce a uniformly thin film disc. This disc was then cut into rectangular shapes, the length, width and thickness of which were determined accurately using a digital micrometer. The rectangular samples were then mounted in a film clamp in the TA Instruments Q800 dynamic mechanical analyzer and an isothermal protocol was run to determine the Young's modulus of the size films. The protocol used was:

Step 1. Heat to 25°C
Step 2. Isotherm at 25°C for 3 minutes
Step 3. Stress-Strain investigation with load ramp of 0.1N min^{-1}

The stress-strain curves were plotted from the data obtained from this investigation and the Young's modulus was calculated from the gradient of the curves. This whole sequence was repeated to ensure reproducible Young's modulus values for films of the sizes could be obtained with a reasonable degree of accuracy.

Figure 3.3 – Image of film mounted in the DMA prior to a load being applied

3.3.10 Peel Test

Films of the size were created on glass slides as described previously in section 3.2.4. This method produced films with a thickness of 50±5 μm.

The force binding the film to the glass slide is known as the adhesive strength. This can be determined from the sample by measuring the force required to peel the film from the glass slide. An Instron Extra Servo mechanical tensile testing machine was used for this task.

A variation of the ISO standard 180° peel test [100] was used to determine the adhesive strength of the films. This test is normally used for such a determination but it was found that, at this angle, the peeled film underwent self-adhesion during peeling producing inaccurate results. To counteract this effect a slight tilt to the glass slide was introduced using a small piece of metal wire. This reduced the angle of the peel allowing it to be performed without this self-adhesion occurring.

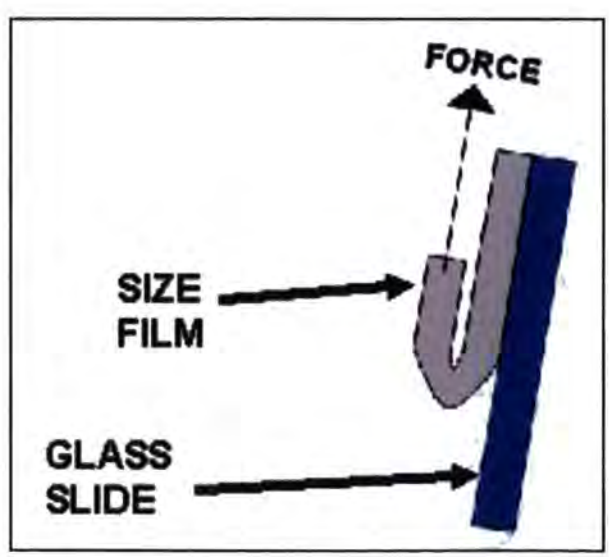

Figure 3.4 – Schematic diagram of the modified peel test which measures the adhesion of the dried size to glass surface

The new peel angle range was calculated using trigonometry as the diameter of the wire and the distance of it from the slide were known. It was found that the peel occurs at an angle of 171° during the initial stages of the peel and at an angle of 168° in the final stages of the peel.

Initial peel stage

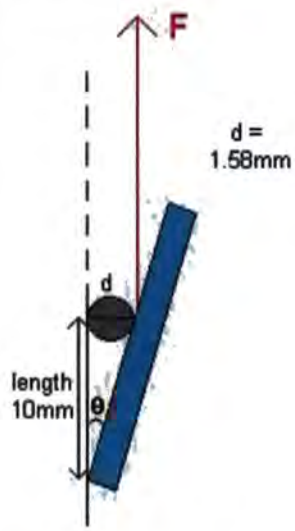

$\tan \theta = \frac{\text{diameter of wire}}{\text{length}}$

$\tan \theta = \frac{1.58}{10} = 0.158$

$\theta = \tan^{-1} 0.158 = 9°$

Therefore initial peel occurs at 171°

Final peel stage

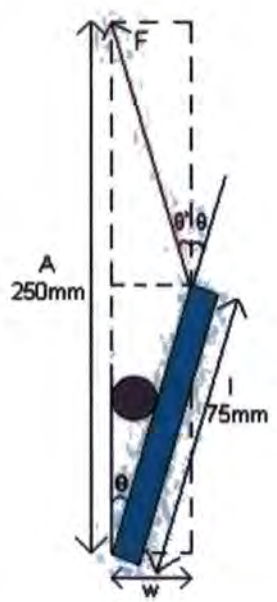

$\theta = 9°$ $l = 75mm$

$\sin \theta = w / l \rightarrow \sin 9 = w / 75$

$w = \sin 9 \times 75 = 11.7mm$

$\tan \theta' = w / A = 11.7 / 250 = 0.0468$

$\theta' = 3° \rightarrow$ an increase of 3° from initial angle

Therefore final peel occurs at 168°

Figure 3.5 – Calculation of peel angle at start and end stages

Range of peel = 171-168°

The instrument was set to peel the film at a rate of 20 mm min^{-1}. This whole sequence was repeated to ensure reproducible values for the adhesive strength of films of the sizes could be obtained with a reasonable degree of accuracy.

Figure 3.6 – Image of the peel test being performed on a coated glass slide.

3.3.11 Lap Shear Test

A variation of the ISO standard lap shear test [101] was undertaken to determine the cohesive strength of the dried size. Two glass slides, which had been coated with wet size, were positioned approximately 10 mm apart and a third slide was placed on top of these binding them all together upon drying to create a pyramid structure. The top slide was off-set so that the interfacial area was much larger for one of the base slides. Therefore, when a force was applied to pull the two bottom slides apart the cohesion of the smaller interfacial area (x) will fail first. It is this smaller area which can then be investigated to determine the cohesive strength of the different sizes. The slides were also investigated for the presence of size on both surfaces to ensure that cohesive failure rather than adhesive had occurred. An Instron Extra Servo mechanical tensile testing machine was used to determine the cohesive strength of a dried size and it was set to pull the slides apart at a rate of 5 mm min^{-1}.

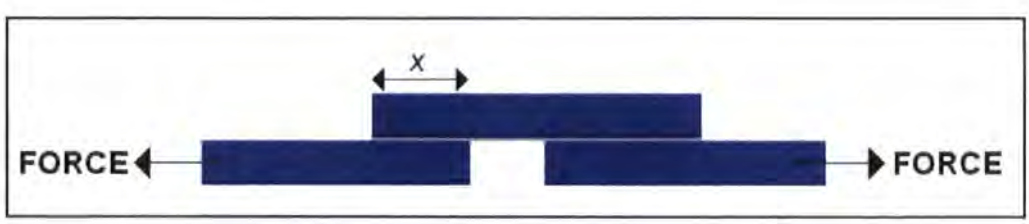

Figure 3.7 – Schematic diagram of the two point lap-shear test used to measure the cohesive force of the dried size binding two glass slides together

Pyramid type samples as shown in figure 3.7 were produced using the above procedure. These samples were then cured in an oven at 130°C for 16 hours.

Initially a cure temperature of 70°C was attempted but it was found that the size did not dry sufficiently over 16 hours, which produced a weak bond between the two glass interfaces that was too small to measure. This was overcome by increasing the temperature to a value greater than the boiling point of water, which is present in excess in the size. This enabled the solid content of the size to bind the glass surfaces together, increasing the strength of the cohesive bond to a magnitude which the testing instrument could measure.

Three slides were used rather than two for this determination due to the orientation and inflexibility of the clamps mounted in the instrument. Initially a two slide sample was attempted but it was found that the sample failed when it was mounted in the instrument clamps. This occurred because the clamps are aligned at 180° but the two slide sample has a step present which produces a lateral force in the interfacial bond. Because this lateral force is stronger than the cohesive strength of the bond it causes it to fail before any force is applied to shear the slides apart. By using three slides mounted in the pyramid arrangement the clamps are aligned and there is no lateral force acting on the bond. This whole sequence was repeated to ensure reproducible values for the cohesive strength of films of the sizes could be obtained with a reasonable degree of accuracy.

Figure 3.8 – Image of the lap shear test being run on the pyramid sample

3.3.12 Contact Angle Measurement

Films of the size were created on glass slides as described previously in section 3.2.4 and the static contact angle of the dried size was then determined using deionised water and styrene (supplied by Fluka) as wetting liquids. The wet size itself was also used as a wetting liquid on bare glass slides to determine how the size initially adheres to the bare glass surface during sizing.

A Ramé-Hart NRL 100-00 goniometer was used to investigate the wetting nature of the samples by measuring the contact angles made by a dropping liquid on the sample. The goniometer consists of a height adjustable stage on which the sample is placed and a focussing lens with a rotating cross-hair etched onto it. This cross-hair produces a tangent line to produce a quantifiable contact angle measurement for the droplet; a light source is also present on the goniometer to illuminate the sample. When the sample has been set at the correct height so that the horizontal cross-hair line is level with the surface of the sample, a single droplet of liquid is placed onto the surface and left for 60 seconds to equilibrate. The stage is then positioned so the edge of the droplet lies directly on the intersection of the two lines in the cross-hair. The lens is rotated until the cross-hair forms a tangent with the outer edge of the droplet and the angle is recorded from the scale present on the lens. This tangent angle corresponds to the contact angle of the sample and the manufacturer has stated that the value is correct to within ±2°.

This whole sequence was repeated to ensure reproducible values for the contact angle of films of the sizes could be obtained with a reasonable degree of accuracy.

3.3.13 Wet-out Rate

Glass fibres, in the form of a chopped strand mat, are treated with the size being investigated which binds them together. This sized mat is then placed onto a wet-out rate detector which has been developed in the labs at Celanese. The mat sits on a thin piece of transparent plastic which is present to protect the instrument and a 5 mm thick metal plate with a circle cut out (diameter 50 mm) is placed on top of the mat to keep it in place. 25 ml of polyester resin is poured into this hole in the plate directly onto the mat to fill the gap. The light source is then placed over the hole and the initial time is recorded. When the light passing through the mat achieves a particular intensity then the computer stops the timer and the wet-out rate of the size is known. The computer program used for the wet-out rate determination was produced by Pico Technology and was called DrDaq. Polyester resin without hardener or catalyst is used to prevent polymerisation.

The wet-out was recorded as the average of three individual runs to ensure reproducible values could be obtained with a reasonable degree of accuracy.

This investigation was carried out by Dr. Rian van Straeten at Celanese labs in the Netherlands, due to the limited availability and uniqueness of the instrument.

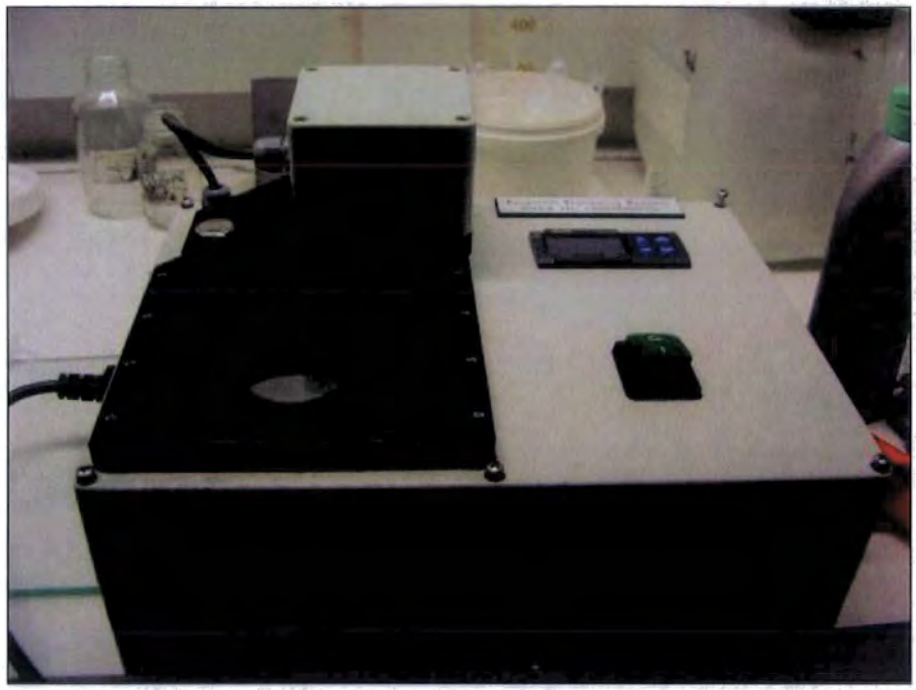

Figure 3.8 – Image of the wet-out rate instrument designed by Celanese

Chapter 4

Results

Size Structure

4.1 Introduction

Many glass fibre size formulations exist; the choice of which should be used is wholly dependent on the final application of the fibres. Fibres used for weaving will generally have an increased amount of film-former present to aid in the binding of the fibres. Alternatively, those used in matting for roofing contain no film-former to promote dispersion during impregnation.[13] Most formulations in existence were created using an empirical process, starting from one found previously to be successful. Subtle changes from the initial formulation are made depending on the end use of the finished fibre products. However, the effectiveness of a glass fibre size could be better predicted from a full appreciation of the chemistry occurring within the size – this is what this investigation hopes to achieve.

The first part of this investigation aims to determine the chemical structure of a typical glass fibre size used in industry. This includes determining the distribution of each component present in the size, specifically whether the components are found in specific areas within the size or if the size exists as a random mixture. This information could then be very useful for predicting whether a hypothetical size formulation is likely to either pass or fail for a particular application or under specific conditions.

4.2 Coupling Agent Location

4.2.1 ESEM Imaging

Electron microscope imaging was undertaken on films of the dried sizes using the standard formulation supplied by Vetrotex as discussed in section 3.2.3. Images were taken of the cross-section of the film to investigate the topography and structure.

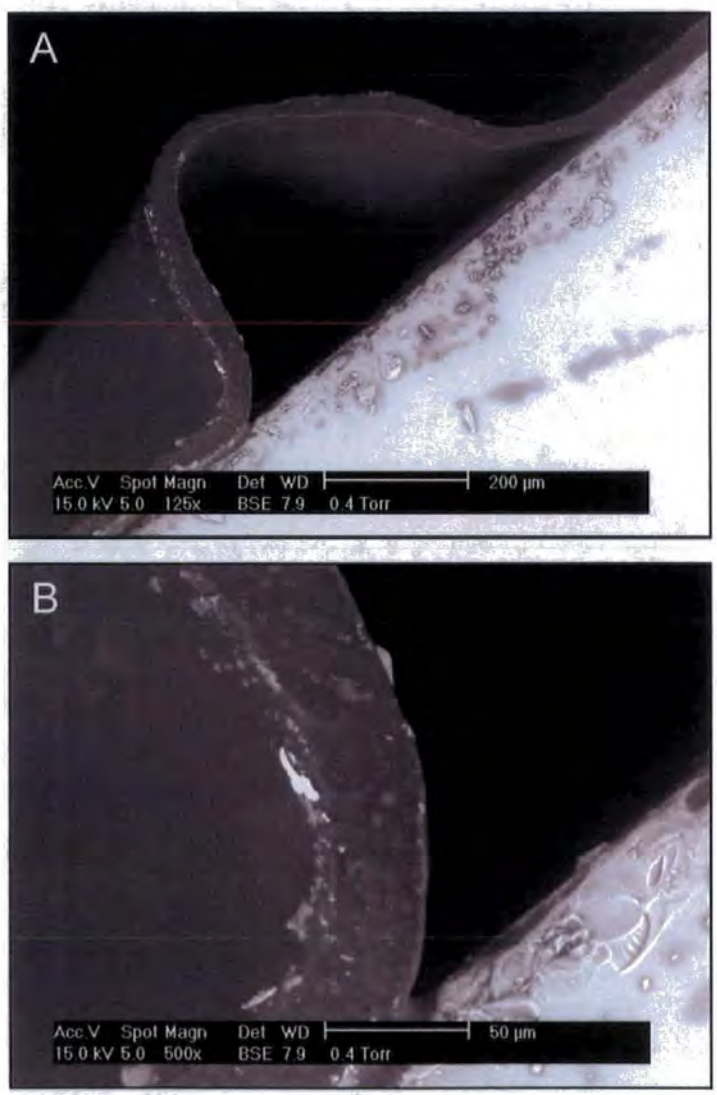

Figure 4.1 – Cross-sectional image of the standard formulation dried size film on a glass slide at: (A) 125x magnification; (B) 500x magnification.

The images in Figure 4.1 are of a film of the dried size which has been laterally forced causing a fold in the surface of the film, creating an area which is not adjacent to the glass.

It can be observed from these images that a lighter band is present in the film at the inner edge of the cross-section which corresponds to the glass interface of the film. This phenomenon is repeated for every other batch of size created using the formulation supplied.

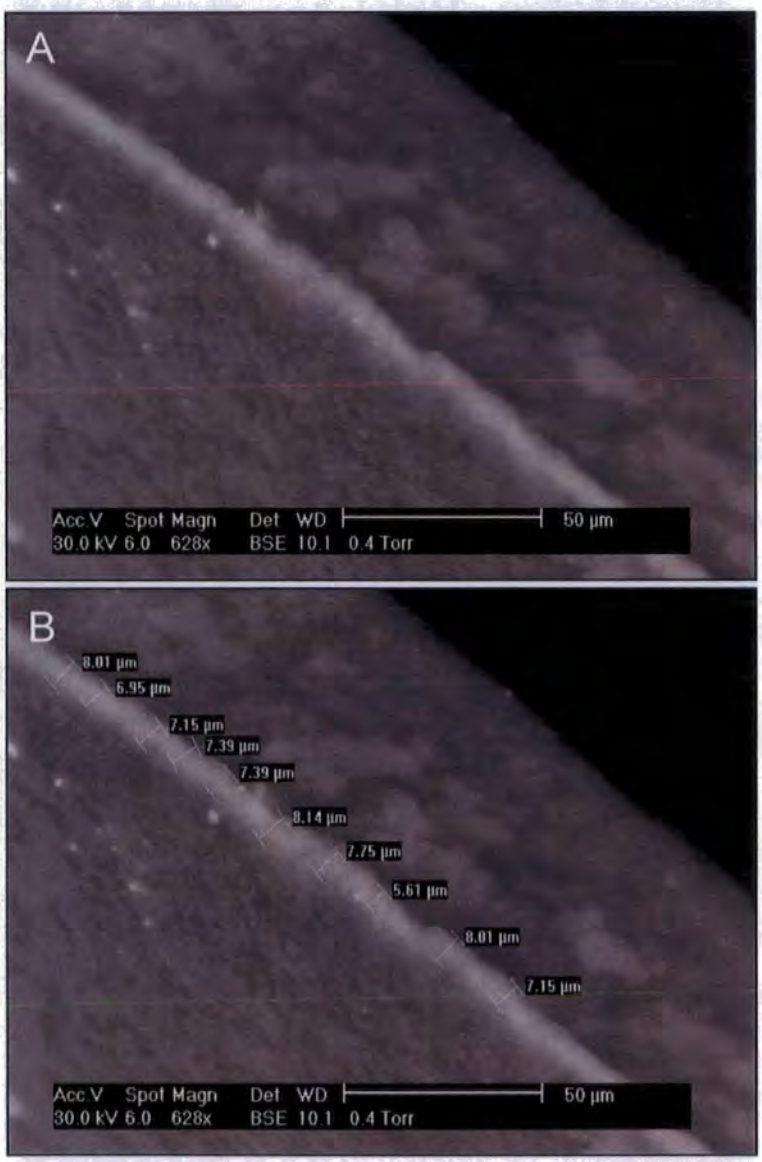

Figure 4.2 – Cross-sectional image of the standard formulation size film on a glass slide at 628x magnification (A) with the thickness of the light band calculated (B).

On closer inspection of this lighter band, it can be observed that it is quite uniform in thickness throughout the film. In Figure 4.2 (B) the lighter coloured band has a thickness range from a minimum of 5.6 μm to a maximum of 8.1 μm.

4.2.2 ATR-FTIR Investigation of Film Interfaces

Attenuation of the IR beam on the instrument allows us to probe the area immediately at the air interface of the dried size. By peeling the film from the glass slide it was also possible to probe the immediate area of the glass interface of the film.

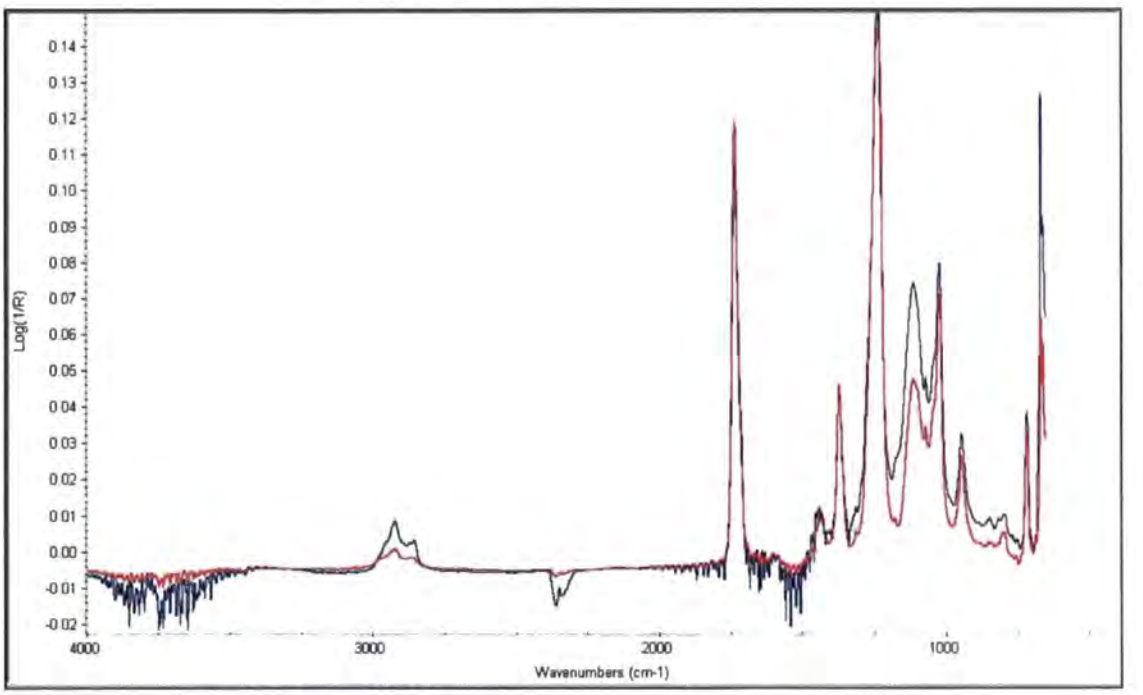

Figure 4.3 – IR spectra of both interfaces of the standard formulation dried size film (red trace – film-air interface; blue trace – film-glass interface).

In figure 4.3 both the air and glass interface of the film have been overlaid on the same graph. Here it can be observed that for the most part the two spectra overlap closely, however the peak around 1100 cm^{-1} (which corresponds to the Si–O–Si stretching vibration) appears to be greater in strength for the film-glass interface than for the film-air interface. This indicates that there are more Si-O bond containing species at the glass

interface of the film. The coupling agent used in the formulation is silane-based therefore this is the most likely cause of the increase in Si-O bonds. This observation is consistent with the literature as coupling agents are known to migrate to the glass surface of a size and lead to improved bonding.[13]

4.2.3 Elemental Analysis of the Dried Size Film

An investigation was undertaken using ESEM-EDX to determine the elemental analysis of the standard composition size as a function of film thickness. A dried film of the size on a glass slide was mounted in the ESEM chamber and analysed.

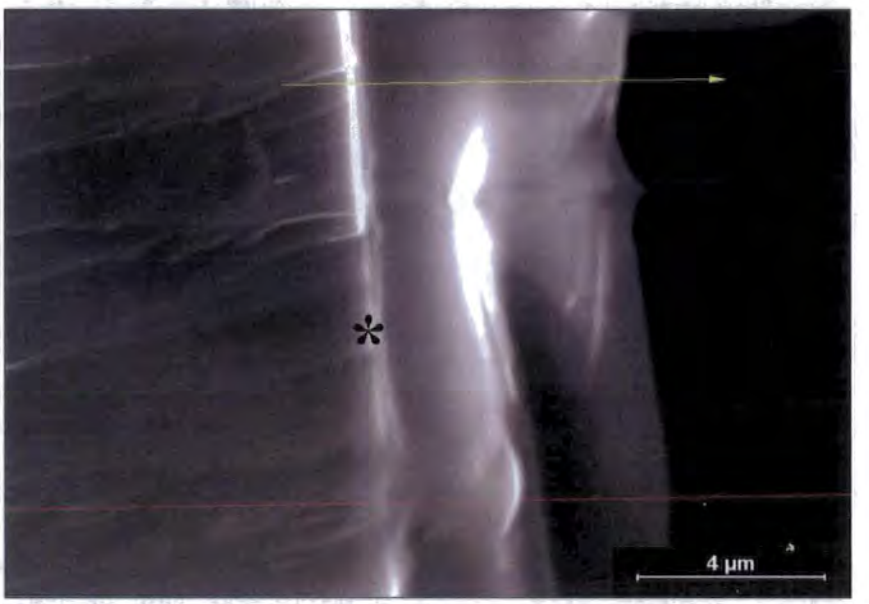

Figure 4.4 – ESEM image of the standard formulation dried size film: Yellow arrow = area investigated by X-ray analysis; * = to the glass-film interface.

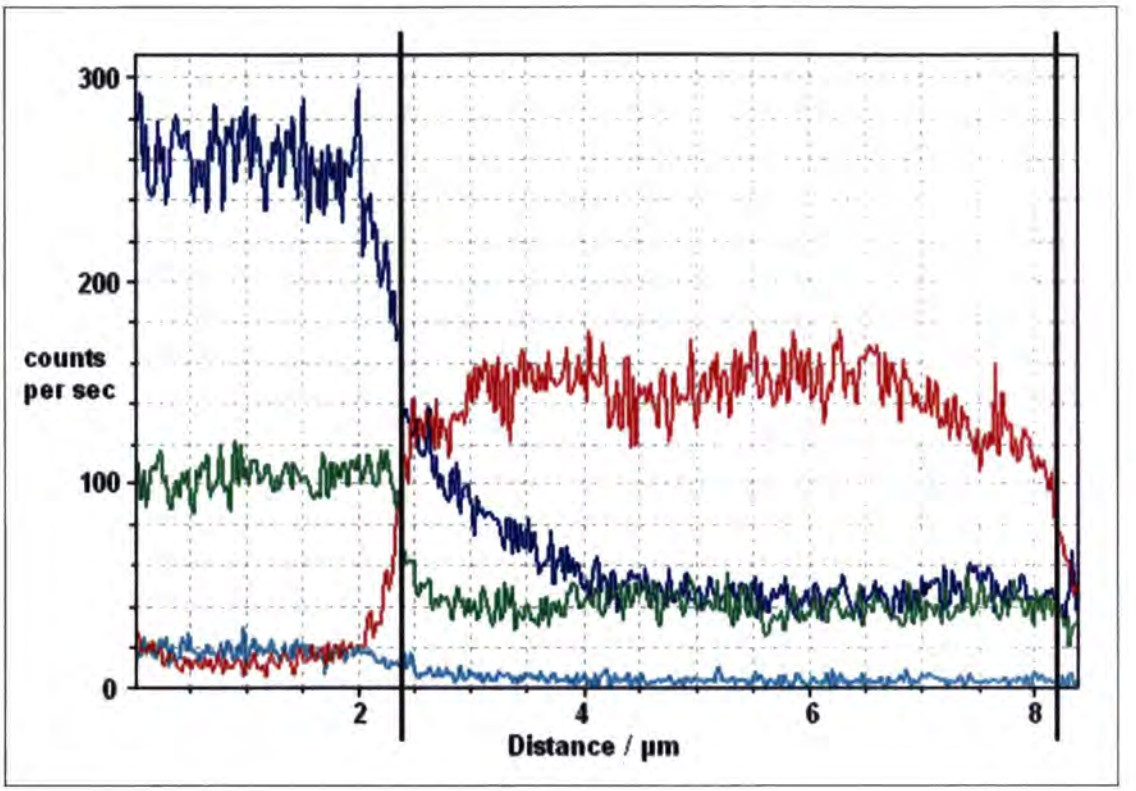

Figure 4.5 – Elemental analysis spectra corresponding to the yellow arrow in Figure 4.4. The left line corresponds to the glass-film interface; right line film-air interface (Element trace: red – carbon, green – oxygen, blue – silicon; cyan – calcium).

The ESEM image (Figure 4.4) shows a cross-section of the dried size film on the surface of a glass slide. The glass area of the sample is on the left and the film is on the right, the interface between the two areas is marked with an asterisk. An X-ray analysis line scan of the area marked by a yellow arrow in the image was performed and the spectrum in Figure 4.5 was produced. The two bold vertical lines indicate the two interfaces of the film, the line on the left is the glass interface and the line on the right is the air interface. This X-ray beam used to probe the sample has a diameter of approximately 0.5µm which indicates that the error in the spectrum above will have an error of the same distance. This occurs due to not all of the beam being in the same

substrate at the same time producing a gradual change in elemental composition rather than instantaneous.

It is observed that, at the glass interface of the film, there is a rapid change in the carbon and oxygen concentrations in the sample, due to the difference in species being sampled. A similar rapid change would also be expected in the silicon concentration, as the glass would contain a large amount of silica which the film should not. However, a gradual decrease in the silicon concentration instead is observed, this is much longer than that observed for the other elements which are attributed to the error of the instrument. This indicates that silicon-containing species are present in the film at the glass interface. As the distance from the interface increases, the concentration of the silicon species decreases until it reaches a plateau. This confirms the theory of migration of the silane-based coupling agent to the glass interface of the size during drying, to aid it bonding to the glass.

It is important to note that the concentration of silicon present in the film does not fall to zero; instead it levels out at a low content. This indicates that an excess of coupling agent (the silicon containing species) is added to the size to ensure strong bonding to the glass. The excess is required due to the large surface area of glass present in the fibrising process; in our system there is a significantly lower surface area of glass in comparison to the amount of size used to coat it.

4.3 Lubricant Location

4.3.1 Ion Beam Analysis of Size Film

Ion beam analysis was used to create a depth profile of the dried size film. It was initially undertaken to study further the area at the glass interface of the film, to try to find additional evidence for the location of the coupling agent additive as part of the investigation detailed in section 4.2. Unfortunately it was not possible to probe to any significant depth of the film due to limitations caused by its dimensions. The ion beam used on the samples had to be weak so as not to destroy the thin film, making only short probe depths possible with a reasonable degree of accuracy. When the energy was increased to attempt to probe deeper into the film, it was found that the ion beam would burn straight through the film without producing any useful results.

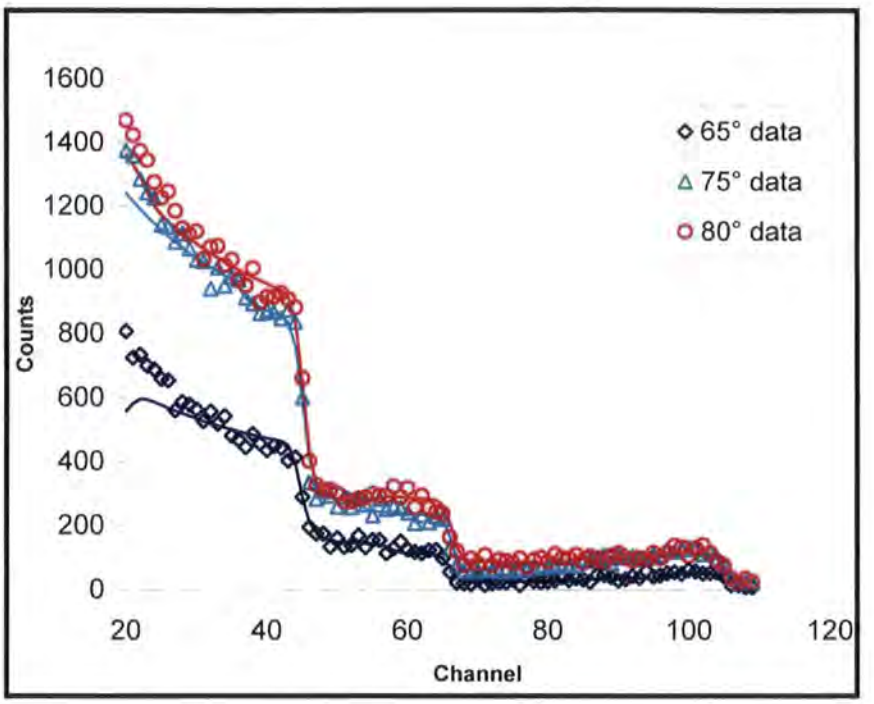

Figure 4.5 – Rutherford back-scattering (RBS) spectra of the standard formulation dried size film. Points on the diagram correspond to experimental data obtained; curves represent the best fit.

Initial attempts to fit the data assuming that the composition solely consisted of PVAc ($C_4H_6O_2$) and the coupling agent were unable to replicate the large step in the data around channel 45, which is due to the threshold energy of recoils from carbon. It was thought that this could be due to the presence of extra hydrocarbons from an as yet unknown source. To negate this extra step an extra species was included in the model with the stoichiometry of C_1H_2; with this modification it was possible to produce data shown as solid curves in Figure 4.5.

By modelling the data produced from Figure 4.5 it was possible to produce a depth profile of the film (Figure 4.6).

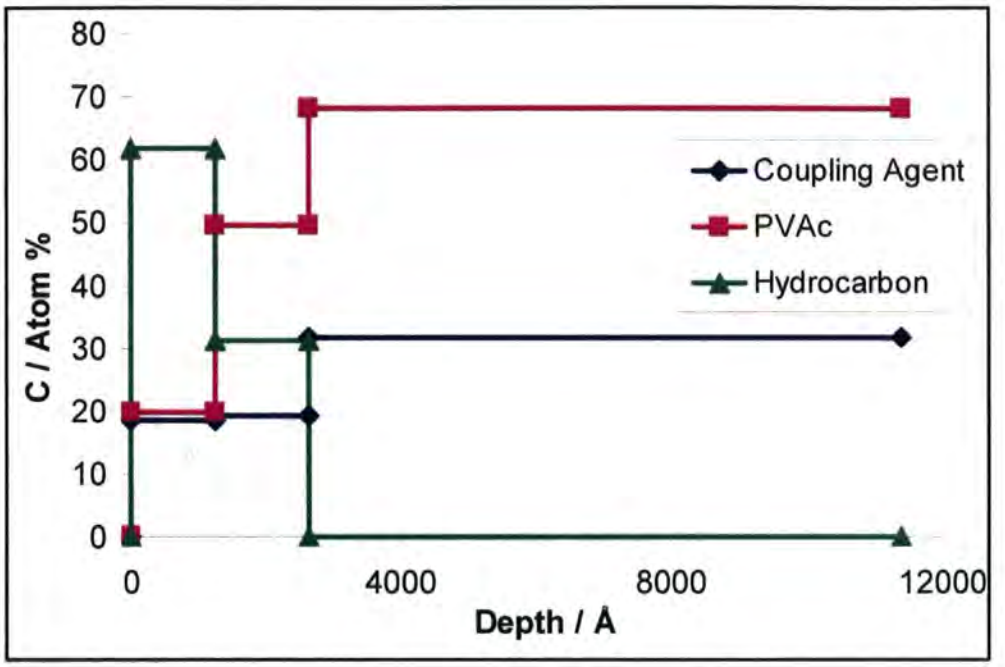

Figure 4.6 – Model of size composition with depth established from the RBS data.

From the model produced, it could be observed that at the air interface of the film a thin layer of a hydrocarbon-based species exists which decreases rapidly at increasing depth. The poly(vinyl acetate) species was found to increase in concentration at a similar rate over a similar distance, with the coupling agent concentration remaining almost constant throughout. A similar trend was found for all repetitions of this experiment leading us to surmise that a hydrocarbon layer is always found at the air interface of a dried film of this size formulation.

4.3.2 Origin of the Hydrocarbon Species

To determine the origin of this hydrocarbon band found at the air interface from the IBA model, three batches of size were produced, each with an additive missing. As there are only five different constituent compounds present in the size formulation, two of which have already been factored into the model, sizes were produced which had either the lubricant, anti-static agent or plasticiser additive missing. It was presumed that the majority of the signal producing the hydrocarbon species would be significantly lower for only one of the sizes if it were arising from the presence of one particular additive.

Films of the sizes lacking one additive were produced and they were investigated as before by IBA to determine a depth profile of each film.

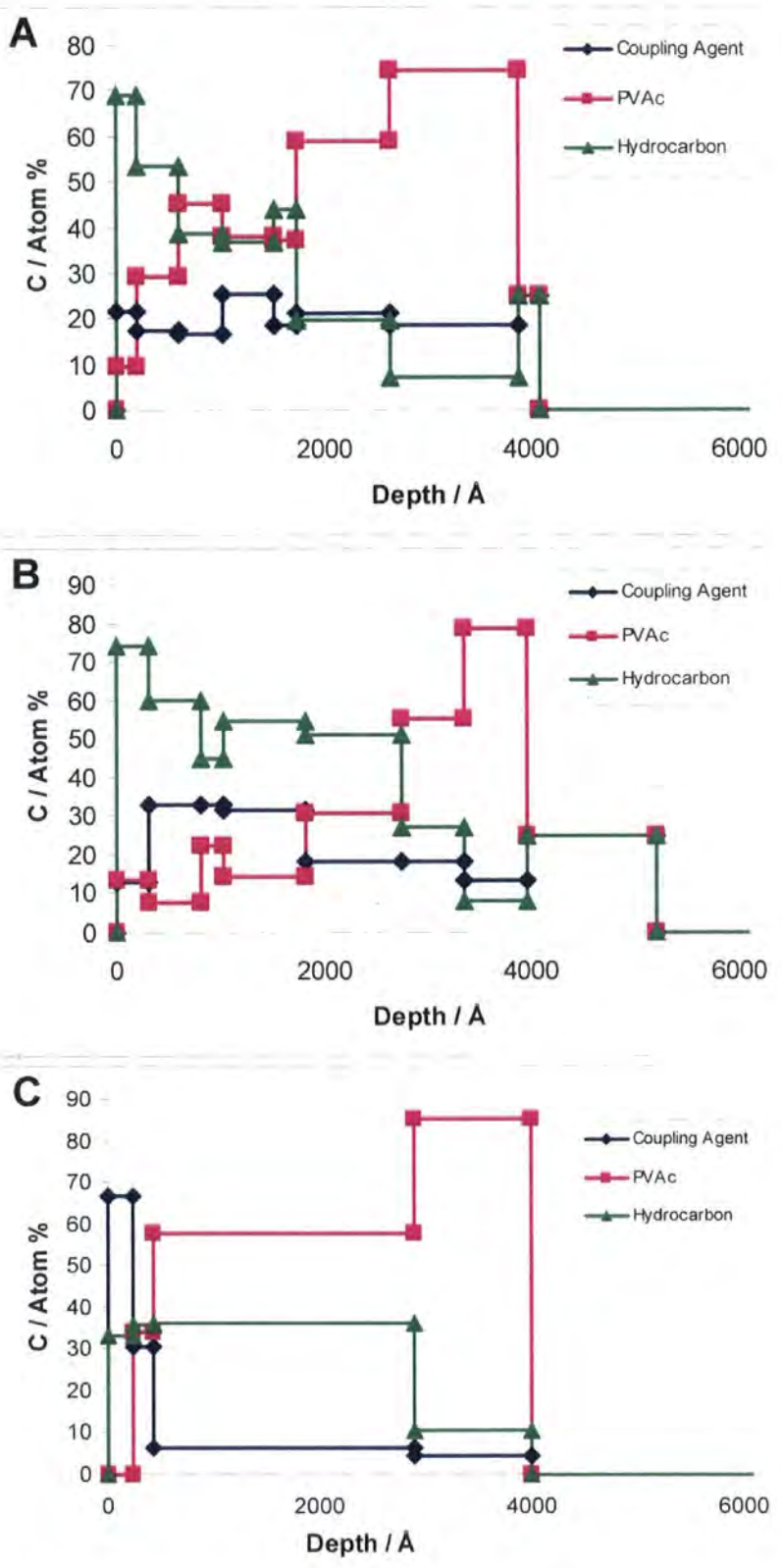

Figure 4.7 – Model of size composition with depth established from the RBS data (A – size without plasticiser, B – without anti-static agent; C – without lubricant).

It can be observed from the depth profiles in Figure 4.7 that the two films lacking plasticiser (A) and anti-static agent (B) both have a large concentration of hydrocarbon species present at the air interface of the film (~70%). However, the size without any lubricant additive (C) has a reduced hydrocarbon species concentration at the air interface (~30%). This indicates that the majority of the hydrocarbon species found at the air interface of the film must originate from the lubricant additive in the size. However, there is still 30% of hydrocarbon species present in the size without lubricant which indicates that the other additives present in the size must also congregate towards the air interface of the film to a lesser extent. This most likely occurs due to the relatively slow drying process used to cure the wet size onto the glass surface, allowing migration of the additives. The plasticiser migrates to the latex particles to aid the plasticity of the film. The anti-static additive migrates to the latex particles to provide an electrical pathway to disperse the build of static electricity within the sized fibre. Migration of the lubricant to the air interface of the film will occur to aid the flexibility of the dried film. However, the lubricant will also be found distributed throughout the film as it provides the dual function of lubricating the film by migration to the latex particles, in a similar manner to the plasticiser and the anti-static additives.

4.4 Ageing Study of Dried Size Films

In the previous section it was shown that a thin hydrocarbon layer, the majority of which arises from the lubricant additive, forms at the air interface of the size film. It is expected that any migration of the additives can only occur during the early film formation stages when the size is still a liquid, allowing movement of molecules to occur. After this stage, the size dries, forming a continuous film where little migration could occur due to the PVAc particles diffusing together. To test this hypothesis, a film of the size was formed and sampled over a number of days to determine whether migration could occur after drying. IBA was used to investigate this by creating depth profiles of the films, as previously undertaken in section 4.3.

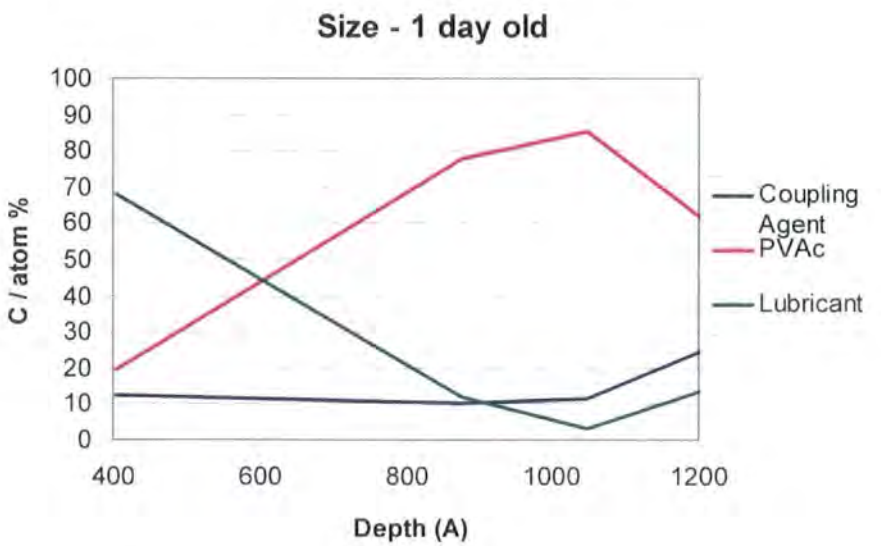

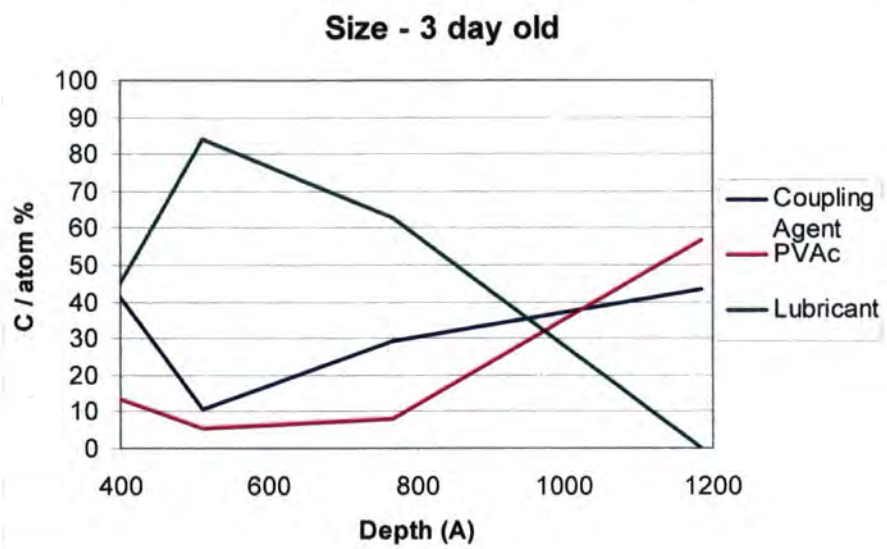
Size - 3 day old
C / atom %
100
90
80
70
60
50
40
30
20
10
0
400
600
800
1000
1200
Depth (A)
Coupling Agent
PVAc
Lubricant

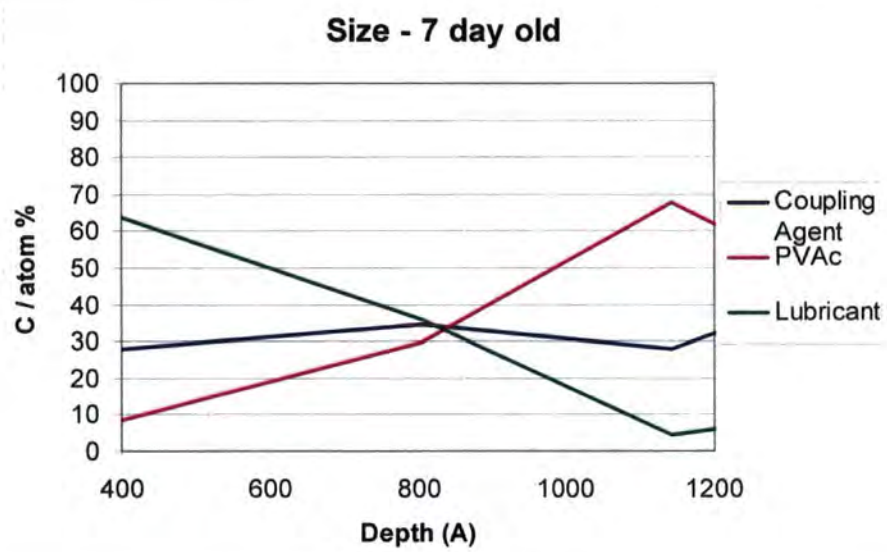
Size - 7 day old
C / atom %
100
90
80
70
60
50
40
30
20
10
0
400
600
800
1000
1200
Depth (A)
Coupling Agent
PVAc
Lubricant

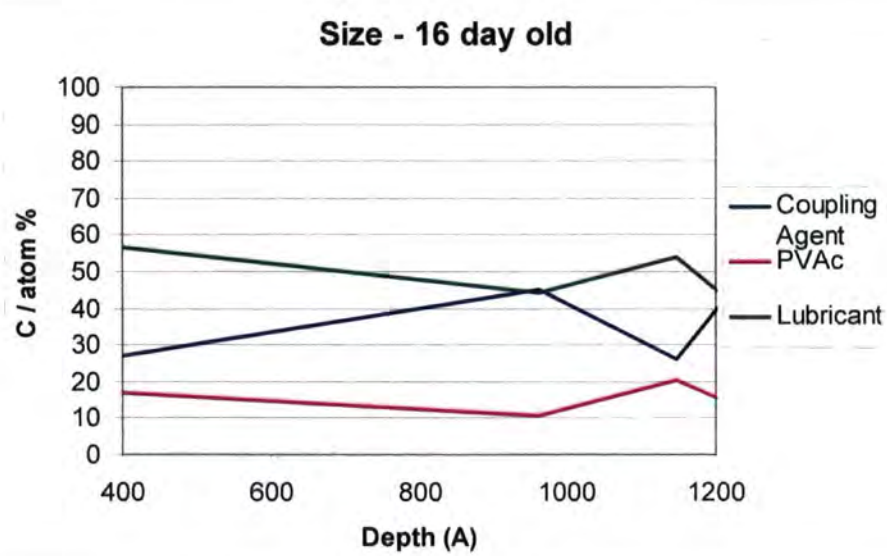
Size - 16 day old
C / atom %
100
90
80
70
60
50
40
30
20
10
0
400
600
800
1000
1200
Depth (A)
Coupling Agent
PVAc
Lubricant

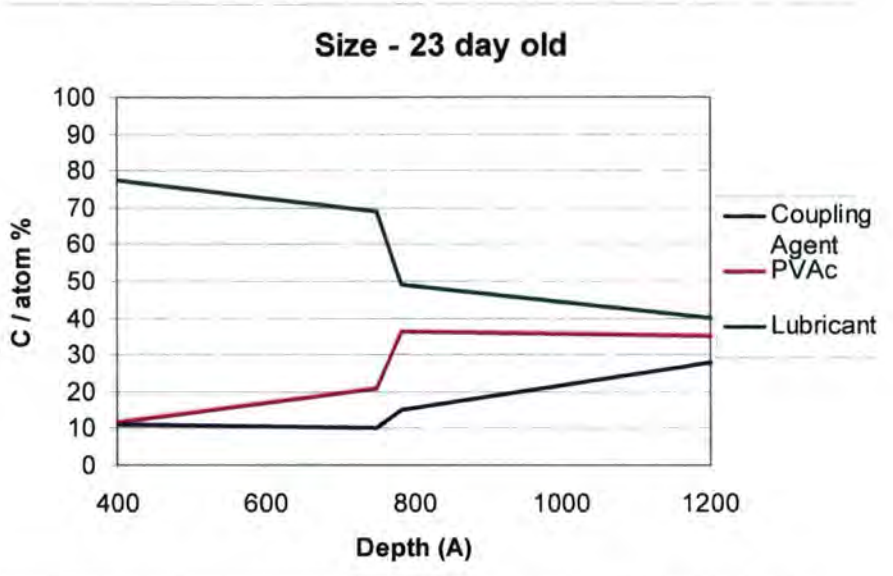

Figure 4.8 – Computer model of depth profile of sizes produced of differing ages

Depth profiles of the size film were investigated at various ages between 1 and 23 days. The resulting profiles show that a general trend can be observed, similar to that already found in section 4.3, where a large amount of lubricant is found at the air interface of the film which reduces at increasing depths. The age of the film does not seem to produce any marked deviations from this trend, although some anomalies do arise mainly in relation to the thickness of the lubricant band. This is most likely due to different areas of the film being investigated for each analysis. Different areas of sample are required due to the high energy of the beam which degrades the sample. Repeated investigation of the same area would produce a varying depth profile, due to the area being investigated being degraded repeatedly, producing inaccurate profiles. Any variations in the profile of the film over the whole range of investigation most likely occur due to the non-uniform nature of the migration occurring within the film.

4.5 Conclusions

It has been deduced that a definite layered structure of the size can be observed for glass sizes produced using the standard formulation. Due to the chemistry occurring within the size during film formation, it can be hypothesised that migration of the coupling agent and lubricant would be expected for sizes made from any formulation. A schematic diagram of the standard model for the glass fibre size using the results obtained from this investigation is shown below.

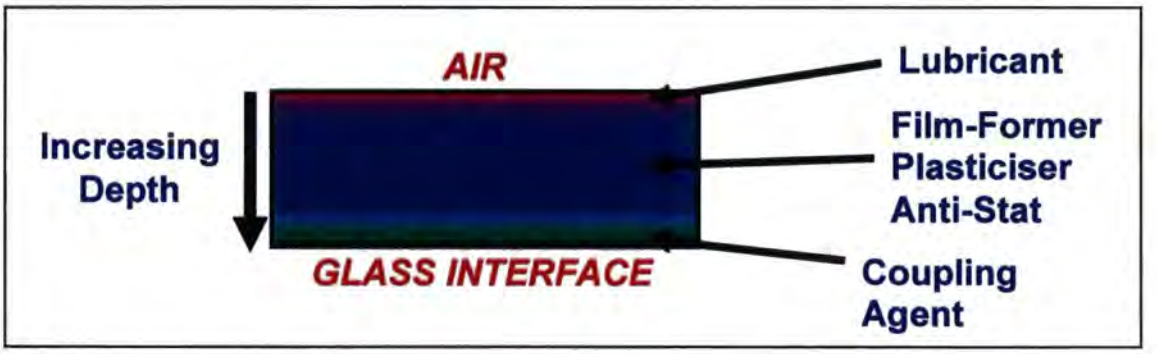

Figure 4.9 – Schematic diagram of the standard model of a glass fibre size

This model illustrates the locations of all of the components present in the formulation used in this investigation. For all formulations it is expected that a similar trend should occur with the coupling agent migrating to the glass interface of the film and the lubricant migrating to the air interface. It should be noted that, although a significant amount of both components migrate, there is also presence of both throughout the bulk of the film.

It has also been shown that migration of the size components does not continue beyond the film formation process and that the age of the size film does not have an effect on the structure.

Chapter 5

Results

Size Performance : Film-Former Effects

5.1 Introduction

Following on from investigative work in the previous chapter based on the standard formulation as discussed in section 3.2.3. it was decided that alterations would be made to the film-former formulation in an attempt to produce physical differences in the PVAc polymer. By varying the amount of first stage monomer and initiator concentration added to the reaction it is known that the particle size and molecular weight will increase respectively. [13] The sizes produced will then be tested in the areas of film formation, wetting, clarity and strength to determine whether the varying physical properties produce any trends in the sizes.

5.2 Film-Former Variations

Batches of the film-formers were created by varying the standard formulation as described in section 3.2.3. Both the initiator concentration and the first stage monomer were altered from the original formulation (size 1) to create film-formers and hence sizes which have different physical properties.

Table 5.1 – Film-former formulation differences (concentrations in %)

Size #	1st Stage Monomer Concentration	Initiator Concentration
1	5	100
2	0	100
3	15	100
4	5	12.5
5	5	25
6	5	50
7	5	150
8	15	25

Analysis was undertaken to determine the exact physical properties of the film-formers created. This should determine whether any link is present between the first stage monomer concentration and the polymers particle size as postulated in the literature.[13] Likewise the existence of any link between the initiator concentration and the polymers molecular weight will also be determined.

5.2.1 Molecular Weight

Gel permeation chromatography (GPC) was used to determine the molecular weight of the PVAc present in each of the film-formers created as stated above. An example of the trace obtained from the GPC instrument is shown below in figure 5.1.

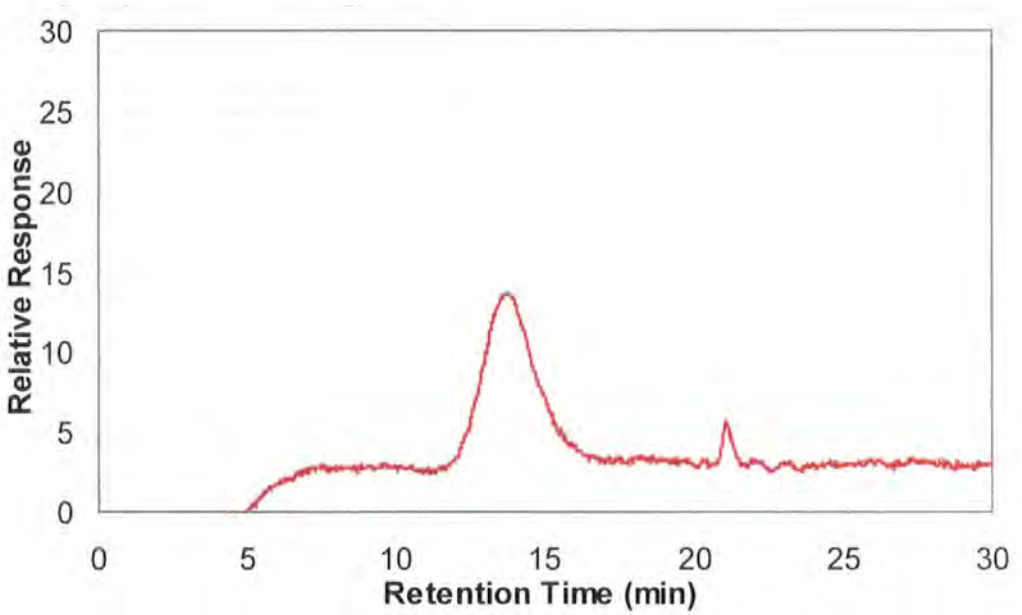

Figure 5.1 – GPC trace of Size 1 using the refractive index detector.

The results obtained correspond to the weight average molecular weight calculated from the initial peak at the lower retention time circa 13 minutes. The smaller peak circa 21 minutes which corresponds to a lower molecular weight most likely arises from the stabilising species used to maintain the polymerisation reaction. The testing of each film-former was repeated three times to ensure accurate results and the error bars reflect the standard deviation of the results.

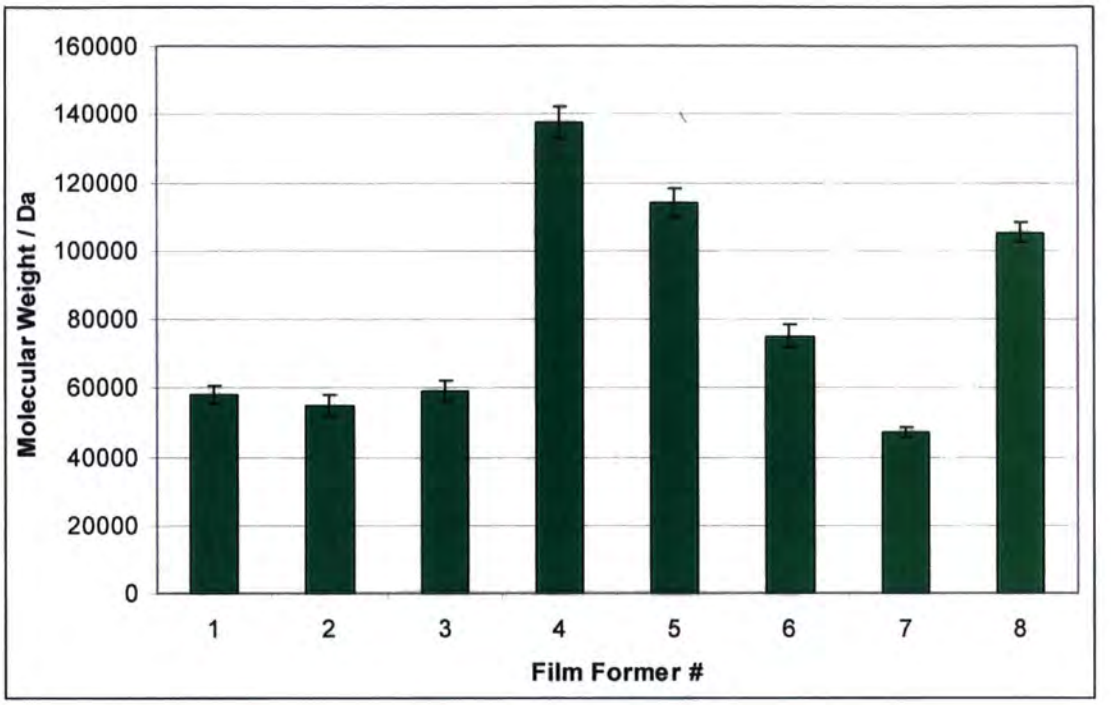

Figure 5.2 – Weight average molecular weight of the film-formers.

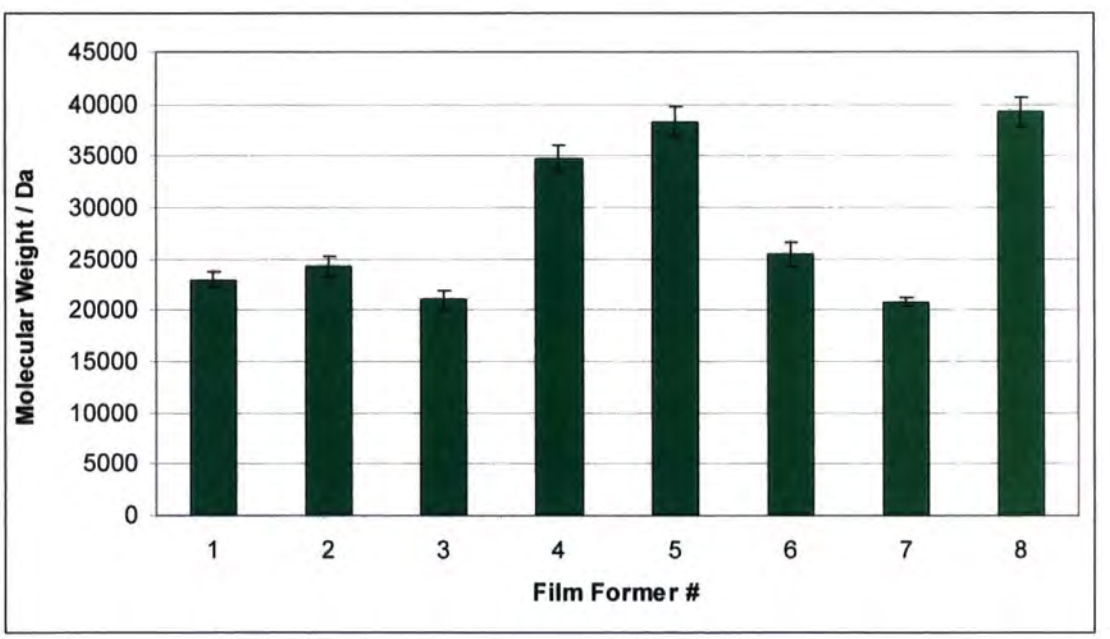

Figure 5.3 – Number average molecular weight of the film-formers.

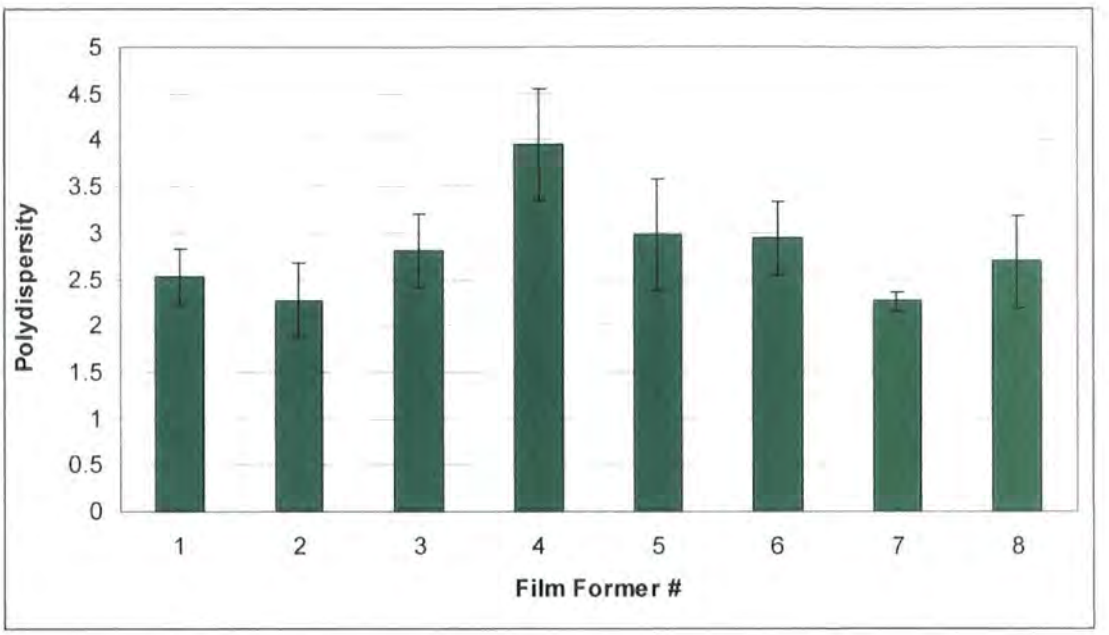

Figure 5.4 – Polydispersity of the film-formers.

It can be observed that the film-formers with the greatest weight average molecular weight correspond to batches 4, 5 & 6. These were produced using a lower initiator concentration than usual and it was found that the lowest initiator concentration produces the greatest molecular weight.

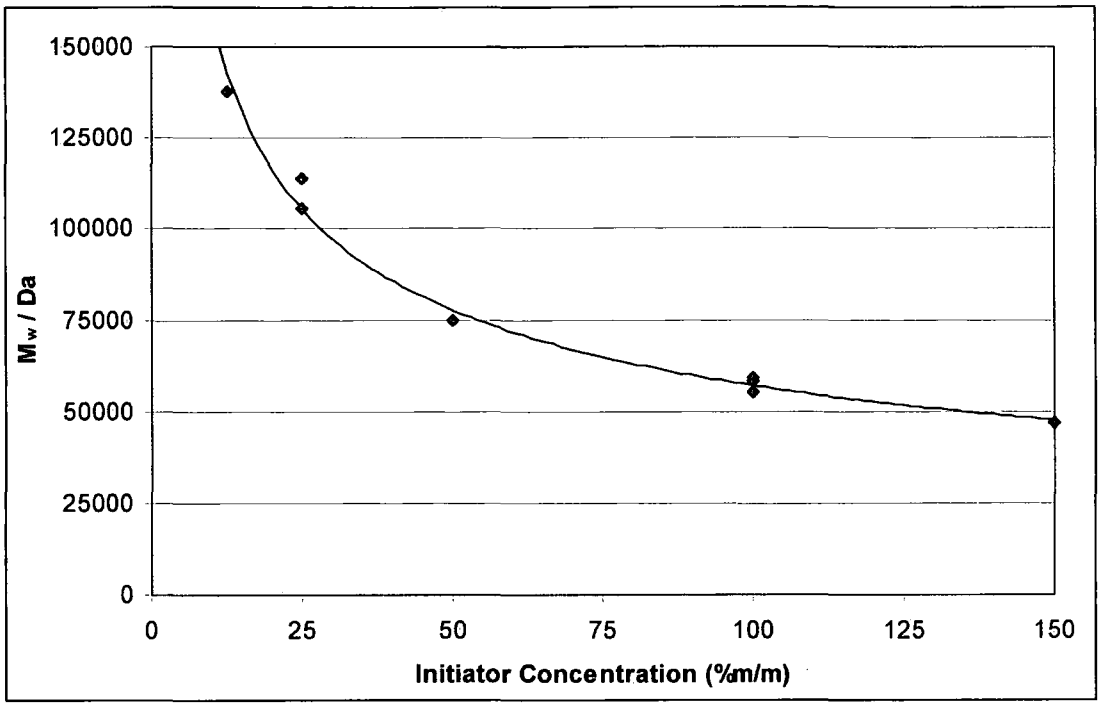

Figure 5.5 – Molecular weight against initiator concentration for PVAc emulsions

Figure 5.5 shows the direct correlation between the molecular weight and the initiator concentration. It is clearly observed that a definite relationship exists between the two confirming what was predicted.[13]

The amount of first stage monomer present in the formulation appears to have no effect due to all molecular weights being similar. The one exception to this is the film-former which also contained a large concentration of first stage monomer as well as a low amount of initiator (sample 8). Due to what we already have learnt regarding the molecular weight it is likely that this arises due to the initiator concentration alone.

Due to the nature of emulsion polymerisations it is known that controlled low molecular weight species can be synthesised with a high accuracy. Relatively low molecular weight species are obtained due to chain transfer occurring between the monomer and the growing polymer chain.[2]

This is a commonly known occurrence for vinyl acetate monomers whereby the chain transfer predominantly occurs on the acetate methyl side chain rather than on the main backbone of the polymer.

5.2.2 Particle Size Distribution

As described previously film-formers were created using the standard formulation although the quantity of first stage monomer in the reaction was altered to create a range of polymer particle sizes.

Two methods of particle size determination were readily available and both were implemented to increase the accuracy of the results obtained.

5.2.2.1 Photon Correlation Spectroscopy

The first method used to determine the particle size was photon correlation spectroscopy. The error bars on the graph in figure 5.7 represent the standard deviation of the distribution for each variation of film-former.

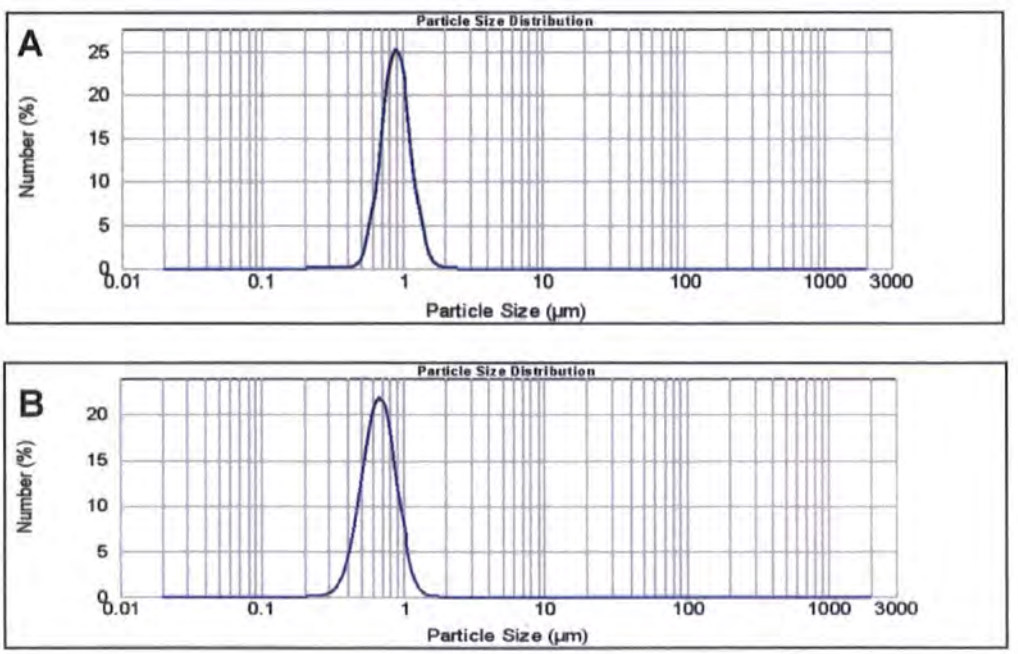

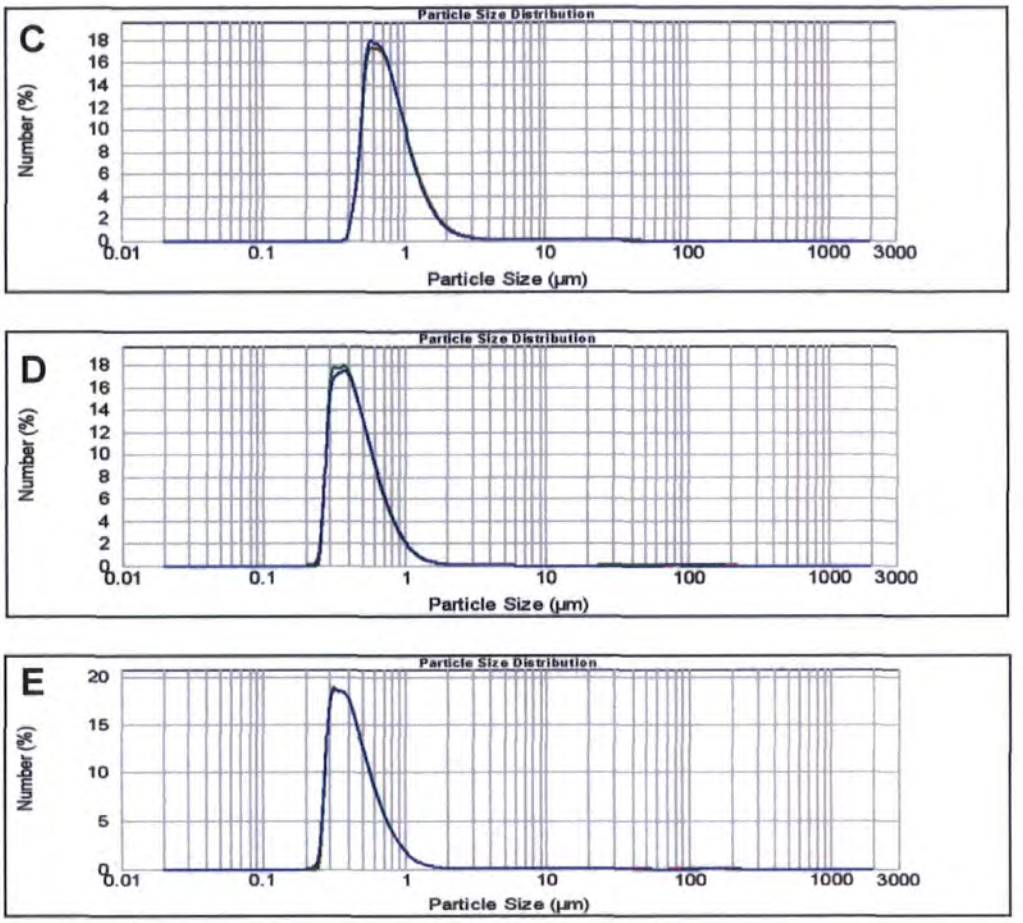

Figure 5.6 – Photon Correlation Spectra for the variation of film-formers

Spectra A = Batch 4; B = Batch 3; C = Batch 8; D = Batch 1; E = Batch 2

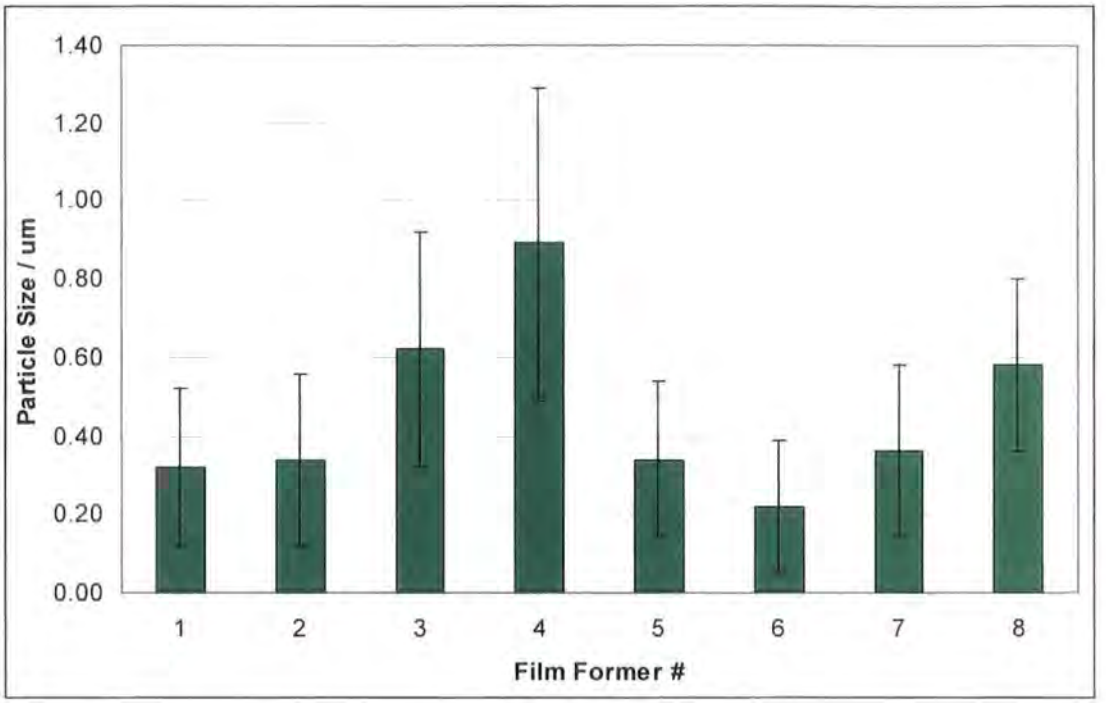

Figure 5.7 – Particle size of the different film-formers calculated by photon correlation spectroscopy

It can be observed that the amount of first stage monomer added to the polymerisation reaction will have an effect on the particle size of the film-former. Batch 3 which had the largest amount of first stage monomer (15%) has a much greater particle size than batch 1 (5%) which also has a greater particle size than batch 2 (0%).

However, it appears that the first stage monomer is not the only physical property responsible for an increase in the particle size batch 4, which has the lowest concentration of initiator, yields the largest particle size. Due to the large difference between the particle size it could be postulated that a very low concentration of initiator has a greater effect on the particle size than an increase of the first stage monomer content.

5.2.2.2 Measurement by Scanning Electron Microscopy

Values obtained for the particle size of each of the batches of film-former were also determined using scanning electron microscopy (SEM). A droplet of each of the film-formers were fast-dried *in vacuo* within the SEM chamber and then viewed. Due to the speed of drying the individual latex particles were unable to coalesce to form a continuous film, hence the individual particles could be observed and their diameters to be measured. An average diameter of each batch was determined using not less than 14 individual measurements per calculation, the error bars represent the standard deviation of the diameters.

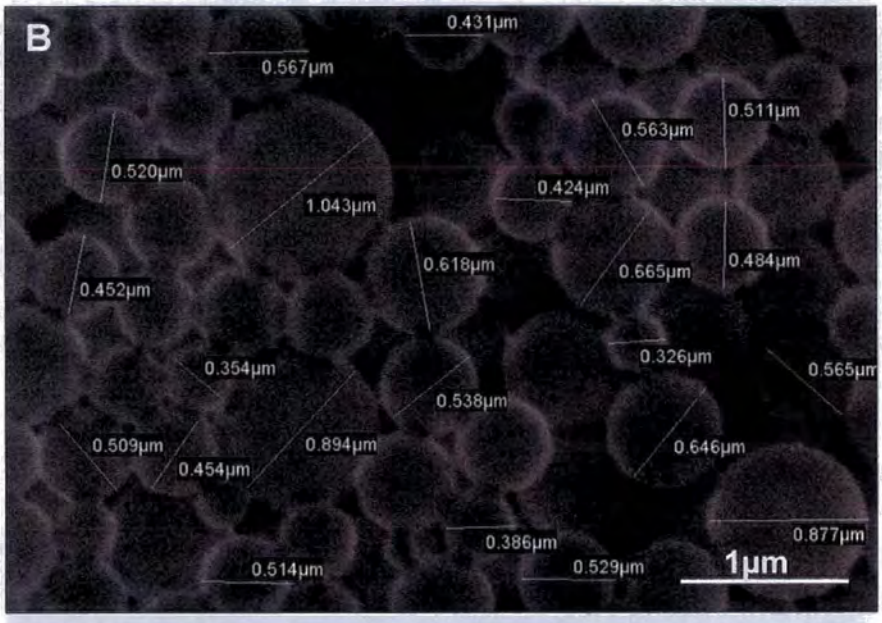
B
0.431µm
0.567µm
0.511µm
0.563µm
0.520µm
0.424µm
1.043µm
0.618µm
0.665µm
0.484µm
0.452µm
0.326µm
0.565µm
0.354µm
0.538µm
0.509µm
0.894µm
0.646µm
0.454µm
0.877µm
0.386µm
0.514µm
0.529µm
1µm

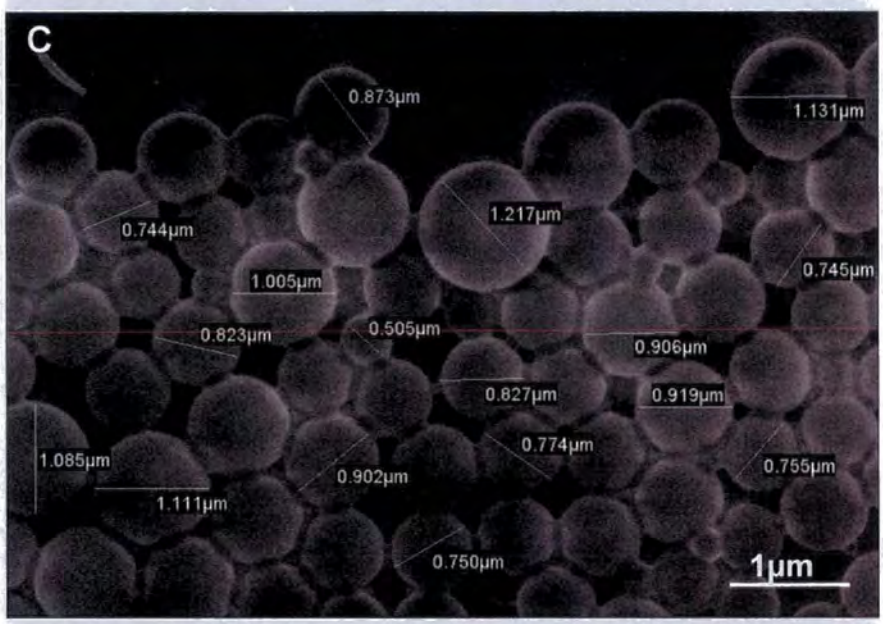
C
0.873µm
1.131µm
1.217µm
0.744µm
0.745µm
1.005µm
0.823µm
0.505µm
0.906µm
0.827µm
0.919µm
0.774µm
1.085µm
0.755µm
0.902µm
1.111µm
0.750µm
1µm

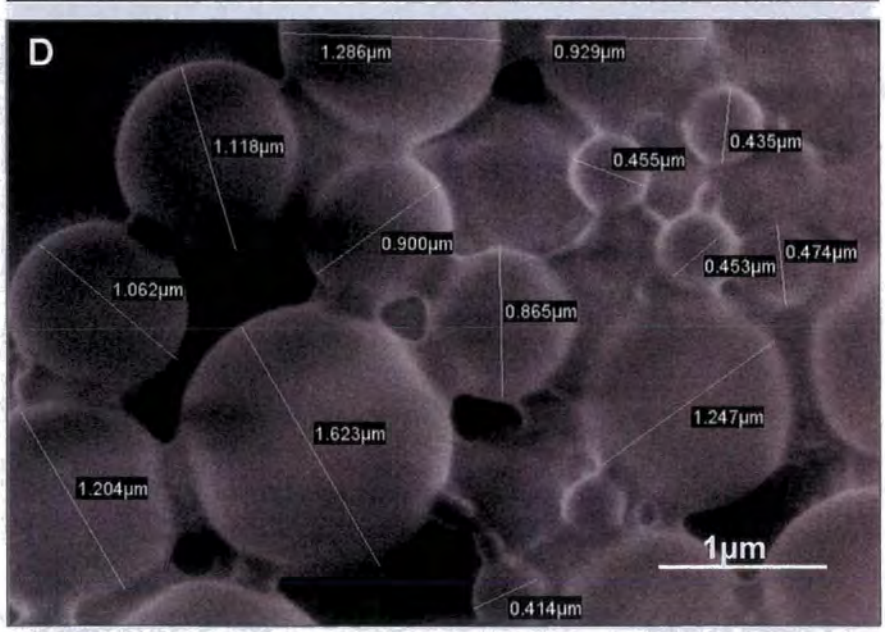
D
1.286µm
0.929µm
1.118µm
0.435µm
0.455µm
0.900µm
0.474µm
0.453µm
1.062µm
0.865µm
1.247µm
1.623µm
1.204µm
1µm
0.414µm

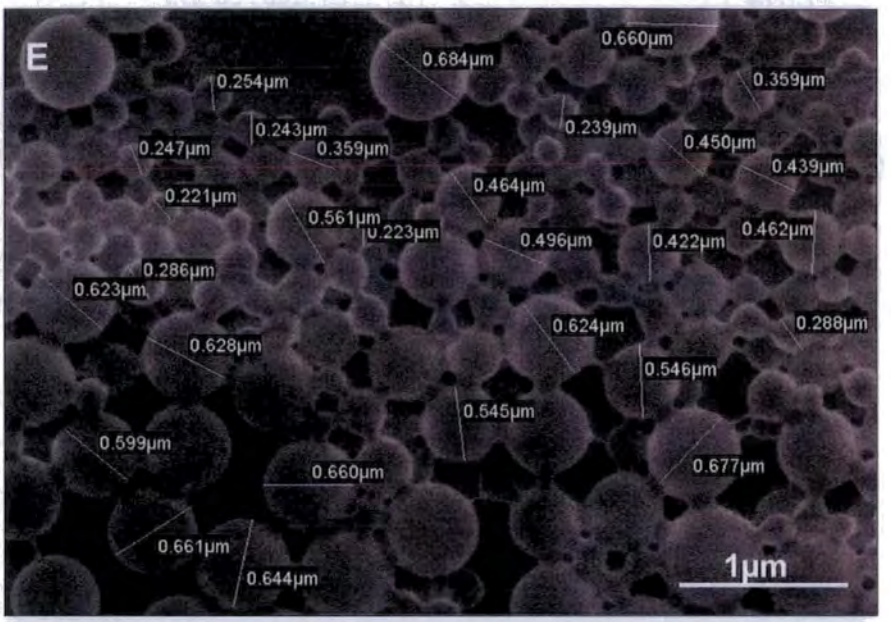
E
0.660μm
0.684μm
0.254μm
0.359μm
0.243μm
0.239μm
0.247μm
0.359μm
0.450μm
0.439μm
0.464μm
0.221μm
0.561μm
0.223μm
0.496μm
0.422μm
0.462μm
0.286μm
0.623μm
0.624μm
0.288μm
0.628μm
0.546μm
0.545μm
0.599μm
0.677μm
0.660μm
0.661μm
0.644μm
1μm

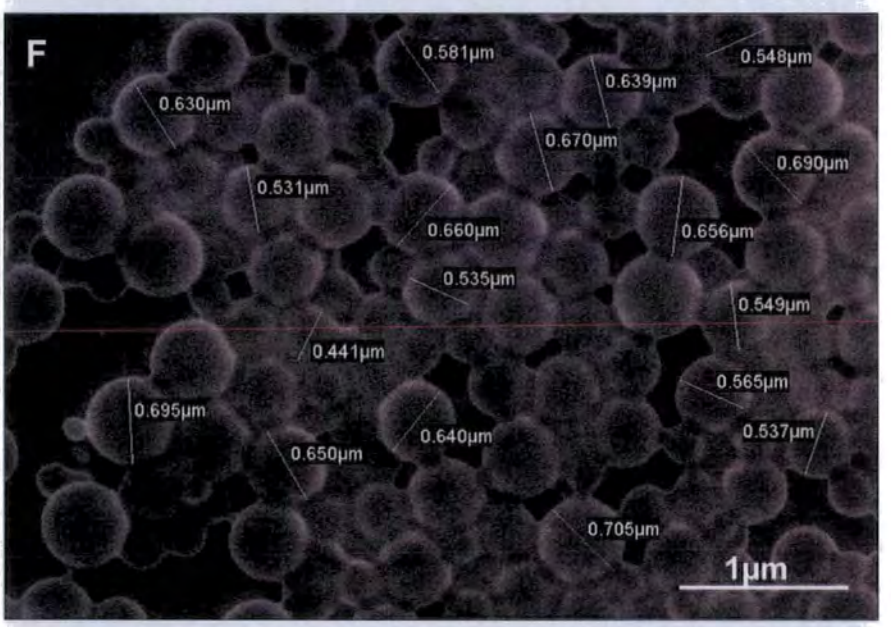
F
0.581μm
0.548μm
0.639μm
0.630μm
0.670μm
0.690μm
0.531μm
0.660μm
0.656μm
0.535μm
0.549μm
0.441μm
0.565μm
0.695μm
0.640μm
0.537μm
0.650μm
0.705μm
1μm

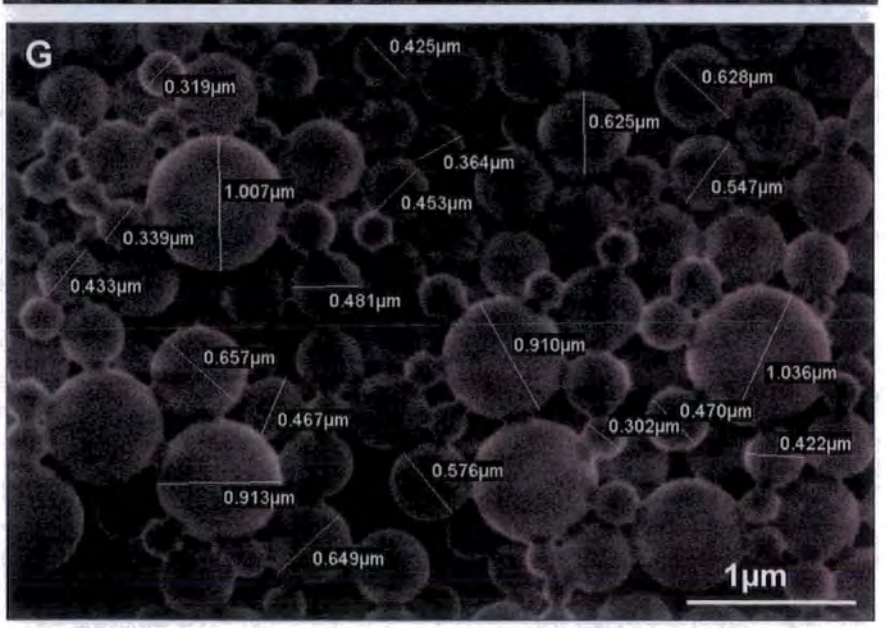
G
0.425μm
0.319μm
0.628μm
0.625μm
0.364μm
1.007μm
0.547μm
0.453μm
0.339μm
0.433μm
0.481μm
0.910μm
0.657μm
1.036μm
0.470μm
0.467μm
0.302μm
0.422μm
0.576μm
0.913μm
0.649μm
1μm

Figure 5.8 – SEM images of the different film-formers including the diameters of a selection of the latex particles.

Image A = Batch 1; B = Batch 2; C = Batch 3; D = Batch 4; E = Batch 5; F = Batch 6; G = Batch 7; H = Batch 8

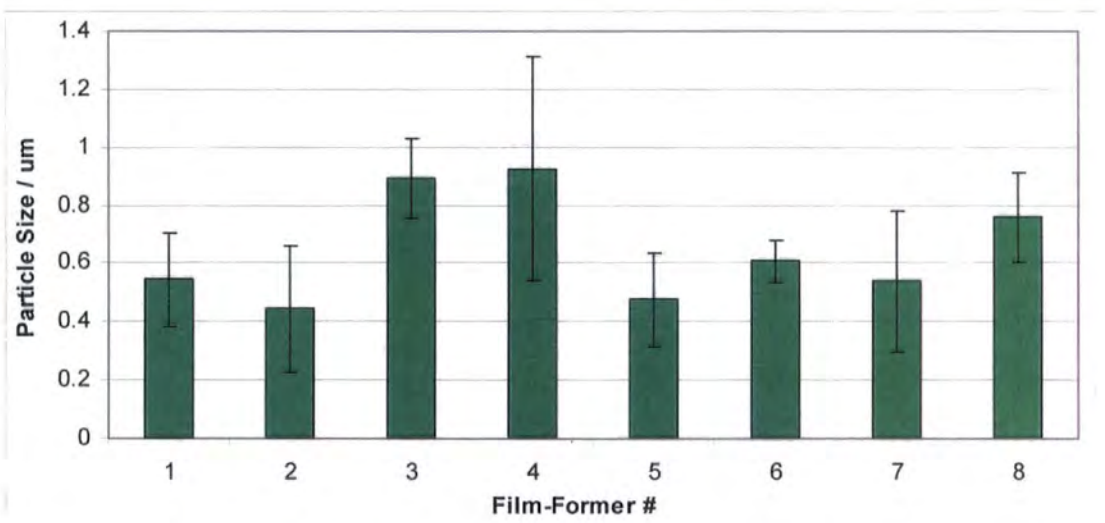

Figure 5.9 – Particle size of the different film-formers calculated by diameter determination via SEM imaging.

Similar results are obtained to those previously described in section 5.2.2.1. Batches 1, 2 & 3 again follow a similar trend within experimental error whereby the particle size is proportional to the first stage monomer concentration used in the polymerisation. Batch 4 also produces the largest particle size which is the same as determined using the photon correlation technique.

Generally the values obtained using this technique are about 50% larger than those obtained using photon correlation spectroscopy due to flattening of the particles. The particles are packed together into a flat, two-dimensional morphology due to evaporation of the water present in the film-former solution. This compresses the spherical particles making them appear wider than those observed previously.

5.3 Film Formation

The mechanism of latex film formation has been discussed previously in section 1.5.2 and it was stated that four individual stages occur. By using scanning electron microscopy it was possible to capture images of the drying of films of our sizes. Films on glass slides were created at staggered time intervals to produce a range of images which illustrate the different stages of drying of the sizes. This was undertaken to determine whether the standard mechanism of latex film formation occurs for all variations of film-former as described in section 5.2.

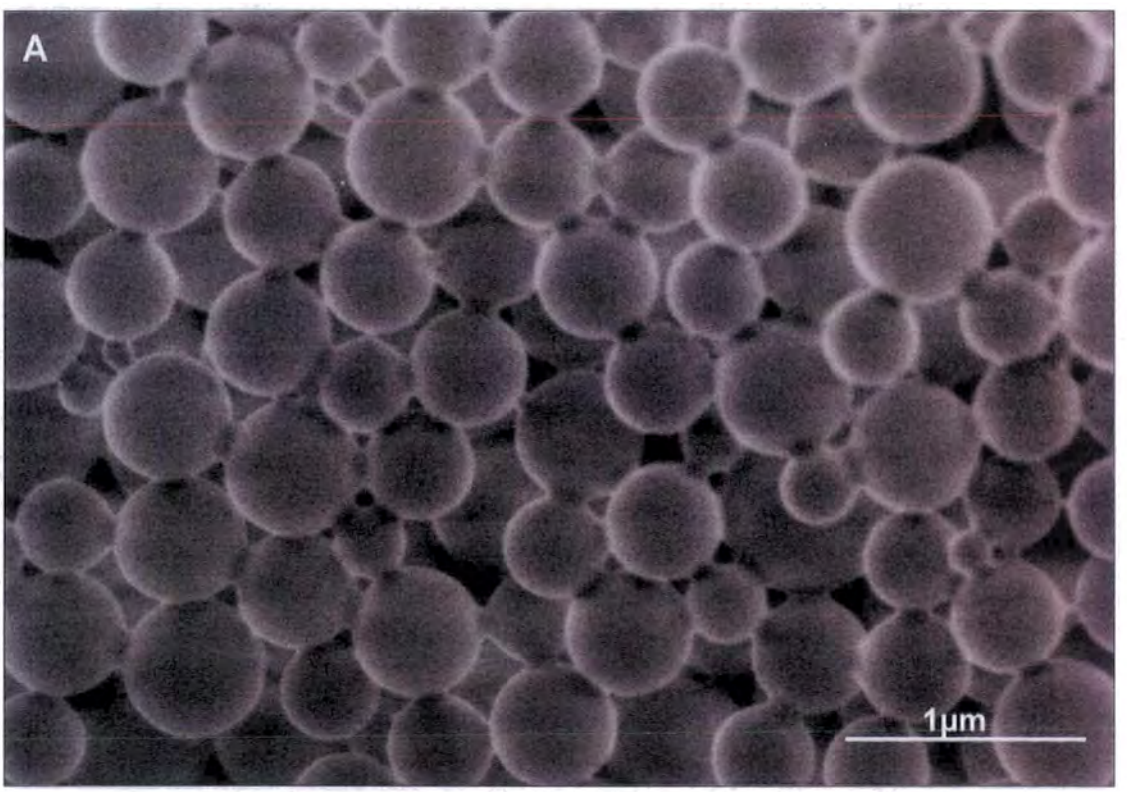

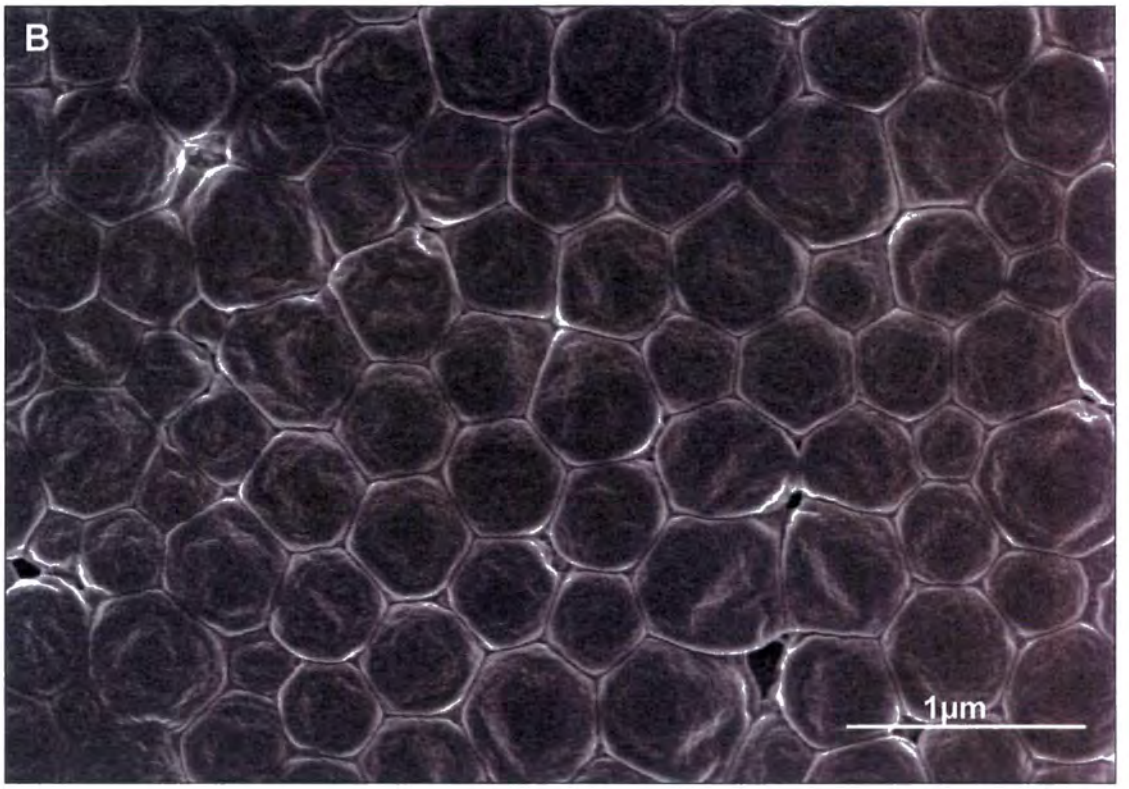
B
1µm

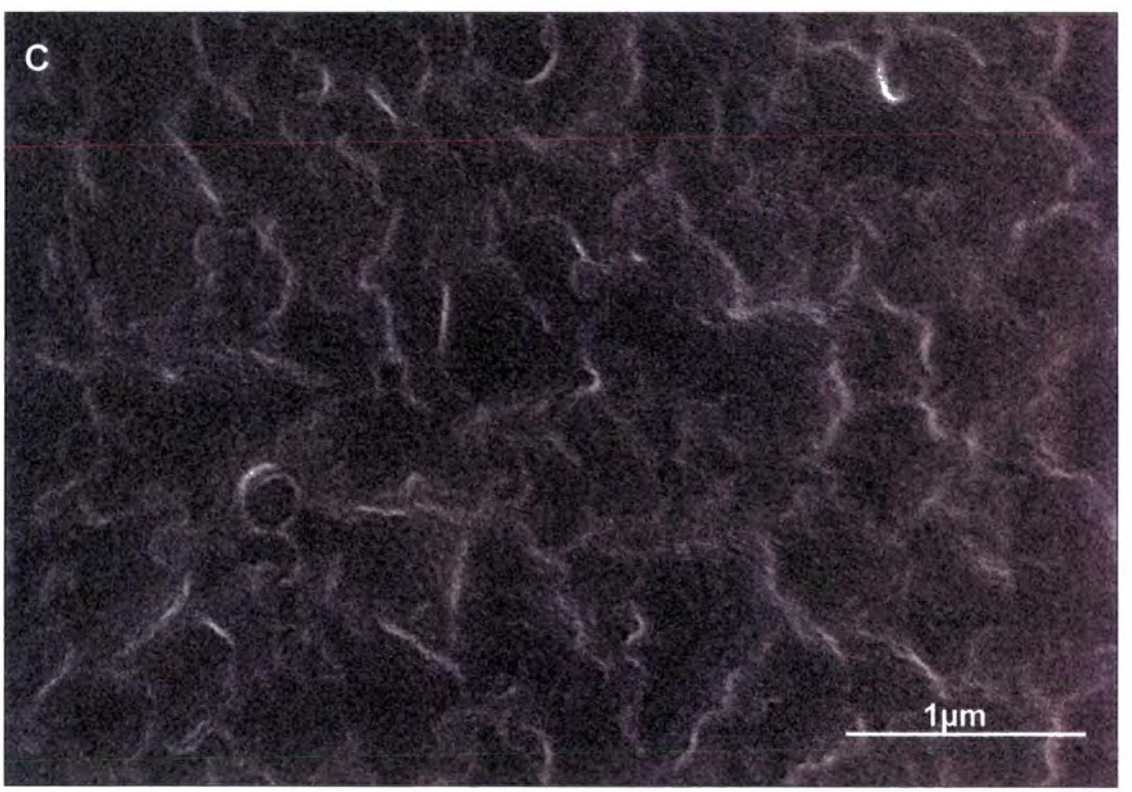
C
1µm

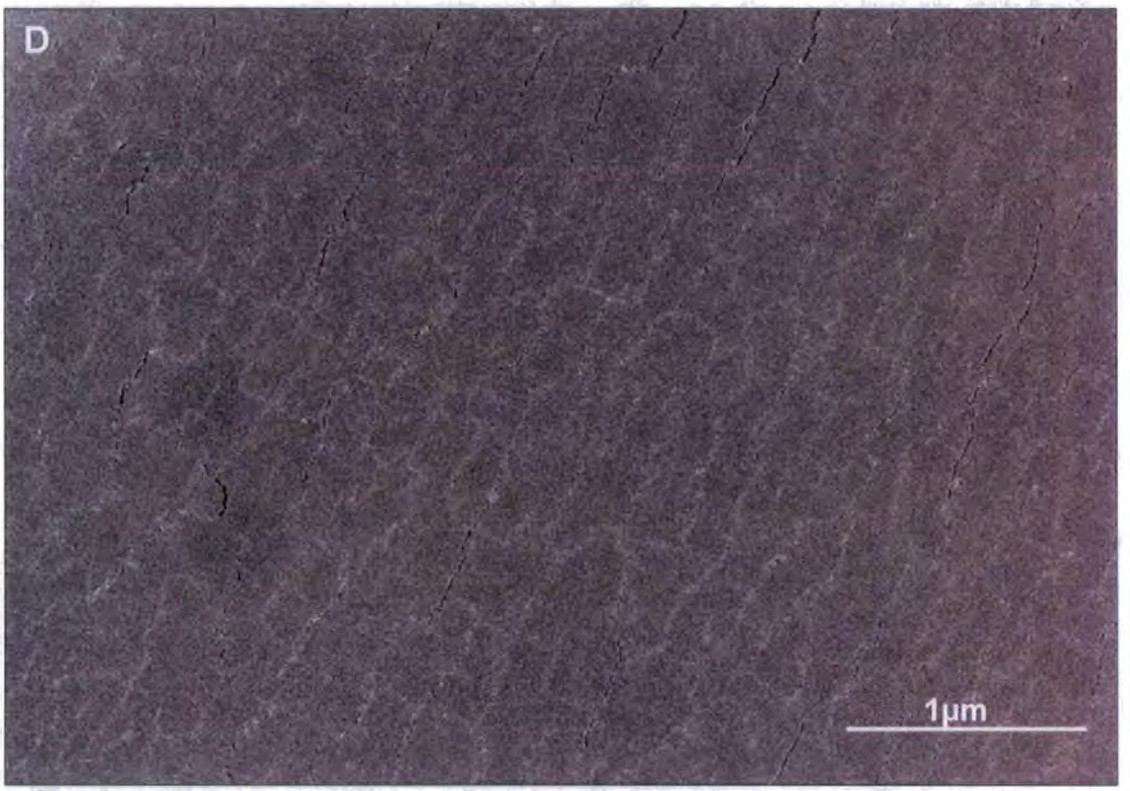

Figure 5.10 - Images of the structure of size 1 at different stages of film formation, undertaken at temperature of 70°C

Image A = Packing; B = Deformation; C = Interfacial breakage; D = Diffusion

Image A illustrates the individual particles packing together due to water evaporation. It is also observed that neighbouring particles are beginning to coalesce slightly indicating that minor breakage of the interfacial barriers occurs early in the mechanism. Image B indicates that thorough packing of the latex particles causes deformation producing honeycombing which minimises the free space between the particles. Image C shows a state between a deformed and continuous film where some structure can be observed due to remnants of the interfacial barriers. Image D shows a continuous film which has been formed due to coalescence of the particles. Some structure can still be observed in the film as white lines which arise from

the hydrophilic species present in the film. These originated from the barriers which surrounded the latex particles and they appear to congregate in set regions in the film.

It was observed that all of the variations of the sizes undergo a similar mechanism (i.e. packing, deformation; diffusion) as seen in figure 5.11. However, some of the sizes appear to form more inhomogeneous films than others, more details of the cause and the effects of this phenomenon are reported in the section 5.4.

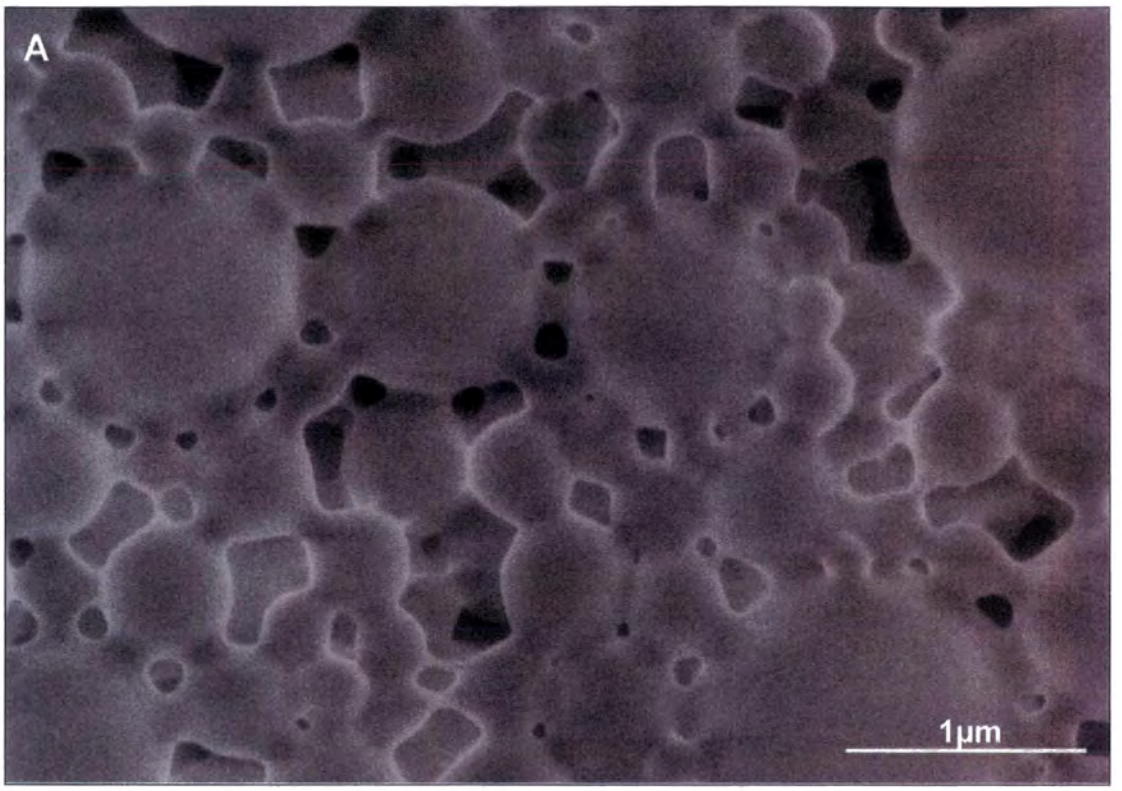
A
1µm


B
1µm

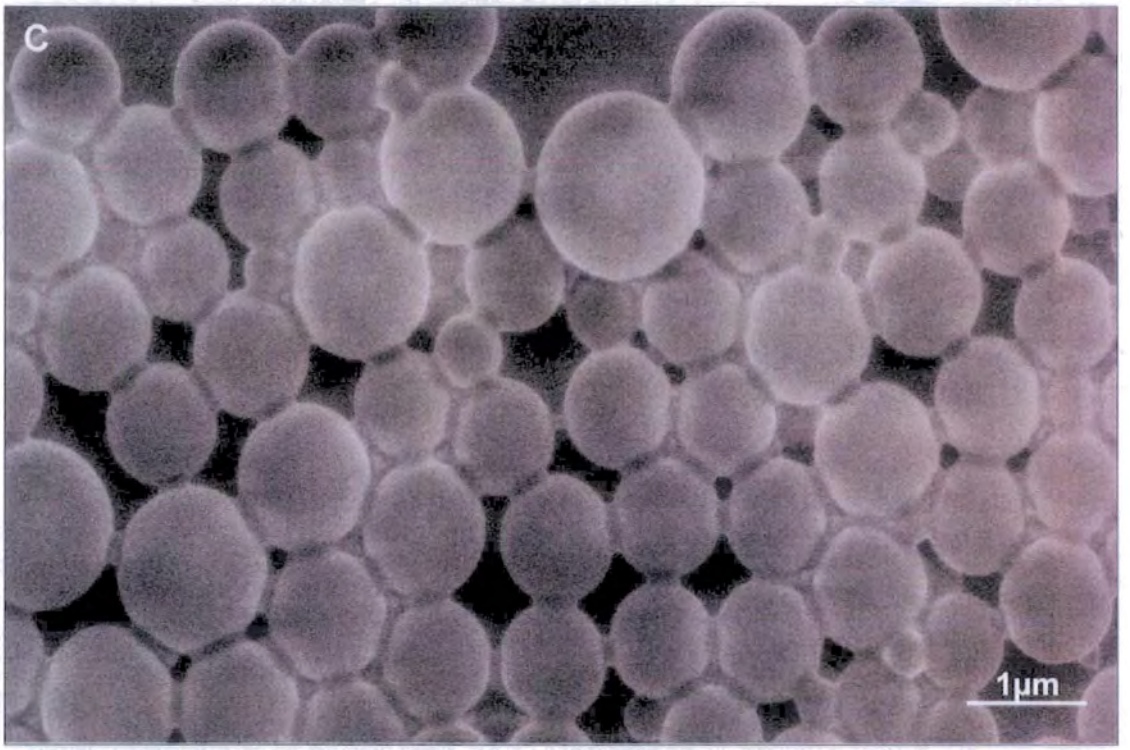
C
1µm


D
2µm

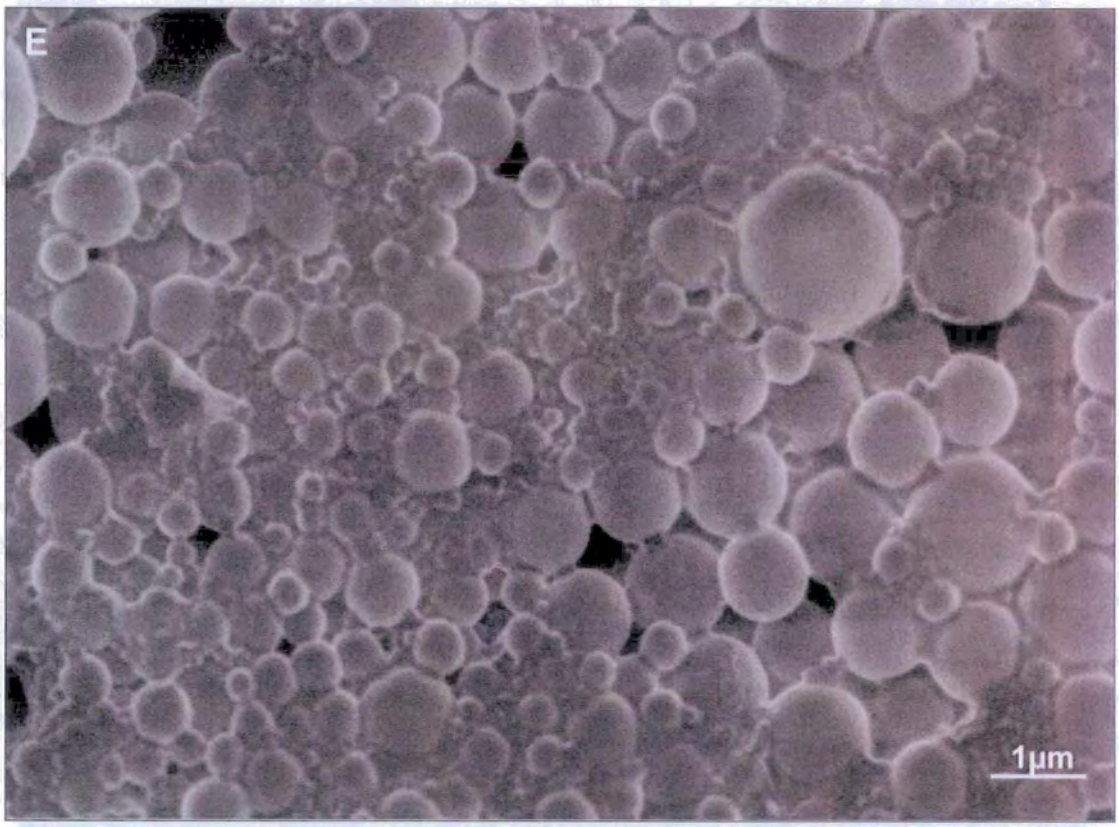
E
1µm

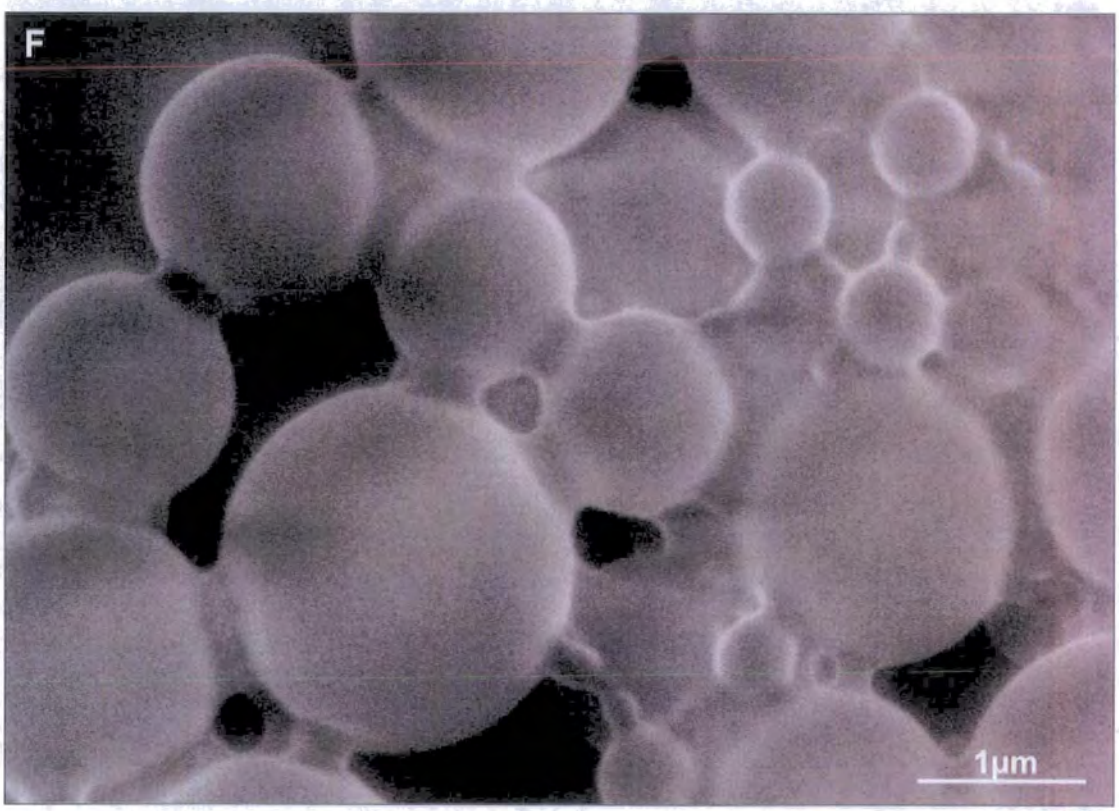
F
1µm

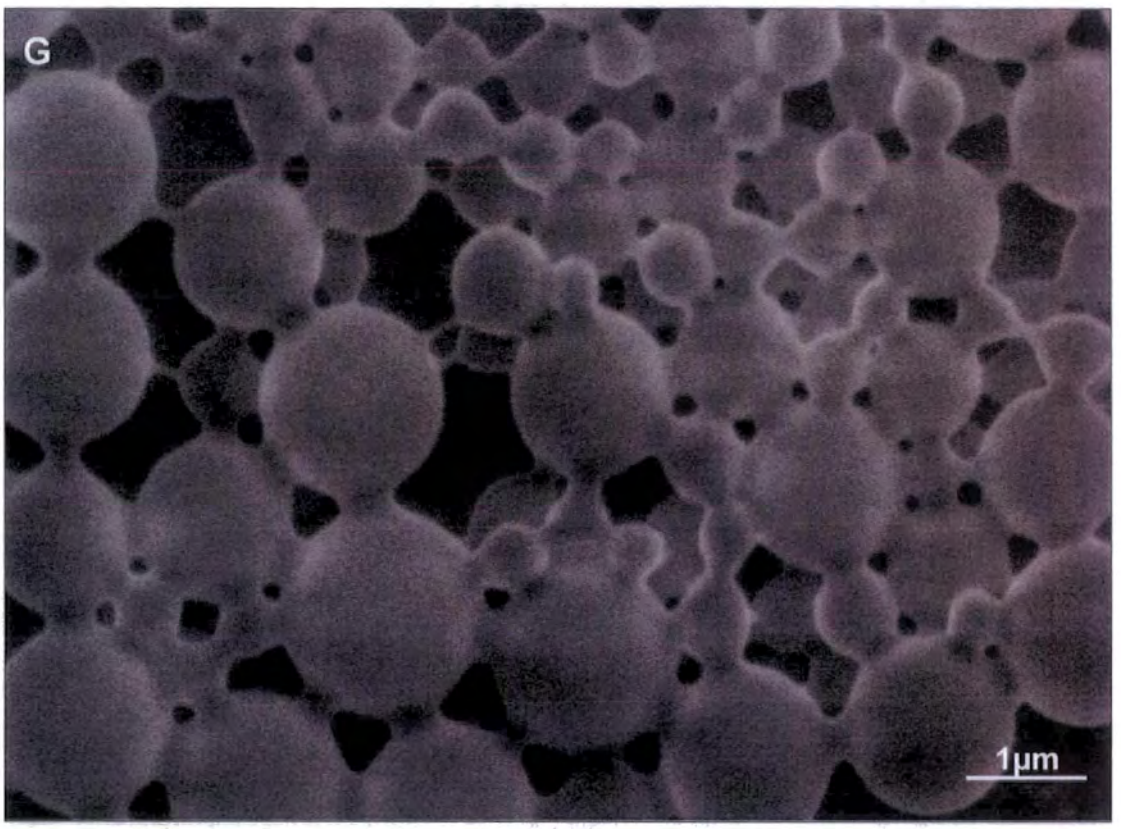
G
1µm

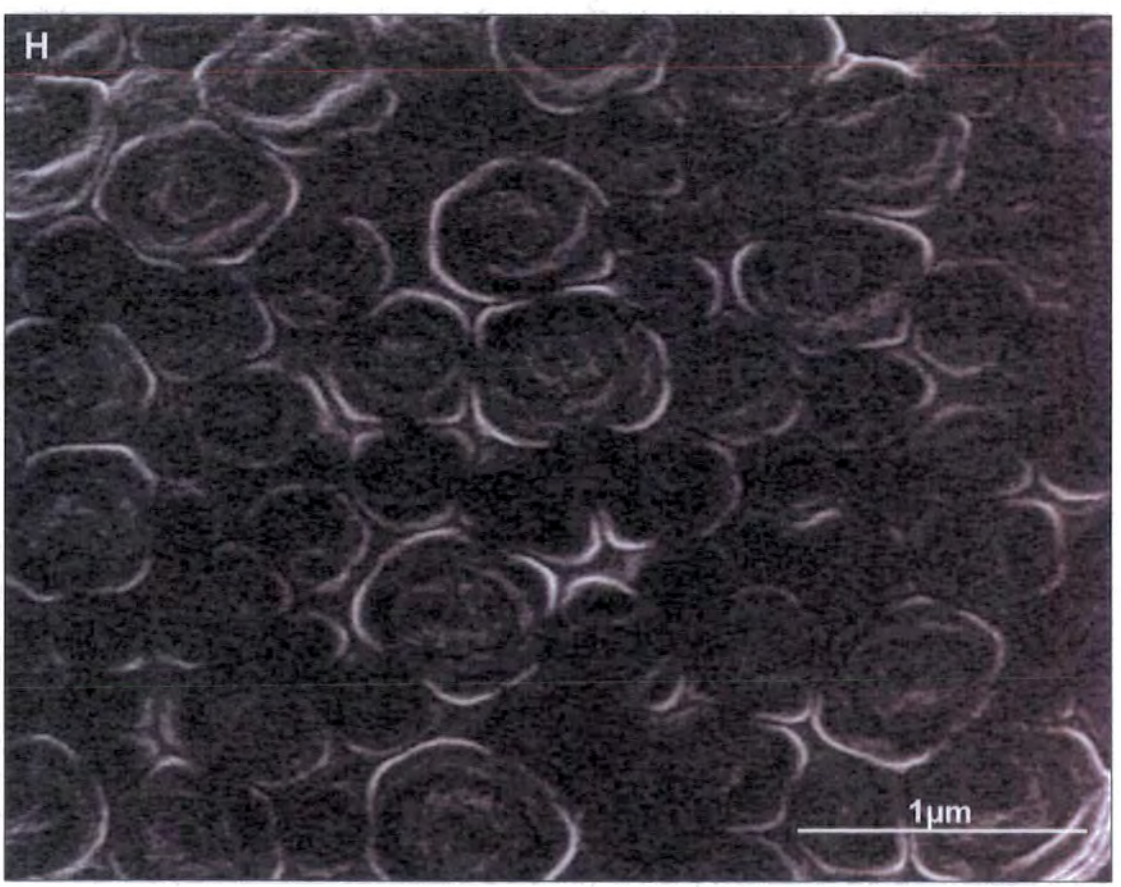
H
1µm

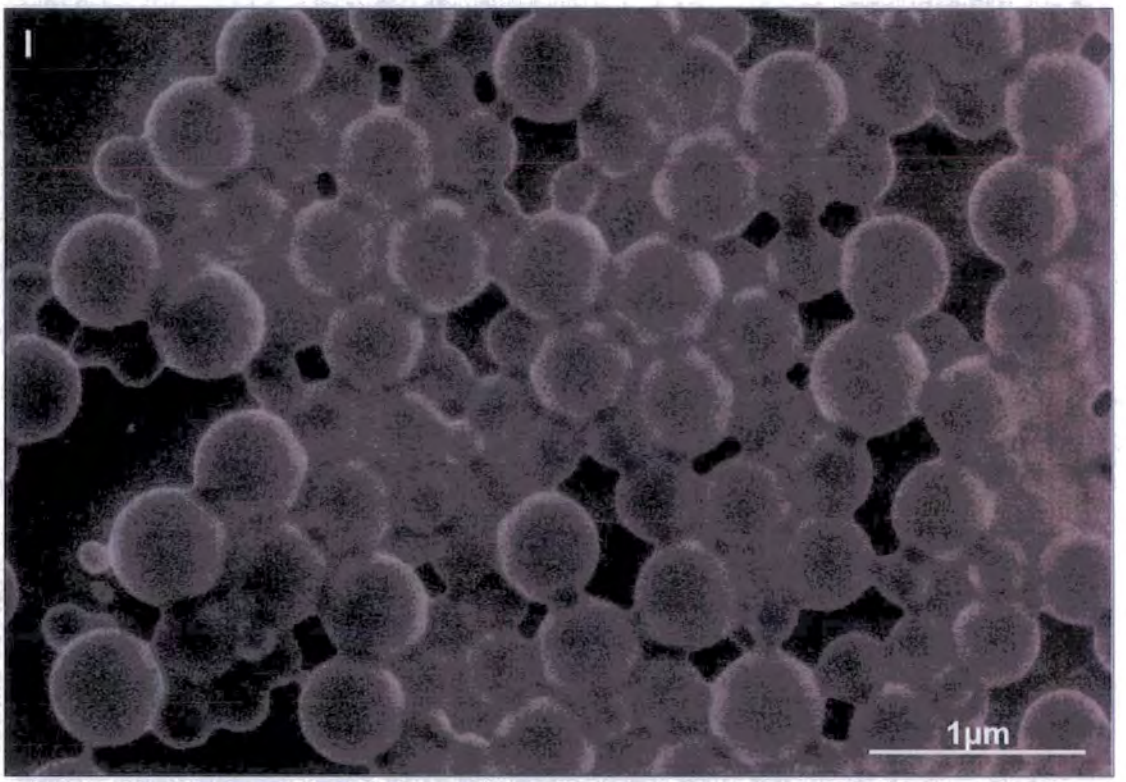
I
1µm

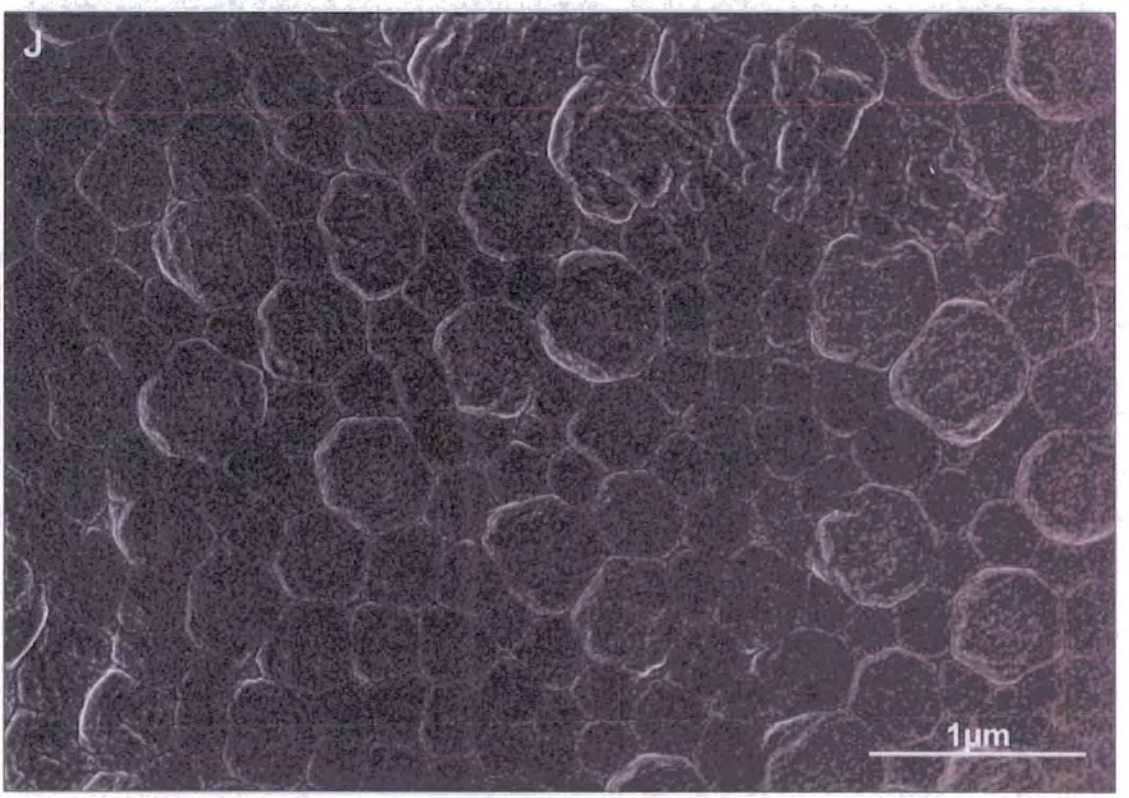
J
1µm

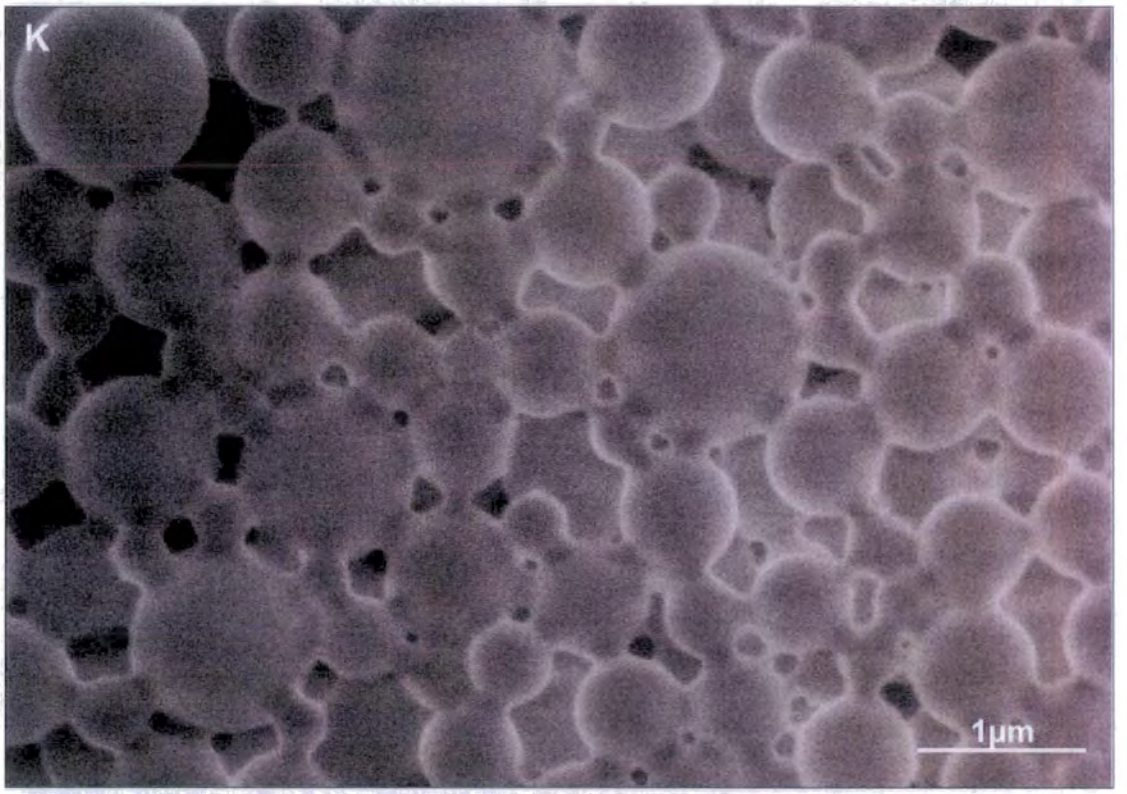
K
1µm

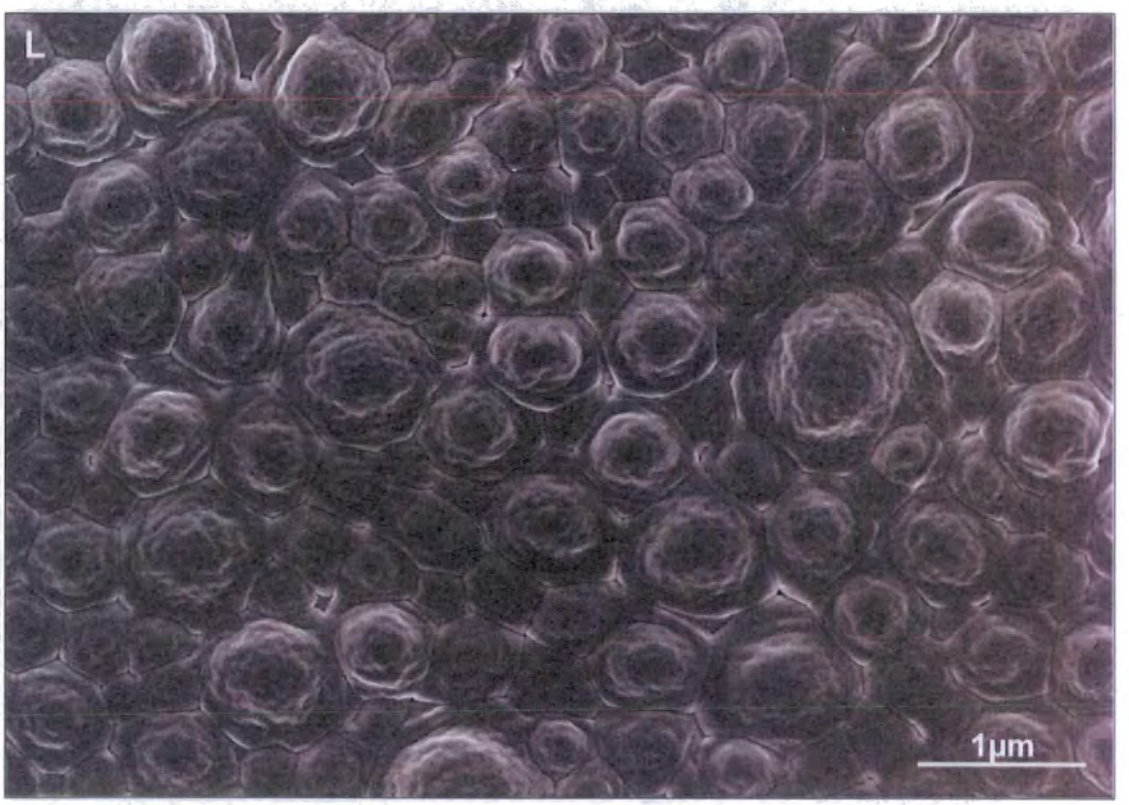
L
1µm

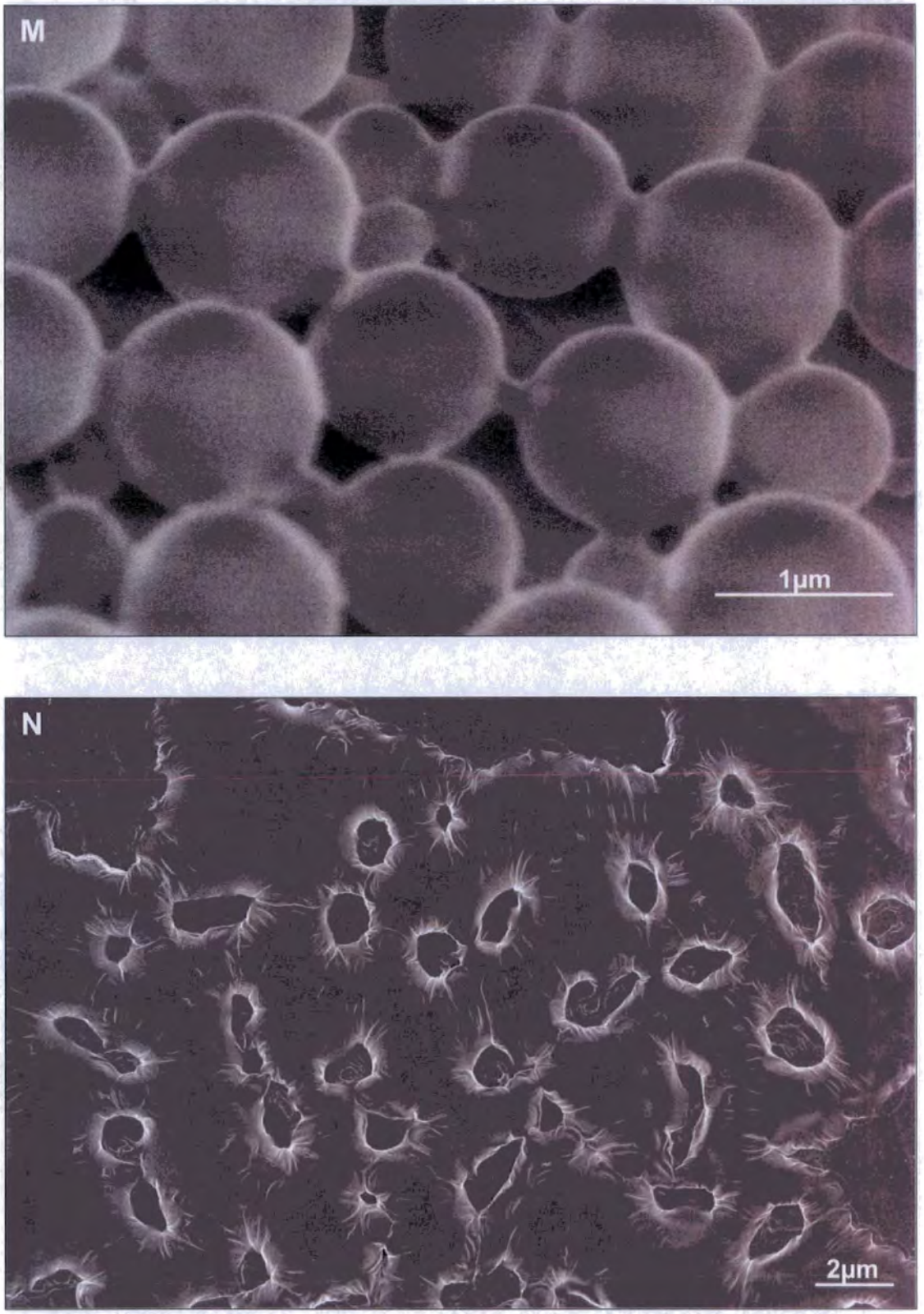

Figure 5.11 – Images of various stages of the film formation process are shown for the remaining seven sizes: Images A & B – Size 2, C & D – Size 3, E & F – Size 4, G & H – Size 5, I & J – Size 6, K & L – Size 7; M & N – Size 8

The speed of drying of the sizes has also been shown to affect the homogeneity of the films produced. The sizes in the images in figures 5.10 and 5.11 were dried at 70°C and produced a continuous film which was found to undergo all stages of the film formation mechanism. However, by drying the samples using the vacuum in the SEM chamber it was possible to stop the size at whatever stage in the mechanism it was at.

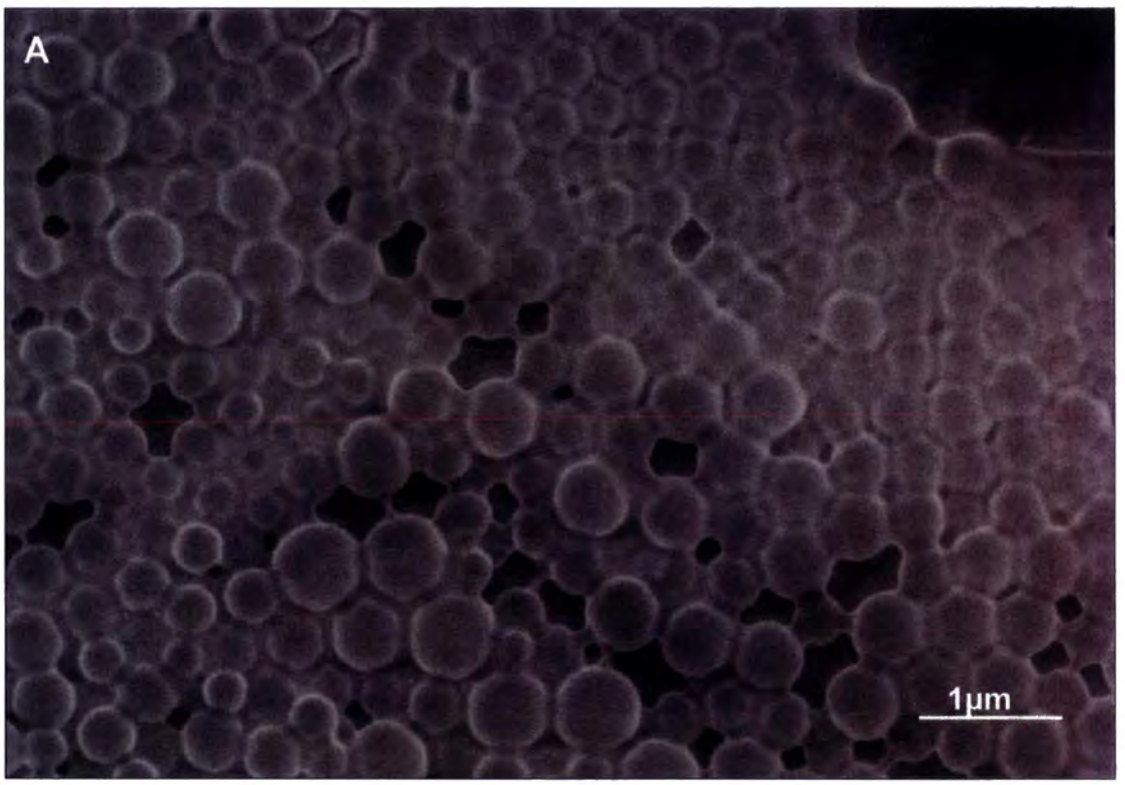

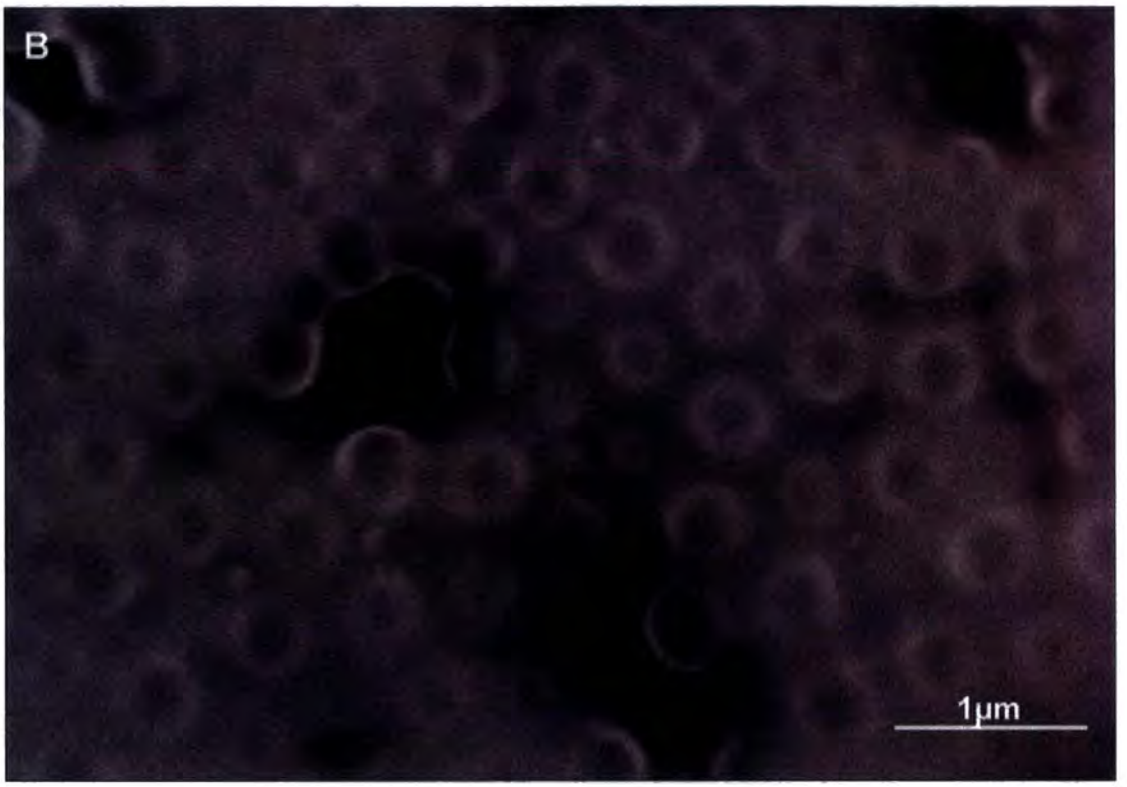

Figure 5.12 – Images of size 1 taken at different stages of drying.

Image A = Vacuum dried immediately after contact with glass;

Image B = Vacuum dried after 60 minutes contact with glass at 70°C.

Figure 5.12 shows images of the size which was dried *in vacuo* immediately following contact with the glass slide (image A) and also one which was allowed to dry for 60 minutes at 70°C prior to drying (image B). It is observed that the size in image B appears to be much more continuous than the size in image A. Image B has a minor amount of particle like nature, however partial diffusion has clearly been initiated. Image A appears to have undergone packing and partial deformation of the particles can be observed, although diffusion does not appear to have been initiated. This indicates that the speed of drying directly affects the homogeneity of the film and also that a fast dried film does not have sufficient time to undergo diffusion.

5.4 Clarity

Absorption spectroscopy was used to determine whether the variations in the size formulation produced an effect on the clarity of the sized fibres. Due to the small and fragile nature of the fibres measurements were instead carried out on flat glass analogues. Any trends present for the sized fibres would be expected to be evident for sized flat glass as it is the coating which will give rise to the effect.

Films were created of the various sizes as described in sections 5.2 & 3.2.4. Visible absorption spectroscopy was used to investigate the clarity of the dried size films.

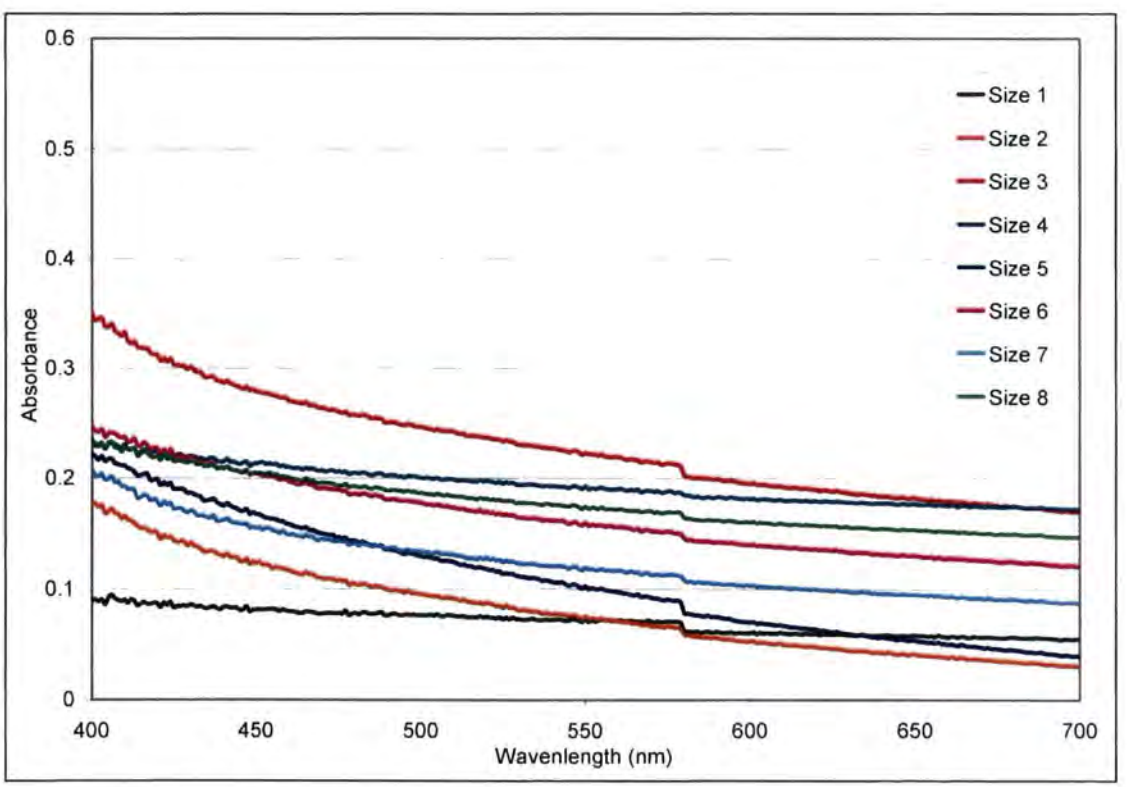

Figure 5.13 – Visible absorption spectra of the different sizes

The absorption spectra of the size alone was determined by calculating the absorbances of the sized glass slide at each wavelength subtracting the absorbances of a bare glass at the corresponding wavelengths.

To produce a value for the clarity of each size a determination of the gradient over the region 400 – 550 nm was undertaken. This region was selected as a distinctive yellowing in the observed colour is observed for the more opaque sizes therefore it is within this region that the majority of the difference in the absorbances should be localised. Each size was repeated three times to ensure accurate results and the standard deviation of the results is expressed in the graph as error bars.

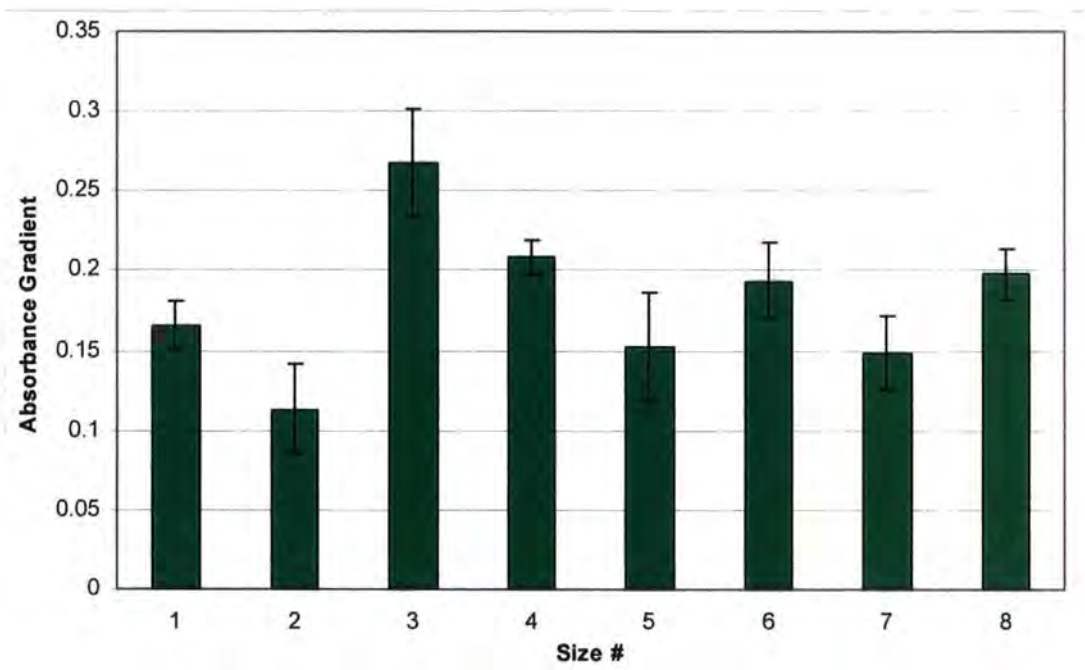

Figure 5.14 – Relative absorption gradients of the different sizes

A trend appears to exist whereby the sizes which produce the largest particles sizes also appear to produce the most opaque sizes. In section 5.2.2 sizes 3, 4 & 8 were shown to have the largest particle sizes and it appears

that these sizes also produce the most opaque films. However, this trend is not directly analogous to that of the particle size as size 4 was found to have the largest particle size and it is size 3 which is the most opaque. This appears to produce a significant amount of error as any variation in the film thickness will cause a change in the absorption of light. All films created had a thickness of 50±5 μm and this 10% variation is the most likely source of error present.

During the initial stages of film formation the latex particles pack together minimising space between particles. This produces stacked particles which will undergo deformation and form a continuous film. However, because larger particles do not pack as compactly as smaller particles voids are created between the particles. These voids promote incomplete breakage of the hydrophilic interfaces leaving the film with remnants of a particle-like structure and hence being inhomogeneous. When light passes through the discontinuous film the interfaces of the particles cause it to be scattered resulting in an opaque film.

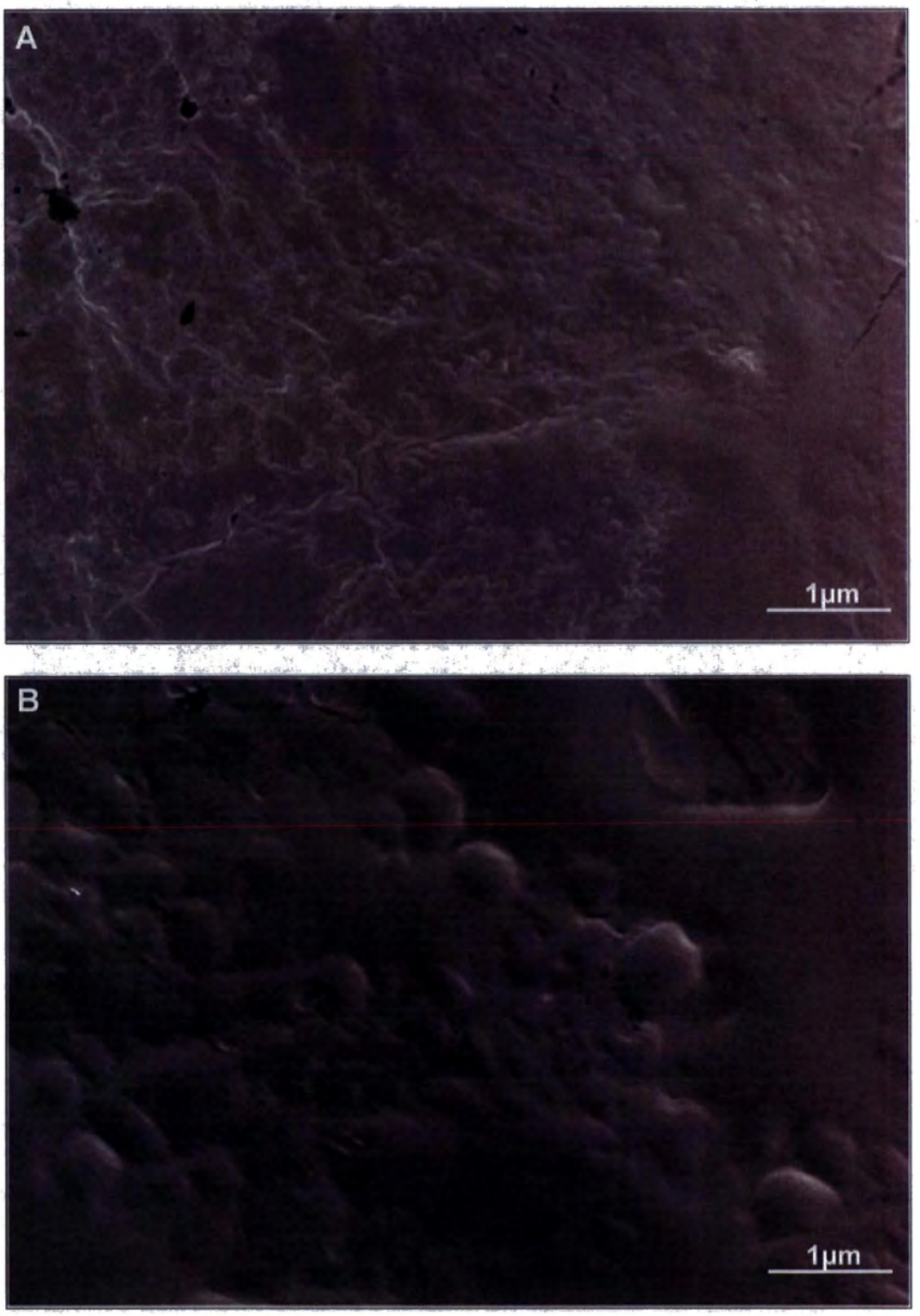
A
1µm
B
1µm

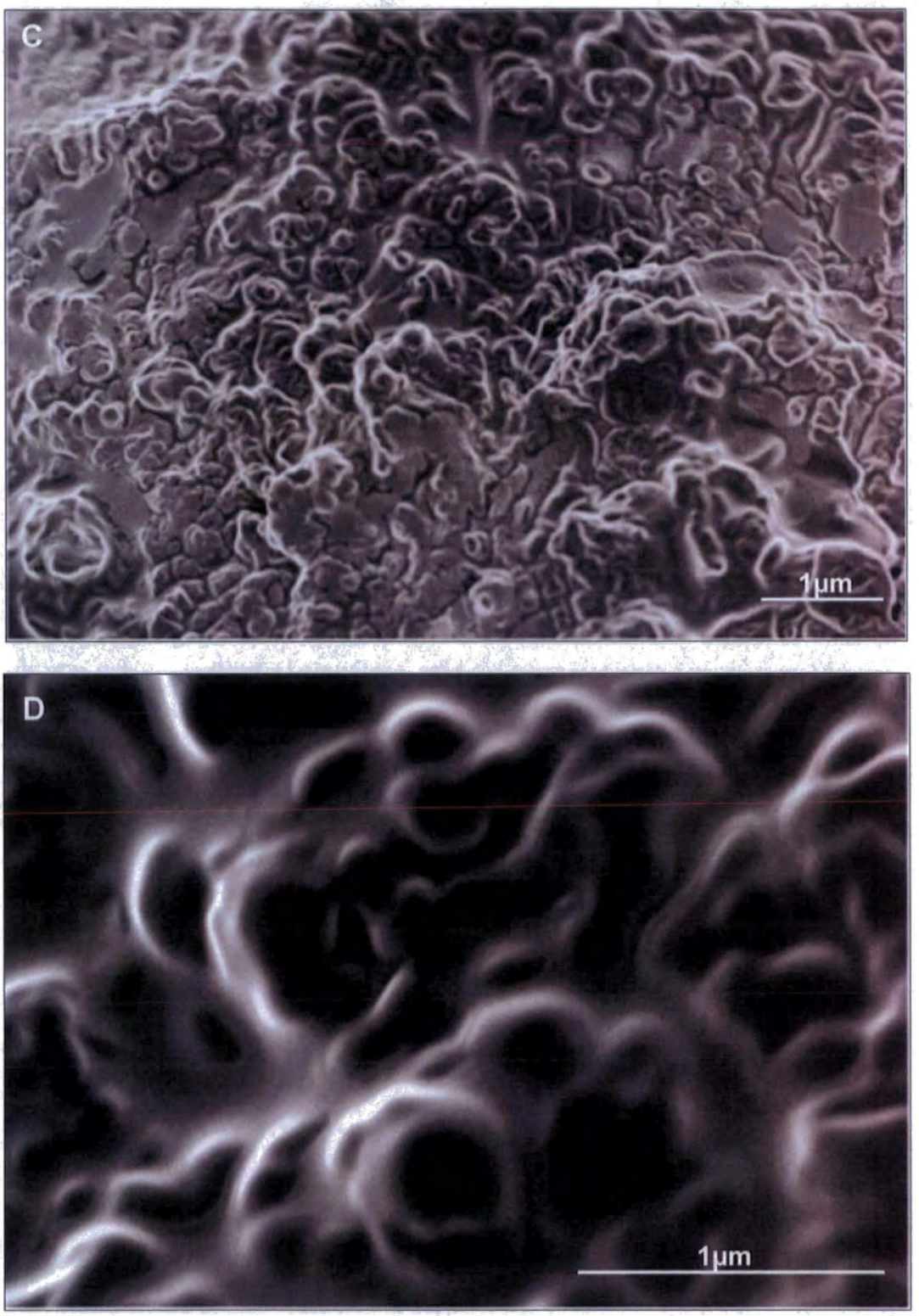

Figure 5.15 – Film coalescence images taken after 24 hours of slow drying

Images A & B = Size 2; Images C & D = Size 3

The effect of inhomogeneity within a film can clearly be observed by scanning electron microscopy. Sizes were dried down slowly at 70°C over 24 hours to create a homogeneous film. In figure 5.15 images A & B show a continuous, homogeneous film without a great deal of structure present which produces relatively low light absorption. This film was created using size 2 which has the lowest particle size and thus creates the most transparent film when dried. Images C & D, created from size 3 which has the largest particle size, produce a large amount of observable structure in the film which scatters light generating an opaque film.

5.5 Wetting Ability

The wetting ability of a size is a vital property as it explains how the size coats a surface and forms a film. In industry the size is deposited onto the glass filaments in the form of an aerosol which is then wound onto a spindle. Due to the winding process filaments are brought in close contact and the droplets are distributed throughout the filaments. During drying the size binds all of the filaments together producing a thicker glass strand. Due to the speed of the winding it is essential that the strength of adhesion of the size to the glass filaments is suitable to increase the chance of cohesion between the filaments. Because of this it is important to determine the adhesive property of the liquid size to the glass, this is known as the contact angle.

5.5.1 Contact Angle

To determine the extent of adhesion between the various sizes and bare glass it was decided to measure the contact angle using flat glass as the contact medium. Although curved glass is the morphology of glass fibres these proved difficult to mount in the instrument and examine due to the small amount of surface area on which to deposit the size. As such flat glass slides were used for the investigation as it is believed that any trends present would exist no matter what type of glass were to be used. Liquid sizes of the variations were created as described in section 5.2 and their contact angles were measured using bare glass slides.

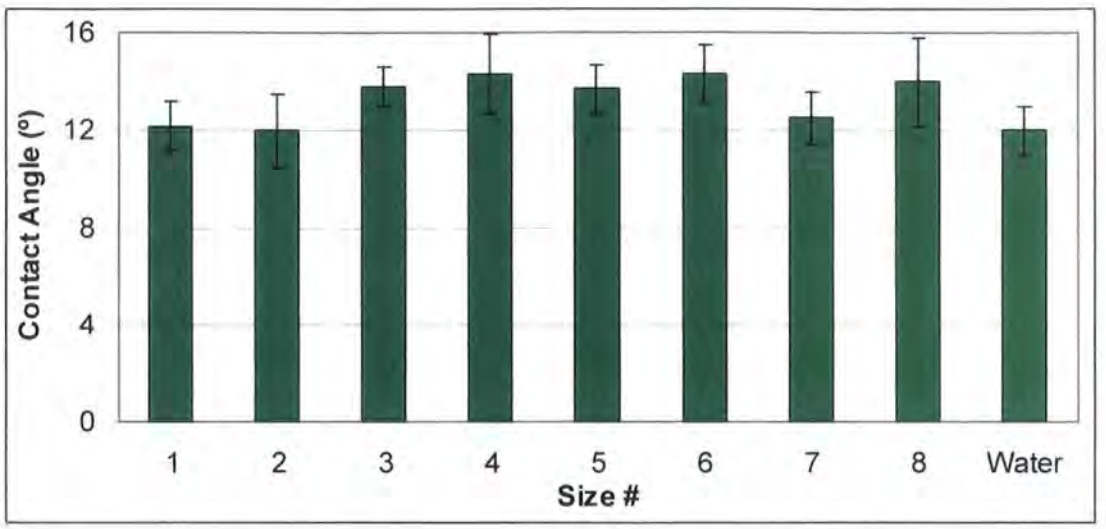

Figure 5.16 – Contact angle of the different sizes wetting bare glass slides

No obvious trend is found to be present due to the lack of any obvious deviation from a standard contact angle. Any slight deviations present fall within the error of the technique which is calculated as the standard deviation from the average of the ten results obtained, these are shown as error bars in figure 5.16. It appears that the differences present in the size formulations do not cause any significant effect in the wetting ability of the size. All of the sizes exhibit a similar contact angle on the glass slides to that of distilled water which is also shown in the figure. This is as expected due to the high water content in the liquid size formulation (~94%) dominating the characteristics of the sizes wetting ability.

The wetting ability of a size can also indicate the ease of which a size can be removed from the glass surface by an impregnating liquid. This factor was investigated by determining the contact angle of a droplet of water on a thin film of each dried size. Dried films of the sizes were created using the technique discussed in section 3.2.4.

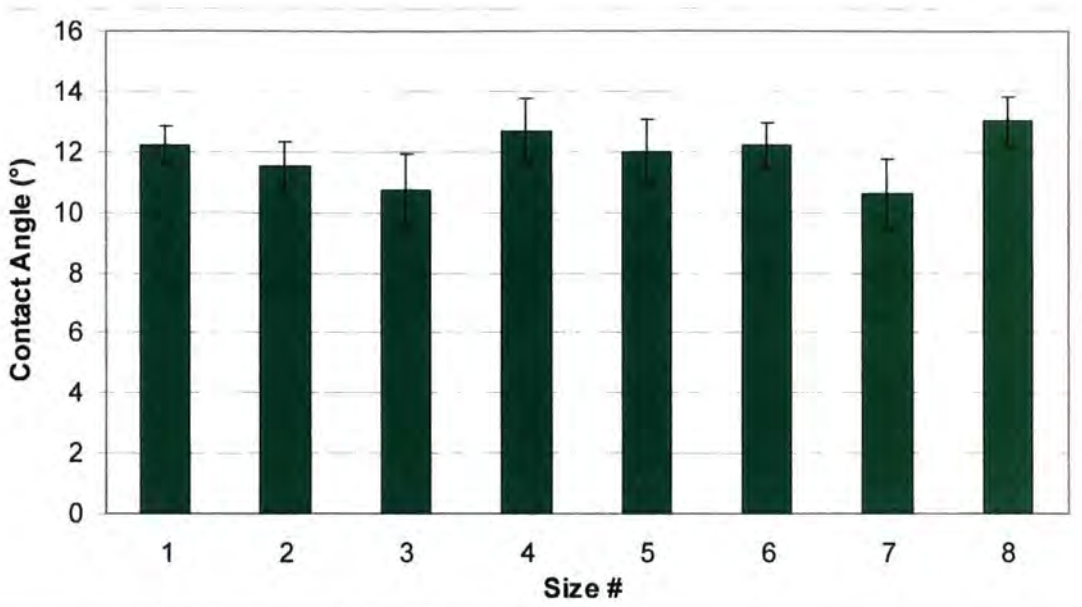

Figure 5.17 – Contact angle of water on films of the different sizes

No obvious trends can be observed as all of the contact angles measured were similar. Any differences which exist can be explained by the error associated with the technique; these are expressed as error bars in the results. The contact angles obtained are calculated as the average of ten measurements.

5.5.2 Fibre Wetting

Following on from the initial investigation of the contact angles it was decided to attempt to determine the effectiveness of the wetting ability of the sizes on bare glass fibres. This was undertaken by investigating the wetting of the fibres for each size at various stages of film formation to determine whether any differences between the sizes can be observed.

Prior to the investigation it was necessary to create bare glass fibres which could be wetted with the different sizes. All fibres are sized during production meaning that those which were to be wetted had to have their original size removed from the surface of the glass. This was undertaken by placing a quantity of the fibres on a heating stage within an environmental scanning electron microscope (ESEM). The temperature of the heated stage was set to 800°C which burnt the size from the glass surface and images were captured throughout.

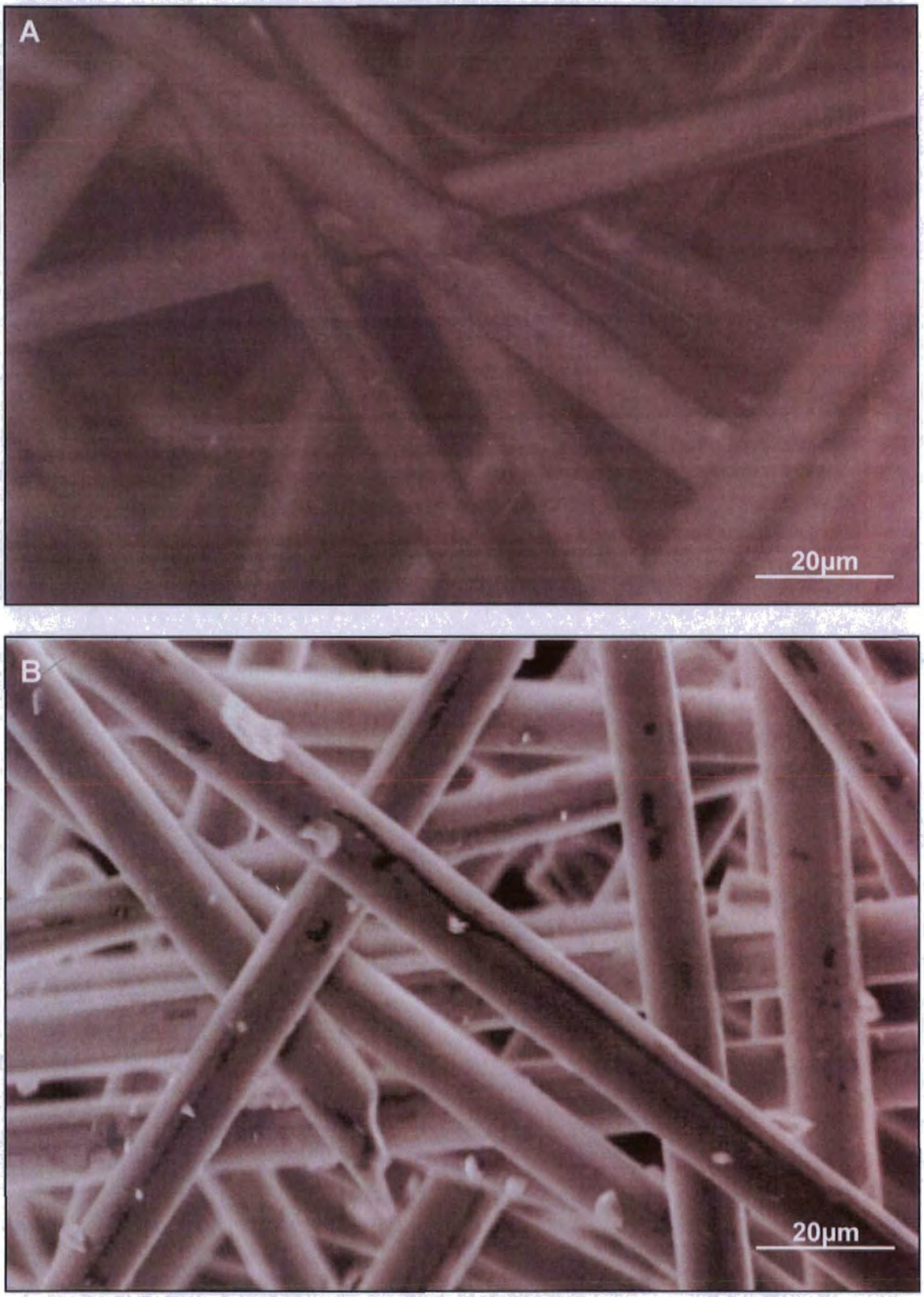

Figure 5.18 – Images showing effect of removal of size from glass fibres.

Image A = Size present (taken at 31°C); Image B = Size removed (taken at 800°C)

Figure 5.18 illustrates the difference between bare and sized fibres. Many more defects and an increased amount of surface detail can be observed on the bare glass fibres in image B whereby in image A the fibres appear smooth. This lack of surface structure is due to the presence of the size on the fibres masking any deformation.

The bare glass fibres were then removed from the ESEM chamber and placed in a dessicator for storage. The heating stage was then exchanged with a wet stage and a quantity of the bare fibres were placed in a small dish on the stage within the ESEM. A droplet of the size was then placed in the dish and the ESEM chamber was sealed. Images were recorded of the size drying slowly onto the glass fibres at a sample temperature of 4°C and a water vapour pressure of 500 Pa.

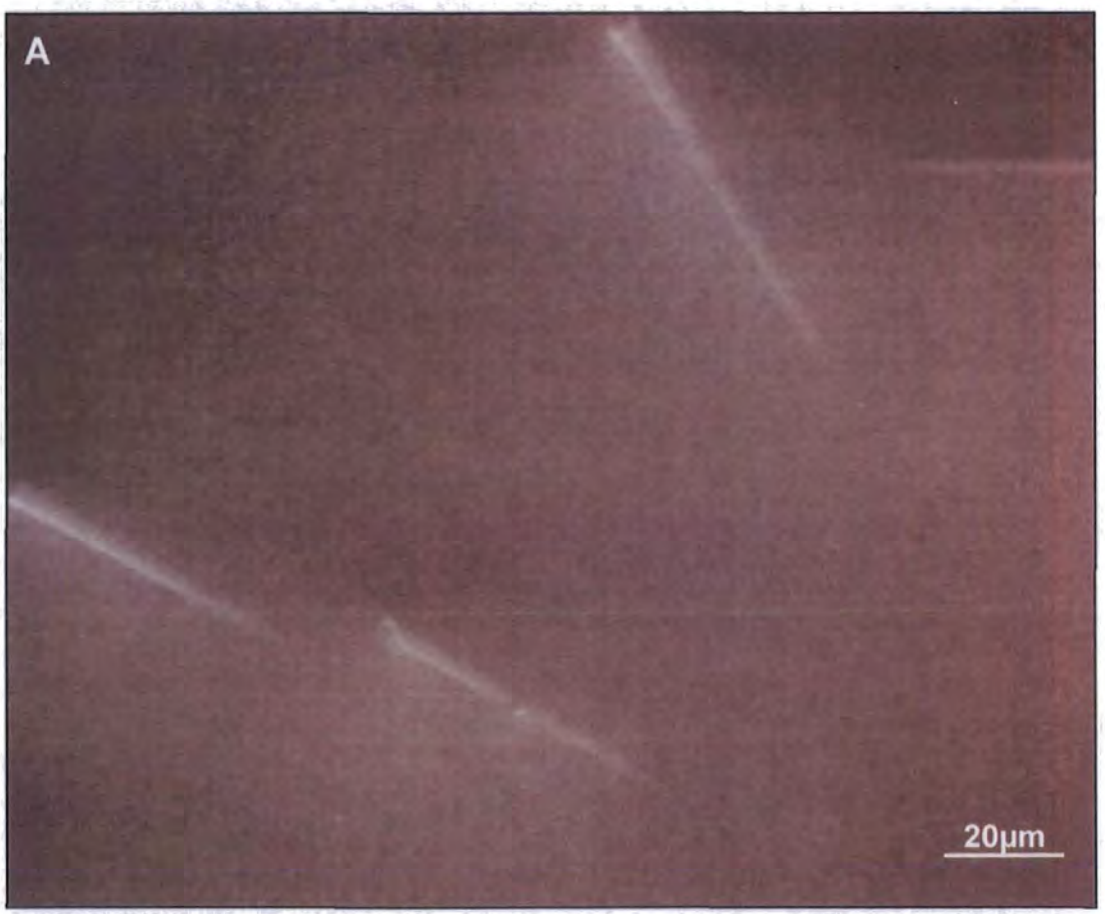

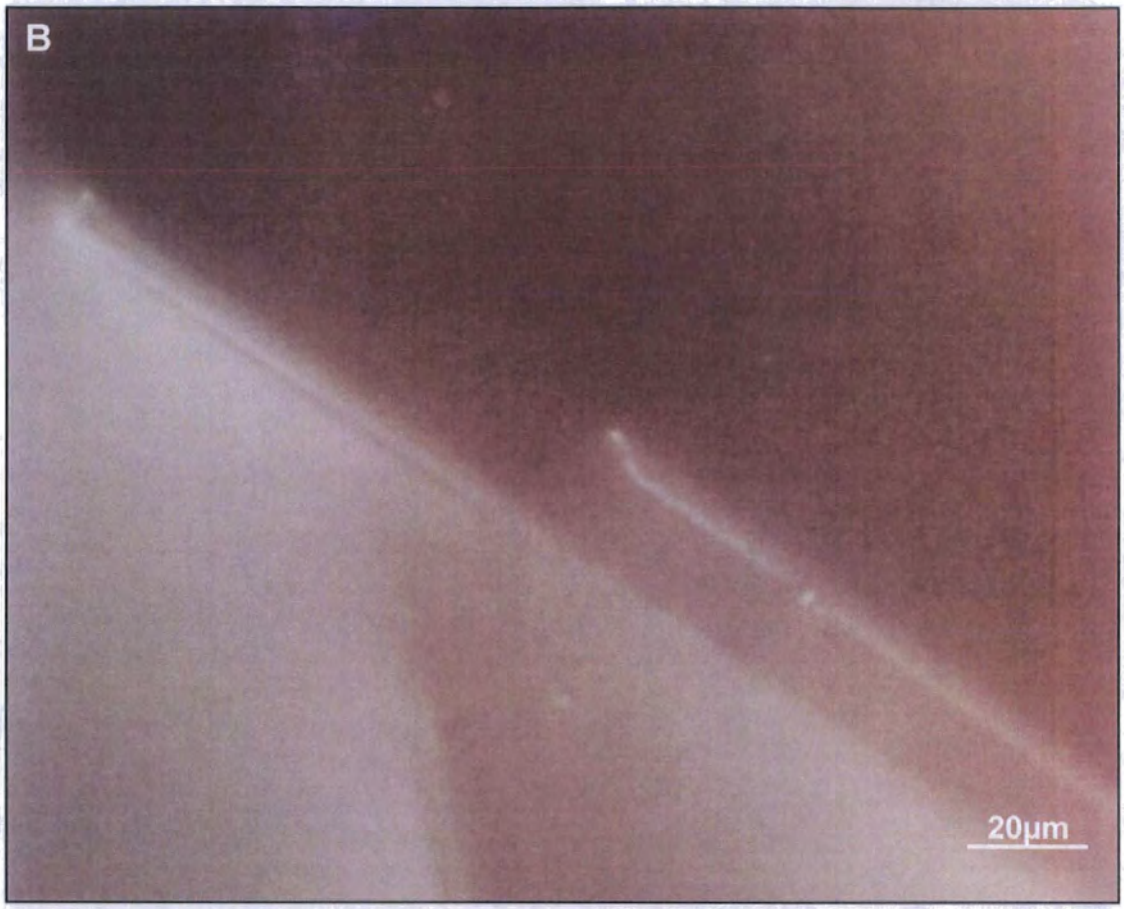
B
20µm


C
20µm

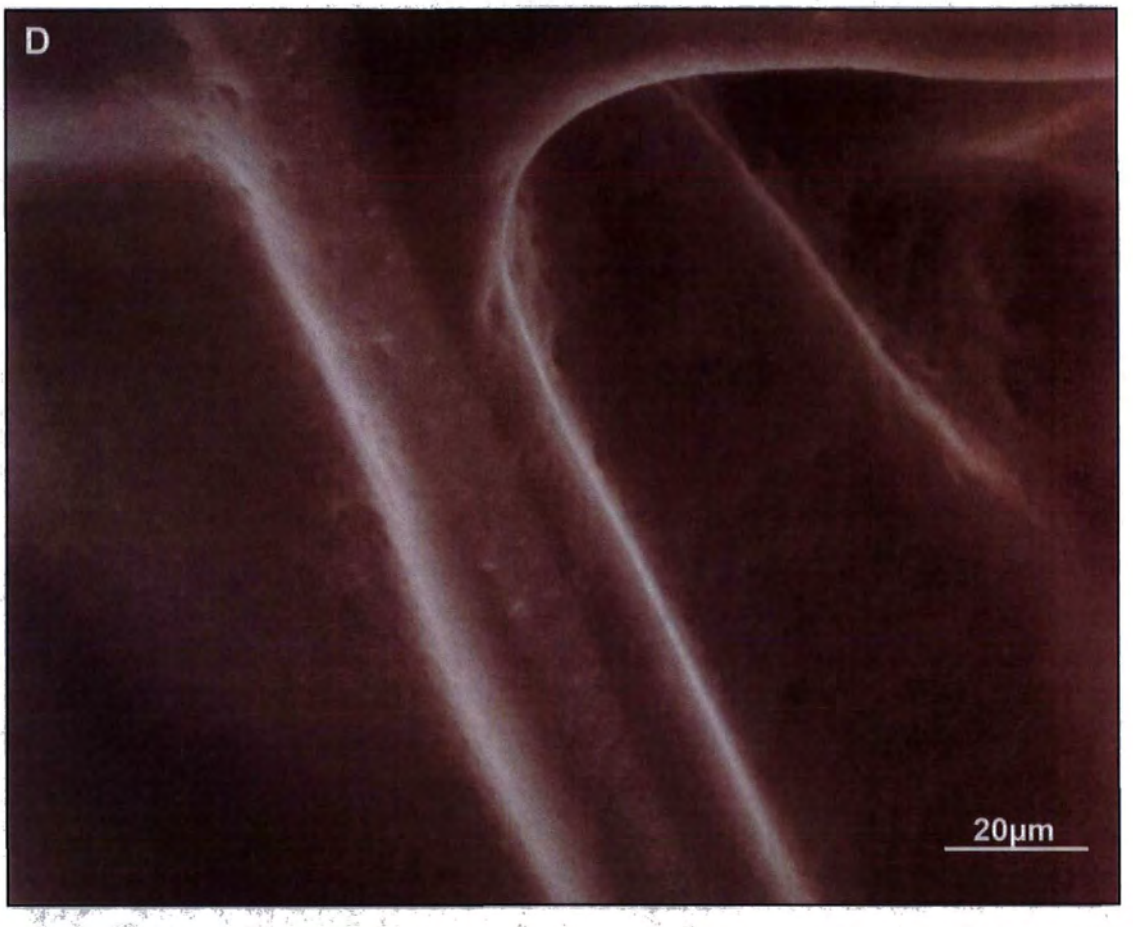
D
20µm

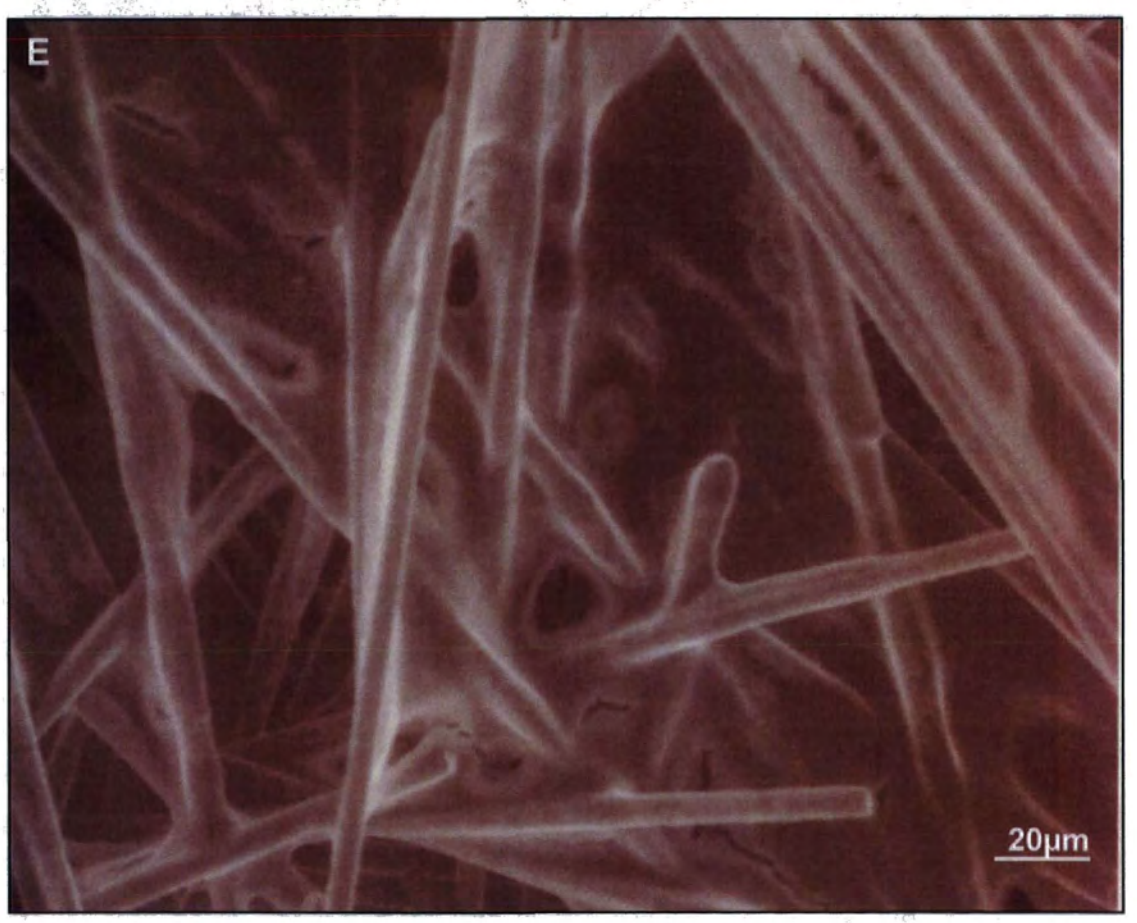
E
20µm

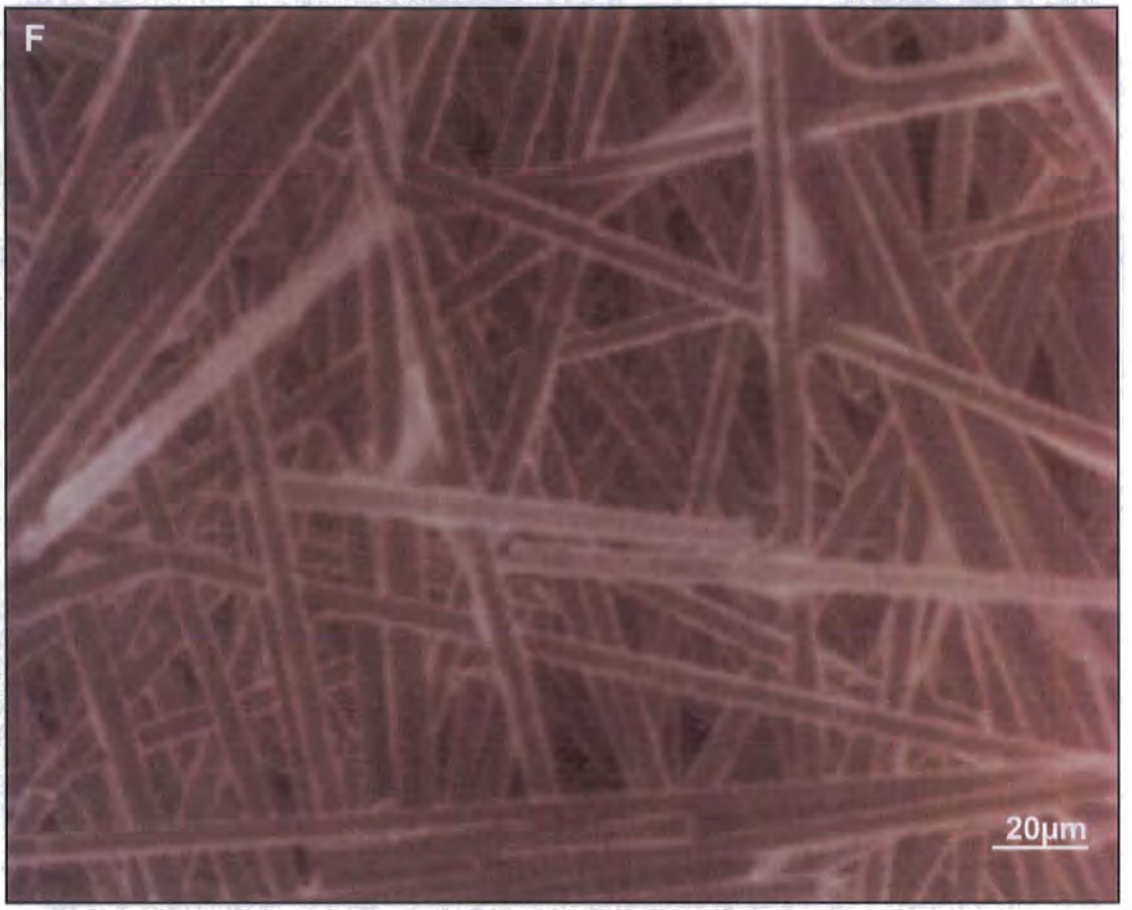

Figure 5.19 – Images showing different stages of size 1 drying on bare glass fibres

Image A = Size after 0 s; B = 120 s; C = 240 s; D = 480 s; E = 600 s; F = 900 s

The images in figure 5.19 show the drying process for glass fibres coated using size 1. It was found that all of the other seven variations produced similar images using the same time-frame and vapour pressure.

During evaporation of the water in the size (images A & B) it begins to adhere to the glass surface of the fibres (image C). The thickness of the adhered size is relatively large at this point (image D) due to a large amount of water still present. As drying continues the thickness of the adhered size decreases and the viewed images can be distinguished as individually sized fibres (image E). Eventually evaporation of the water in the size is complete and fully sized fibres are formed (image F).

Due to ESEM using a water vapour atmosphere to conduct electrons producing an image it was possible to investigate the wetting of these newly sized fibres. By increasing the vapour pressure slowly to 900 Pa whilst keeping the sample temperature constant at 4°C it was possible to condense water from the chamber atmosphere onto the sized fibres.

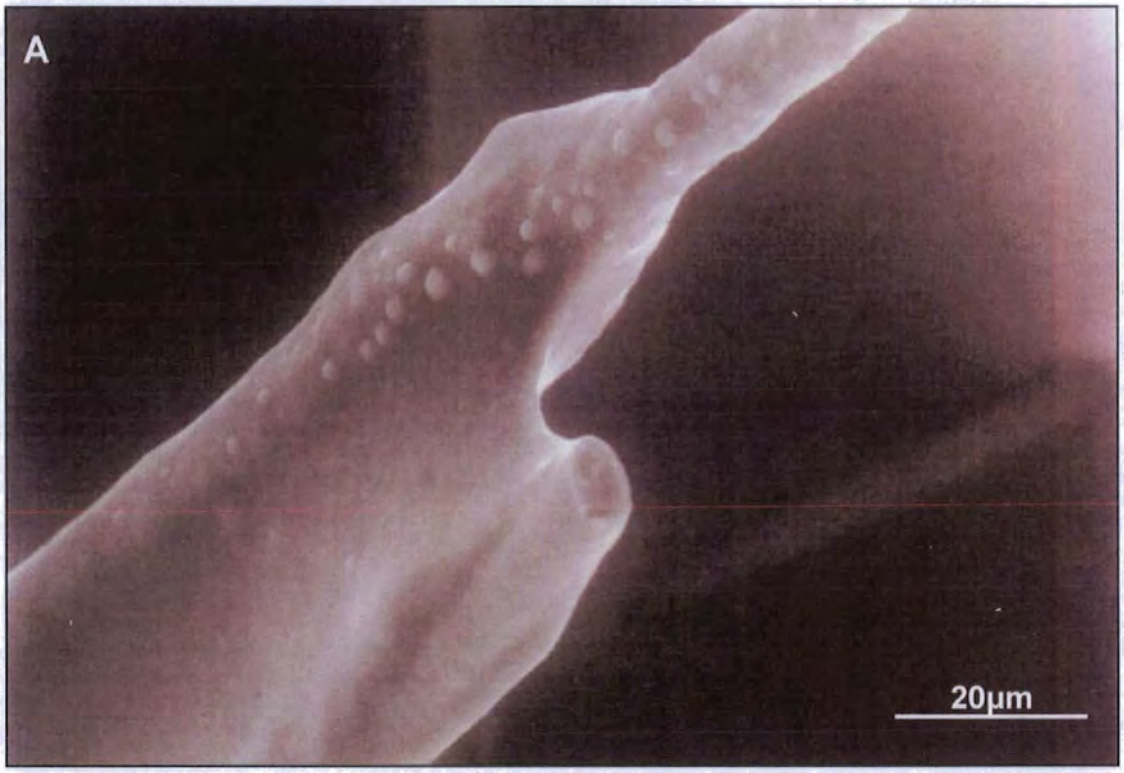

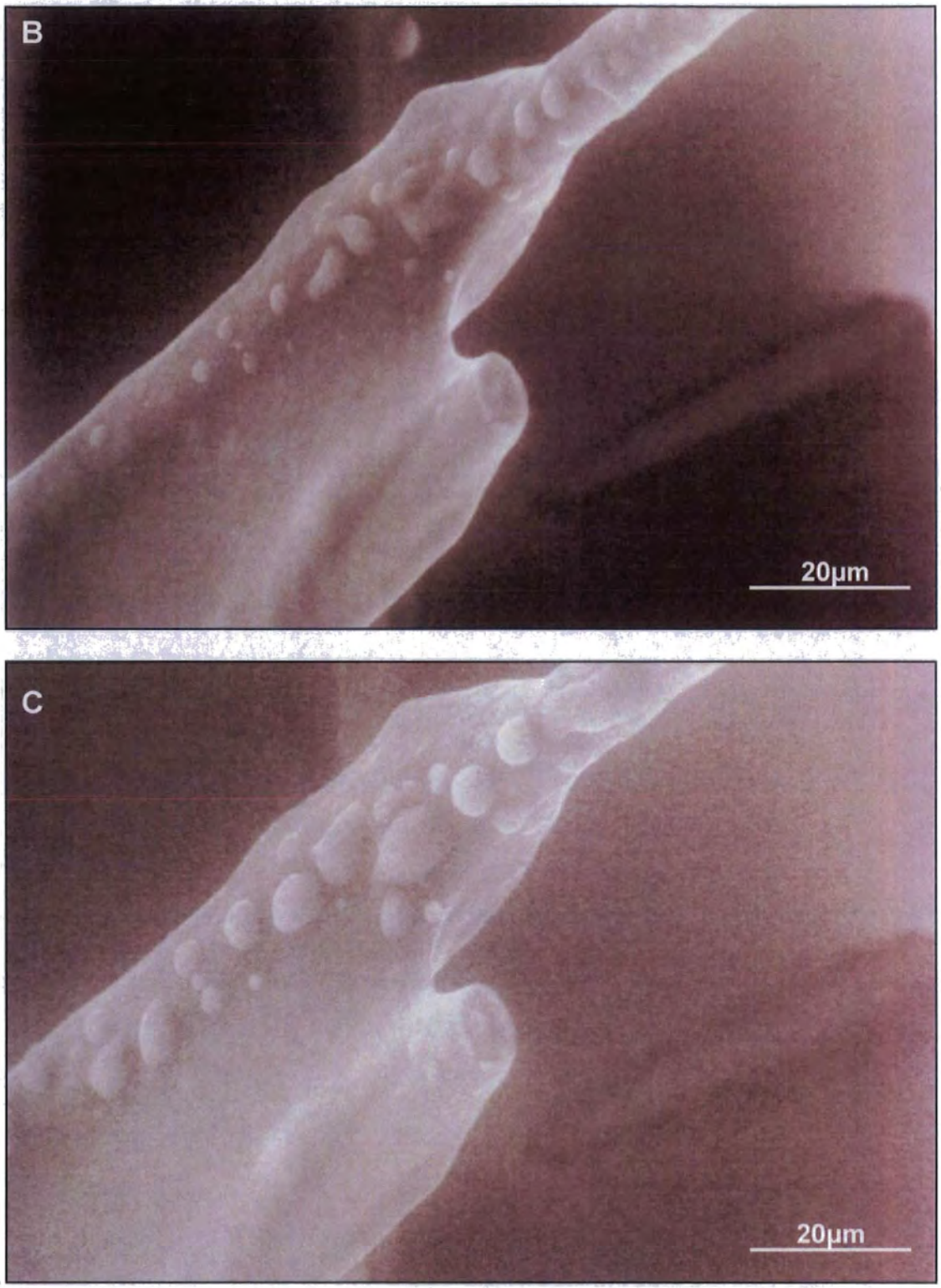

Figure 5.20 – Images showing initial stages of wetting of newly sized glass fibres

Image A = at 500 Pa; B = 550 Pa; C = 600 Pa

A small amount of wetting causes fine water droplets to form on the sized fibres as observed in figure 5.20.

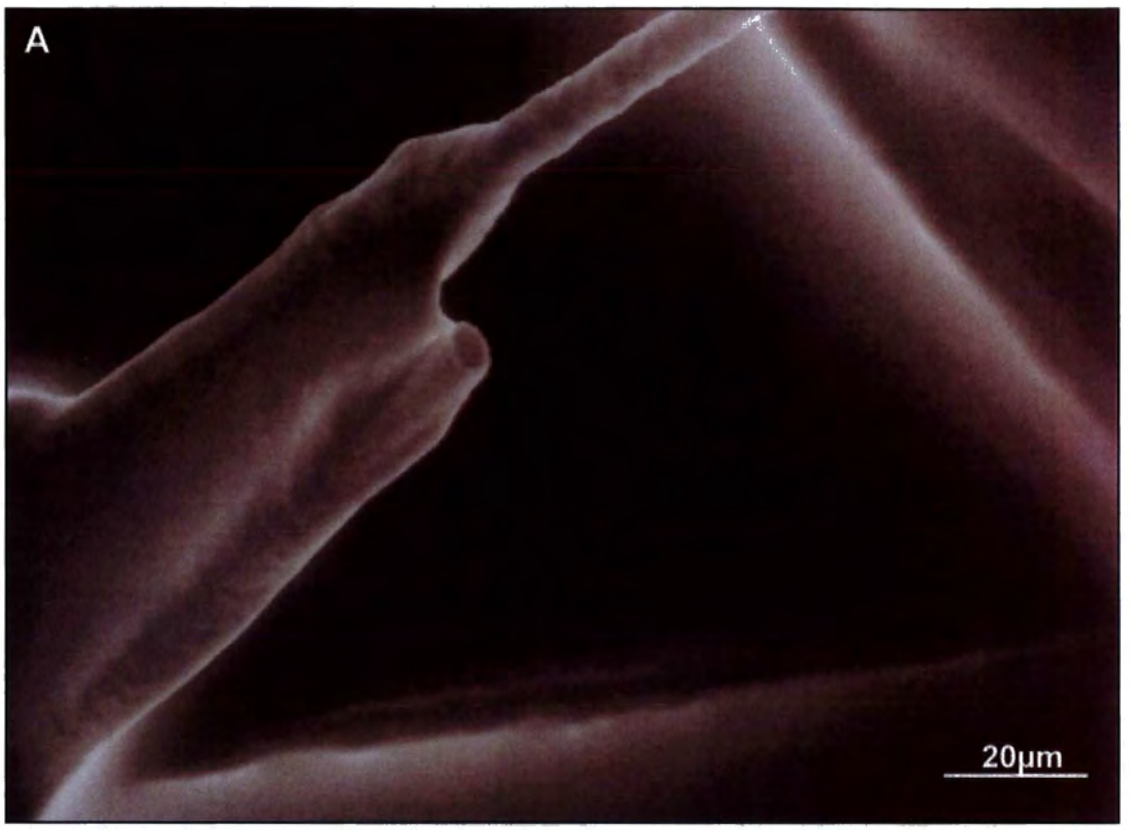
A
20µm


B
20µm

Figure 5.21 – Further images showing wetting of sized glass fibres with size 1

Image A = Size at 800Pa, 0s; B = 800Pa, 240s; C = 800Pa, 360s

The images in figure 5.21 show the sized fibres being re-wetted immediately following a drying step probably due to incomplete drying. This indicates that prior to complete drying the mechanism of drying is reversible as it can be rehydrated and then redistributed on the glass fibres. This theory is confirmed below in figure 5.22 where it can clearly be observed that a redistribution of the size on the glass fibres has occurred following successive wetting and drying steps. Evidence of this was found for all variations of the sizes produced indicating that this phenomenon appears to be independent of the polymer's physical properties.

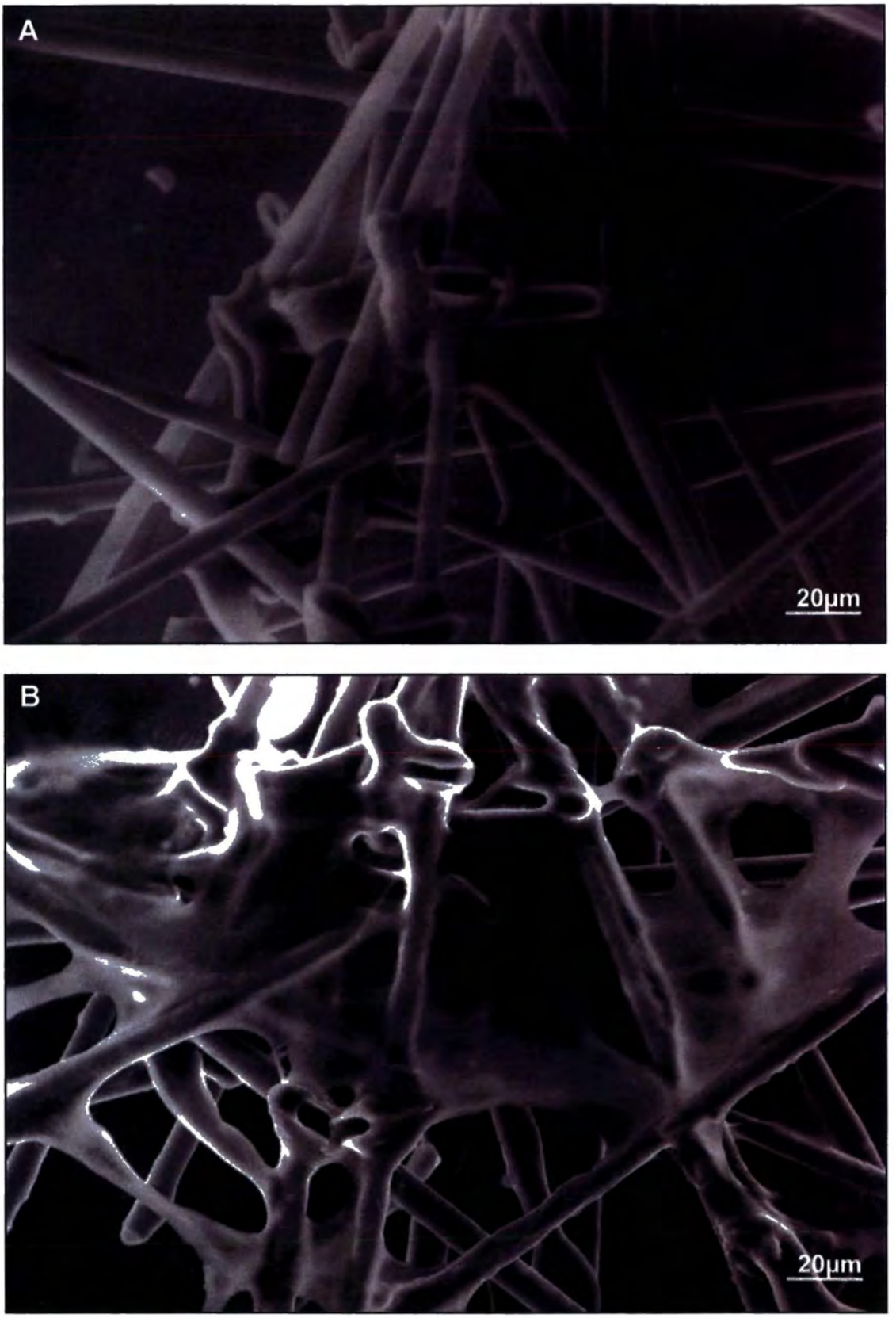

Figure 5.22 – Images of sized fibres using size 1before and after drying and re-wetting. Image A = Sized fibres; B = Fibres after successive wetting and drying.

5.6 Wet-out Rate

The wet-out rate for the variations of liquid sizes created as described in section 5.2 were determined using the custom built detector as described in section 3.3.13.

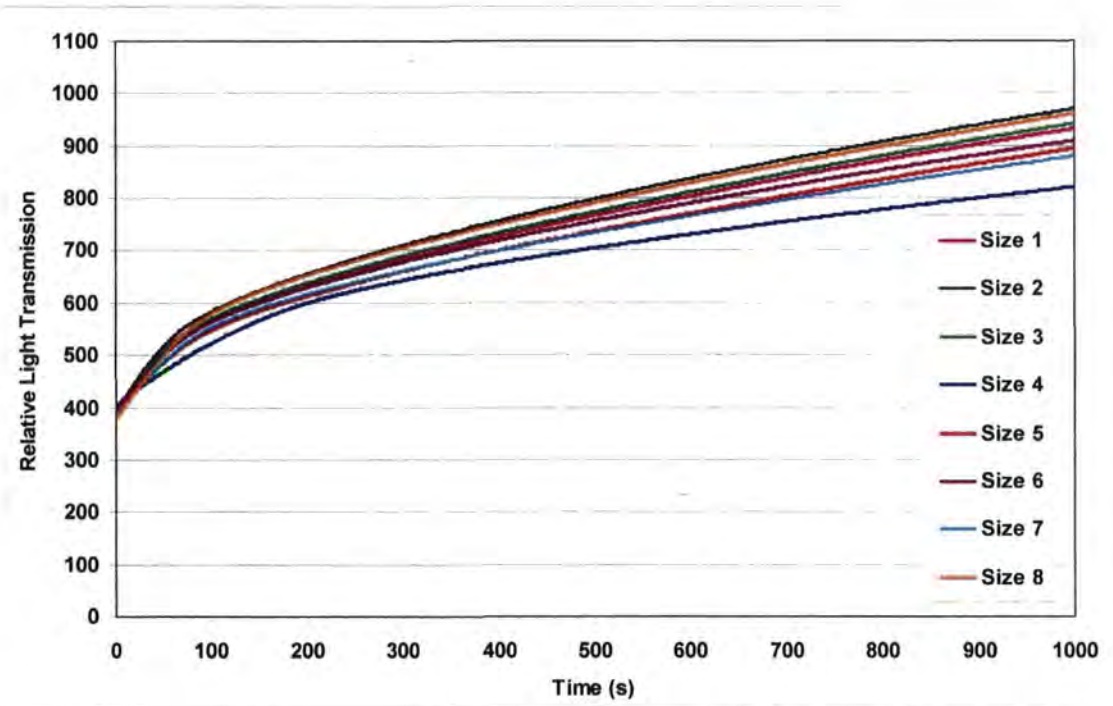

Figure 5.23 – Wet-out rate spectra of the different sizes

The transmission of light increases over time as the size is dissolved from the surface of the fibres by the styrene wetting agent. The wetting agent dissolves the size on the glass fibres allowing the fibre matrix to unravel producing more voids between the fibres in the cloth. These voids allow a greater intensity of the light to pass through to the detector producing the plot shown above in figure 5.23.

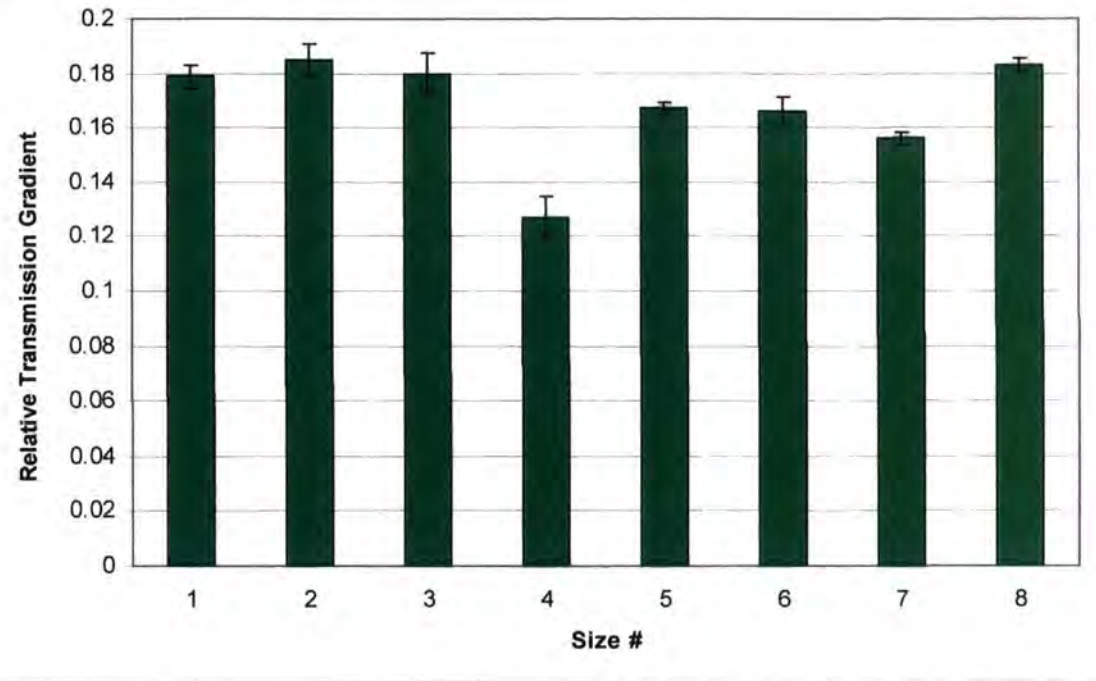

Figure 5.24 – Relative transmission gradients of the different sizes

The testing of each size was repeated three times to ensure accurate results and the associated error bars present reflect the standard deviation of the results about the average value obtained.

The gradient of the light transmitted was determined from the individual spectra of the sizes and the wet-out rate was calculated for the region greater than 300 seconds. To calculate the wet-out rate of each size. This region was selected as there are no inflections present which could invalidate the results obtained. As the wet-out rate should be a continuous value up until the point of complete solubility of the size then any trends observed should be similar no matter which area of investigation is used.

All of the sizes investigated produce a similar wet-out rate except for that of size 4. Size 4 has the largest particle size and it has been shown that this physical property can also affect other tests related to the homogeneity of the film created. It has been shown previously in section 5.3 that

inhomogeneity of the dried size film increases with increasing particles sizes. From this it could be hypothesised that a discontinuous film would be more readily wetted by a solvating species due to the system not being continuous. Voids and inhomogeneous regions present in the film would be sites where wetting could initiate which would facilitate a faster wet-out rate.

However, it is also observed that sizes 3 and 8 (which have similar particle sizes) produce similar wet-out rates to other sizes which have low particle sizes indicating that other factors also affect film formation in size 4.

The most likely explanation is that the formulation of the film-former in size 4 differs too much from that of the standard formulation. By using a much weaker initiator concentration we have produced a polymer which will not undergo typical film formation. Instead an inhomogeneous film forms under drying with regions containing dense amounts of polymer dispersed amongst many voids as is observed by SEM in figure 5.25.

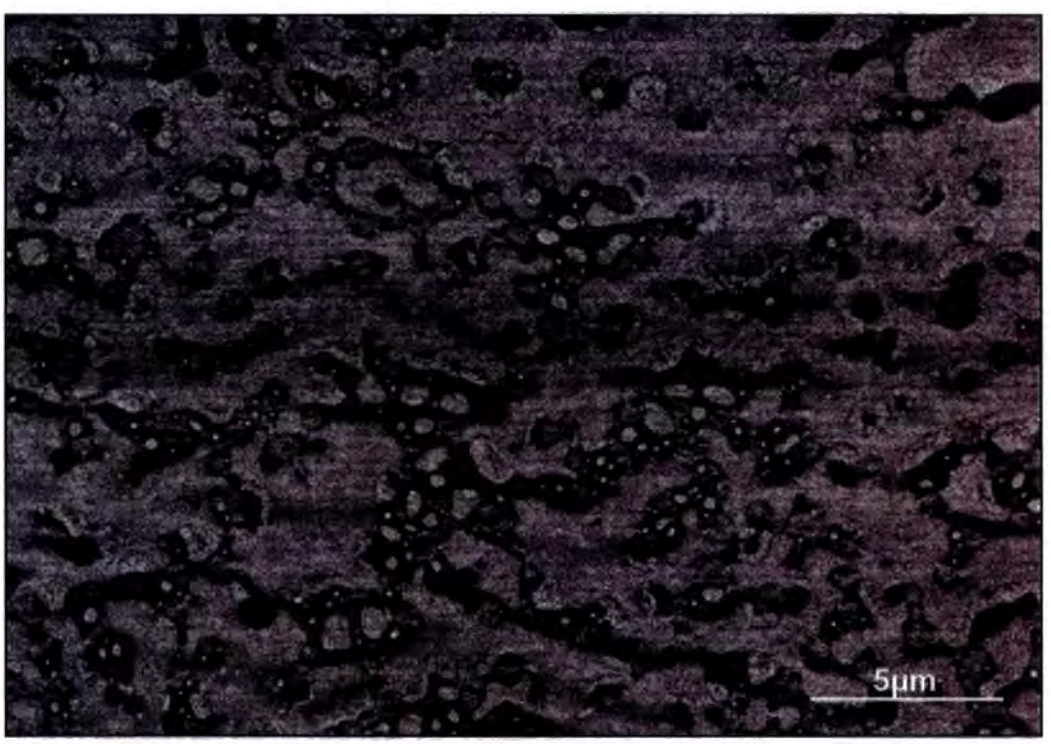

Figure 5.25 – SEM image of the film produced from drying of size 4

5.7 Adhesion

Films of the different size variations were produced as described in sections 5.2 & 3.2.4. Due to the thickness of the film being relatively constant it was possible to determine the adhesive strength of each dried size as a direct analogy of a determination of the strength required to peel the sized film from a glass slide. Peel tests for each size were repeated fifteen times to ensure accurate results were produced. The associated error bars depicted reflect the standard deviation of the results obtained.

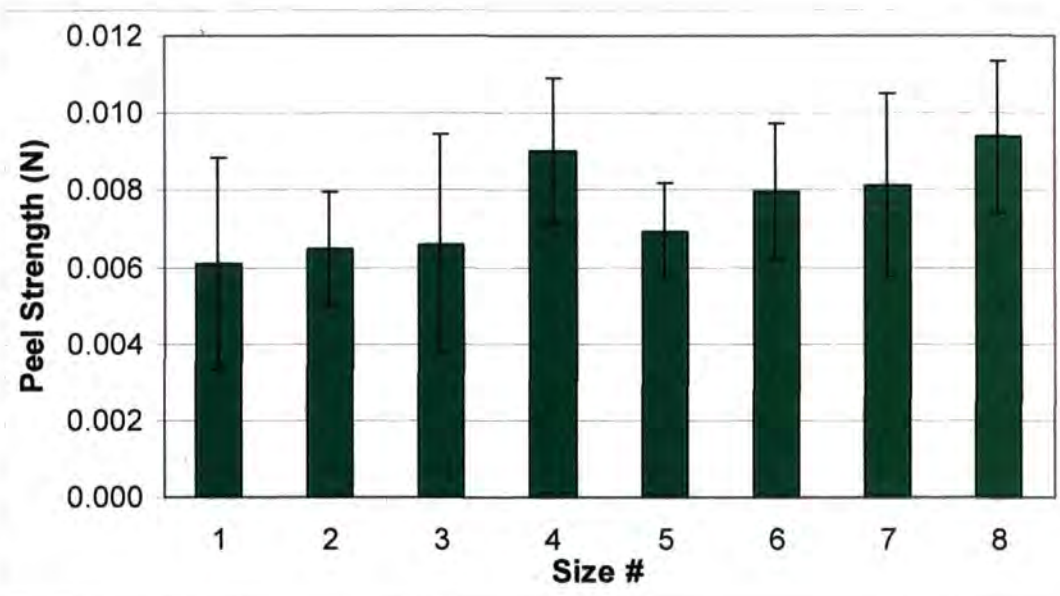

Figure 5.26 – Adhesive strength calculated for each variation of size.

All of the sizes produce a similar amount of adhesive strength using this technique. Any slight trends which may exist could be masked due to the relatively large error associated with the technique.

Error in the technique primarily arises due to the instrumentation used. The machine used is primarily utilised to measure the impact forces of much

tougher materials such as high strength polymers and metals. The forces required to measure the physical properties in materials such as these are much stronger than that required for a peel test therefore it is at these higher orders of magnitude where the calculated force will be most accurate.

Other factors which will affect the associated error include any variation in thickness of the films and also the effect of any external forces. Thickness variations will have a large effect as the test requires comparable samples to have the same thickness. It is stated that the films produced have a thickness of 50±5 μm, this is a variation of 10% of the total thickness which could produce a significant variation in the results obtained. External forces present may also produce a significant effect on the result obtained. Due to the adhesive strength being very small any lateral forces such as a gust of air acting perpendicularly to the peel could affect the force measured.

Due to the large amount of error present in this technique, coupled with the lack of any obvious trends, it could be surmised that a peel test is not an adequate method of determining the adhesion of a size.

5.8 Cohesion

Batches of the different size variations were produced as stated in section 5.2 and lap shear samples were created as described in section 3.3.11. The testing of each size was repeated fifteen times to ensure accurate results were obtained and the associated error bars reflect the standard deviation of the results obtained.

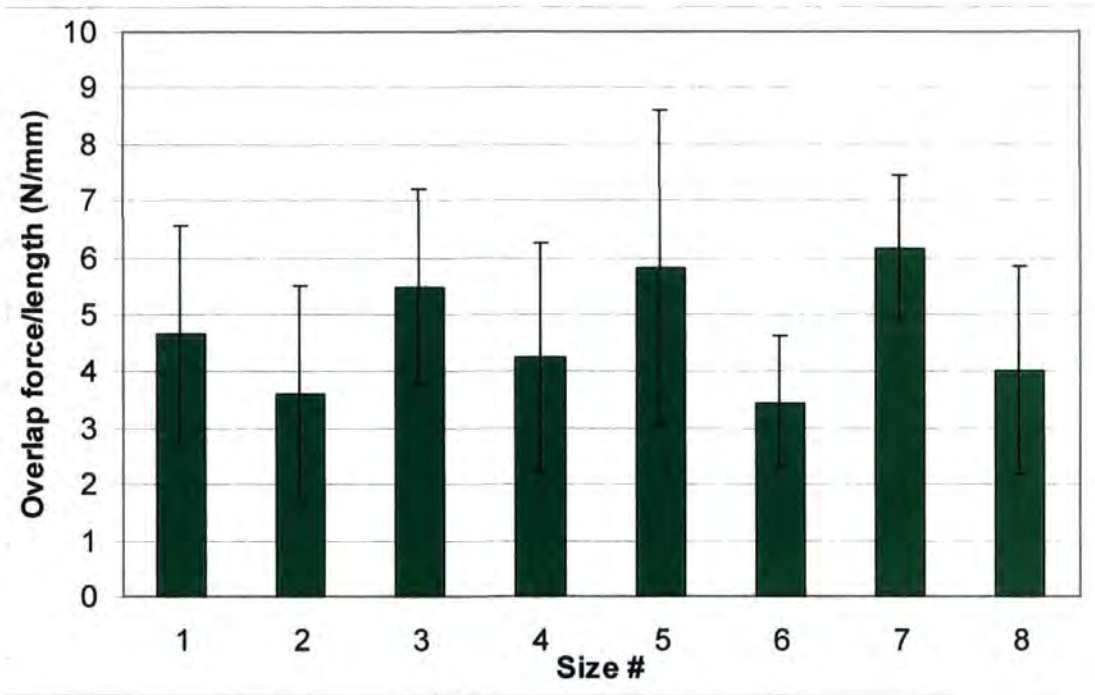

Figure 5.27 – Cohesive strength of the different sizes

It appears that all sizes produce similar levels of cohesion when taking into account the error of the result. The error associated with the technique is large in comparison to the actual cohesive strengths measured. The main reason for this arises due to the variation inherently present in production of

the samples and also the lack of sensitivity of the instrument at low levels which was alluded to in the previous section.

Due to the nature of sample preparation for this technique a significant amount of error arises due to the variable amounts of size thickness found between the glass slides. All samples were prepared identically, however a slightly different amount of liquid could have migrated between the slides during drying which could produce a significant difference in results obtained. Unfortunately it was not possible to measure the exact thickness of the dried size due to the small amount of solid content remaining on the glass surfaces after drying. What little amount of size was present was distributed randomly between the upper and lower glass slides.

Due to the large amount of error present in this technique coupled with the lack of any trends observed it could be hypothesised that a lap shear test is not an adequate method for the determination of size cohesion.

5.9 Young's Modulus

During initial investigations it was found that the standard 50 μm thick films used for other investigations were too thin to mount in the film clamp within the dynamic mechanical analyser (DMA). The instrument tended to stretch the films when they were being clamped in place in the mount. Due to this it was decided that films with an increased thickness should be created for each of the sizes. Dried size films with a thickness of 500±20μm were created for each of the sizes and the Young's Modulus was determined.

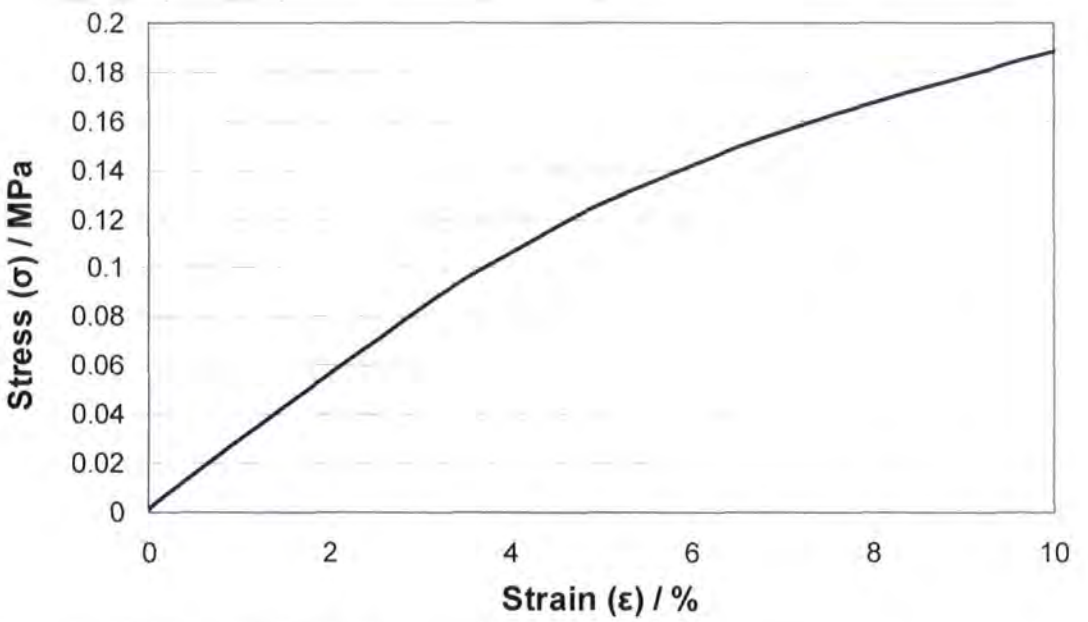

Figure 5.28 – Stress-Strain curve for a dried film of size 1 at 30°C

A stress-strain curve was plotted for each size using the data obtained as shown above in figure 5.28. The initial gradient of the slope before the yield

point was calculated as this equates to the Young's Modulus of the material as stated in equation 5.1.

$$\text{Youngs Modulus} = \frac{\sigma}{\varepsilon} \qquad \text{Equation 5.1}$$

The yield point of a material is the point at which it begins to deform plastically (about 4 MPa in this diagram): before this point the material behaves elastically. The testing of each size was repeated three times to ensure accurate results and the error bars displayed correspond to the standard deviation of the results obtained.

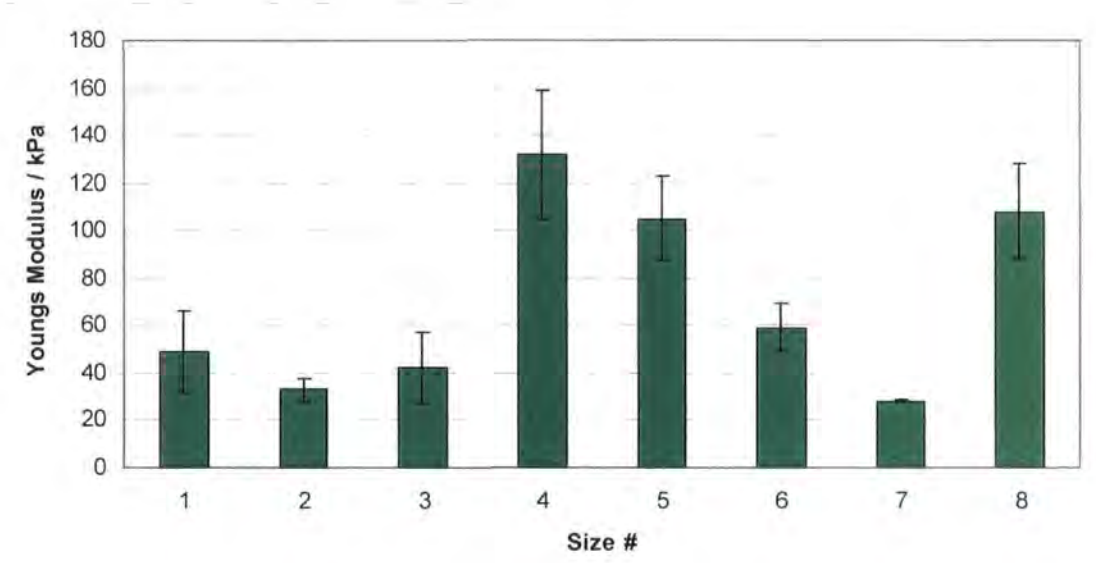

Figure 5.29 – Young's Modulus of the different sizes

From figure 5.29 it can clearly be observed that a significant trend is present which is directly related to the molecular weight of the size. Size 4 contains the film-former with the largest molecular weight and it is found that this size also has the greatest Young's Modulus. Conversely size 7 contains

the lowest molecular weight and the Young's Modulus determined is also the lowest. In fact the entire molecular weight trend is repeated exactly for the Young's Modulus determination.

This trend occurs due to the increasing size of the molecular chains present in the sample causing the rigidity of the polymer matrix to increase. This will cause dried films of the size to be stiffer and therefore the Young's Modulus of the material increases.

5.10 Conclusions

By altering the concentration of specific species in the formulation it was possible to create a range of sizes with different physical properties. These were measured using gel permeation chromatography and photon correlation spectroscopy and it was concluded that the sizes produced contained various particle sizes and molecular weights.

It was found that the size's molecular weight was proportional to the initiator concentration and particle size was proportional to the first stage monomer concentration. However, at low levels of initiator concentration it was found that the particle size was also found to increase even more so than by altering the first stage monomer concentration.

The particle size was also measured using a scanning electron microscope (SEM) whereby an average of each size's particles were determined. The values obtained using this technique were about 50% larger than those calculated using photon correlation spectroscopy due to the particles being flattened during drying *in vacuo* within the SEM.

Using SEM it was possible to determine that all variations of the sizes were found to undergo the complete mechanism of film formation if dried under the correct conditions. A significant amount of drying time was required for complete diffusion of the particles to occur and it was found that fast dried samples using vacuum produced inhomogeneous films. The sizes with the larger particle sizes were found to produce films which retained particle-like structure in them following diffusion. This resulted in the films scattering light

and appearing increasingly opaque, the magnitude of the opaqueness of the film was proportional to the heterogeneity which is related to the particle size.

The contact angle of wetting of a size on a glass surface was found to be similar for each variation. The contact angle of wetting of the dried size films using water as the wetting agent was also found to be similar for all sizes. Images were produced using SEM which also confirm these findings.

It was also found that, prior to the initial drying of the fibres, the wetting process is reversible. SEM images prove that an incompletely dried size will be rewetted under water saturation conditions and will also be redistributed on the glass fibres under a successive drying step.

The wet-out rate of the sizes was found to be similar except for the size with the largest particle size which produced a faster wet-out rate. It is hypothesised that this occurs due to the large particles present in the size presenting voids in the film for which the wetting agent to facilitate wetting.

It was concluded that peel and lap shear tests are not an appropriate method to determine the adhesion and cohesion of a size using heavy duty machinery. Because of the relatively small forces required to peel or shear the films a very sensitive instrument is required to make accurate determinations.

The stiffness was determined as the Young's Modulus of dried films of the sizes and it was found that the stiffness of the size increases with an increasing molecular weight. This occurs due to the increasing size of the molecular chains present in the sample causing the rigidity of the polymer matrix to increase.

Chapter 6

Results

Size Performance : Additive Effect

6.1 Introduction

Following on from the previous section, it was decided to investigate the effect of the other components present in the formulation on the size performance. Batches of size with different concentrations of each component were formulated to determine whether any trends could be observed. Due to time constraints, it was decided that only those tests which were most likely to yield obvious trends would be undertaken. These were carried out so that the results obtained would allow us to understand more clearly the chemistry occurring within a glass fibre size.

Given further time a more thorough investigation of these sizes would have been preferable and would most likely have produced further information regarding the role of each component.

6.2 Additive Concentration Variations

Batches of size were created using variations of the standard formulation as discussed in section 3.2.3. The component additives used were the same throughout the investigation; however the concentration of each varied between 0%-500% to produce a range of sizes of different composition. All of the size component concentrations were altered apart from for the film-former, to create 16 different sizes. The film-former used was that of the standard batch (batch 1) in all variations.

Table 6.1 – Batches of sizes produced using varying additive concentrations.

Batch	Formulation Notes
Standard	Standard formulation, 100% of each component used
0% C	0% of coupling agent component used
50% C	50% of coupling agent component used
200% C	200% of coupling agent component used
500% C	500% of coupling agent component used
0% P	0% of plasticiser component used
50% P	50% of plasticiser component used
200% P	200% of plasticiser component used
500% P	500% of plasticiser component used
0% L	0% of lubricant component used
50% L	50% of lubricant component used
200% L	200% of lubricant component used
500% L	500% of lubricant component used
0% A	0% of anti-static agent component used
50% A	50% of anti-static agent component used
200% A	200% of anti-static agent component used
500% A	500% of anti-static agent component used

6.3 Wetting Ability of Sizes

Batches of the size variations were dried onto flat glass slides as described in section 3.2.4. The contact angle of the surface of films of the dried size were investigated using water as the contact liquid.

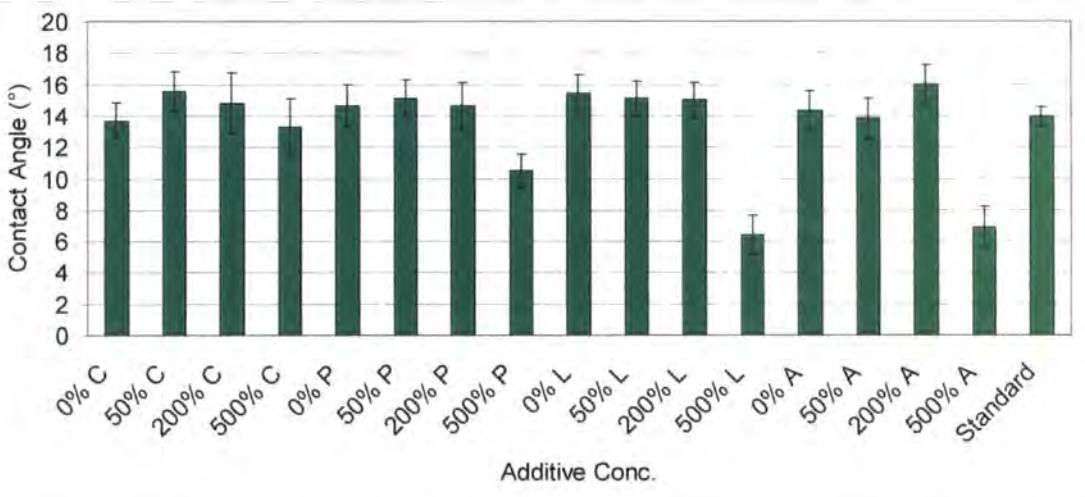

Figure 6.1 – Contact angle investigation of different additive concentrations using water droplets on dried size films.

Water droplets on all of the film variations exhibited similar hydrophilic tendencies. However, the sizes created using an excess of each component (500%) all produced noticeably lower contact angles.

The size created using an excessive amount of lubricant produced films with a noticeably different appearance than all of the others. Film-formation appeared to be non-uniform with fluidic areas inter-dispersed between dry regions. By adding an excess of the lubricant the continuous nature of the film appears to break down, resulting in a dried size with an increased hydrophilic nature. During drying, the lubricant component

preferentially migrates to the air interface of the size (as discussed in section 4), therefore, it is likely that the excess of lubricant present causes inhomogeneous evaporation during film formation. This leads to areas of the film drying at different rates producing areas with different degrees of drying. This is also the most likely reason why the sizes created using the anti-static agent and plasticiser also produce a significantly lower contact angle with water, which indicates a more hydrophilic film.

The size produced using an excess of coupling agent has the weakest effect on the contact angle due to preferential migration to the glass interface of the film. This would not be expected to affect the evaporation stage of the film formation mechanism unlike the other additives.

The wetting ability of the liquid sizes was also investigated by dropping onto bare glass.

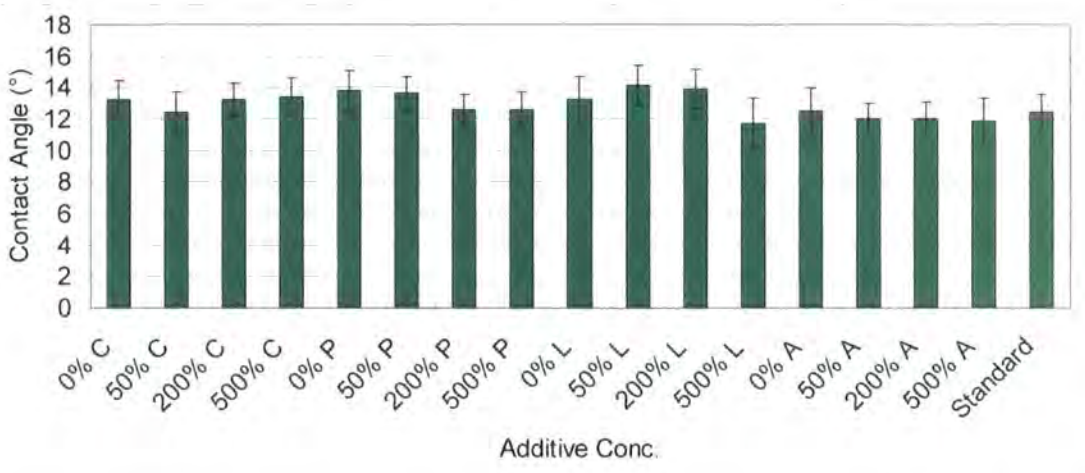

Figure 6.2 – Contact angle investigation of different additive concentrations using size solution droplets on bare glass slides.

All of the size droplets appear to exhibit similar wetting properties when dropped onto a bare glass slide. This indicates that the minor differences

present in the formulation are far outweighed by the excessive water content present in the size solution (>90%). It is already known that water adheres to glass and that glass is a hydrophilic substance [13] therefore all variations of the size formulation are also hydrophilic.

6.4 Adhesion

Samples were prepared using batches of each size as detailed in sections 3.2.4 & 6.2. The samples were mounted in the mechanical testing instrument as described in section 3.3.11 and the films were peeled from the glass slides. The force required to separate the film from the surface was measured and recorded. Each peel test was repeated five times to minimise error and determine accurately the adhesive force of each variation of the size.

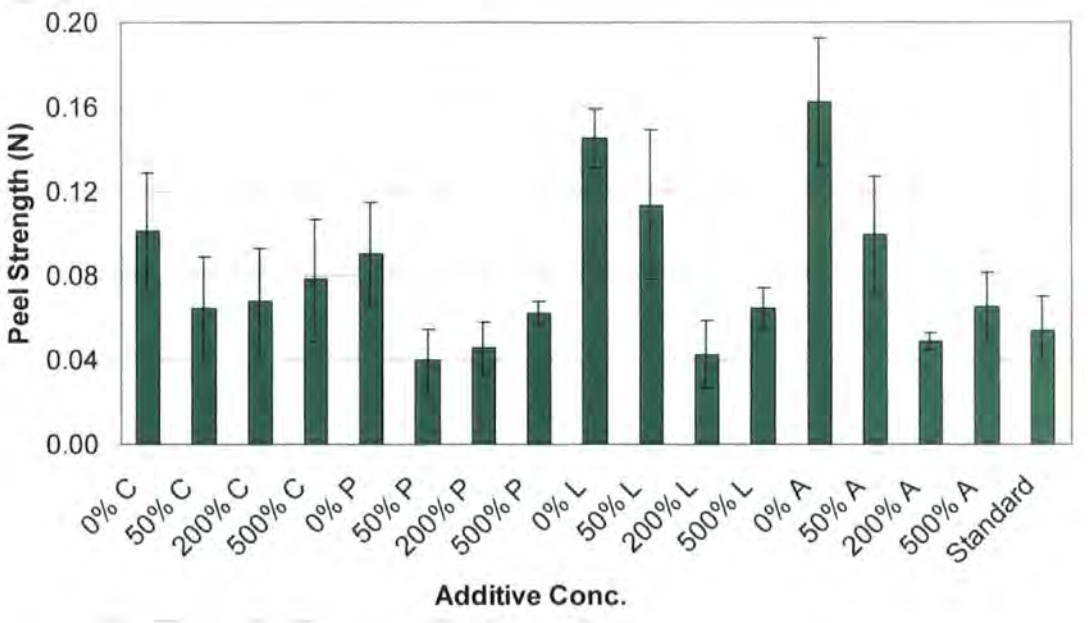

Figure 6.3 – Peel test results for each variation of size formulated.

Errors in comparable adhesion results may arise due to the differing amounts of solid content in each of the variations of the size. As the amount of each component is altered, the solid content of the size will either increase or decrease, leading to a change in thickness of the film. This was negated by determination of the thickness of each of the film variations from the standard

size composition. This was undertaken by measuring the thickness of a dried film of each variation of the size by ESEM.

Table 6.2 – Dried size film thickness of each variation determined by ESEM.

Size	Film Thickness /μm
0% C	37
50% C	40
200% C	54
500% C	73
0% P	32
50% P	36
200% P	46
500% P	60
0% L	29
50% L	35
200% L	51
500% L	70
0% A	35
50% A	39
200% A	48
500% A	63
Standard	42

The results in figure 6.3 were normalised by dividing the calculated adhesive strength by the film thickness to produce a more accurate adhesive strength result for each variation of the size.

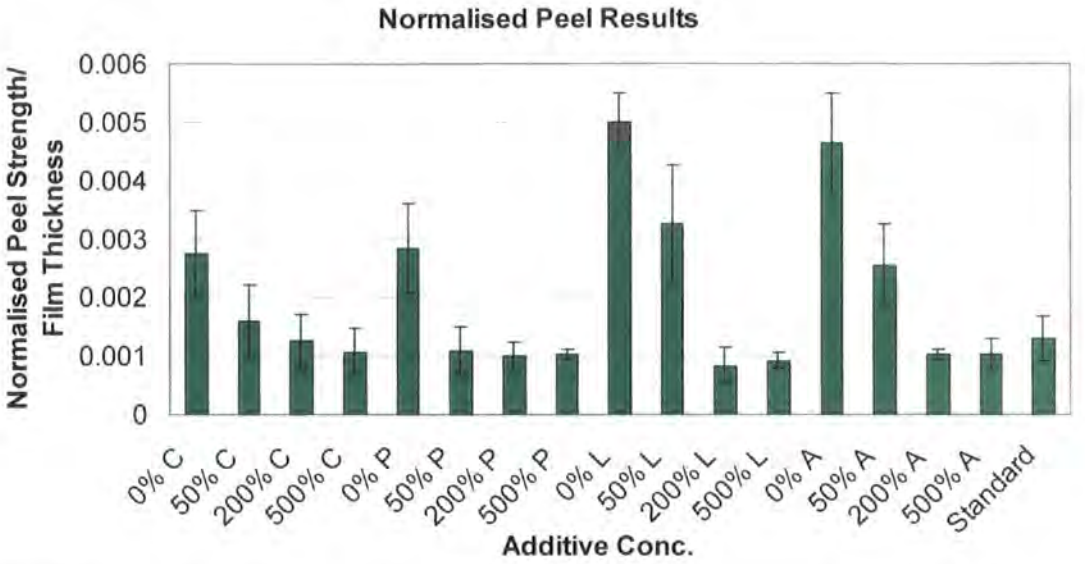

Figure 6.4 – Normalised peel test results for each variation of size formulated.

A trend is observed from the results, where films with a lower amount of additive present produce a more strongly adhesive film. As the amount of component increases the adhesive strength decreases before reaching a plateau at 100% concentration. At this point higher concentrations of component no longer influence the films adhesion to the glass.

The variations with the largest effect on the adhesive strength appear to be those lacking in lubricant and anti-static agent. The lubricant is added to the formulation to improve the flexibility of the dried film, so removing it rigidifies the sample making it more difficult to peel; therefore rendering it more strongly bound to the glass surface. The anti-static agent is also a lubricant which promotes similar behaviour to the excessively lubricated variation. The plasticiser is added to improve further the flexibility of the film and a lack of this causes the film to perform in a similar manner to those already mentioned.

The coupling agent is added to improve the binding of the film to the glass surface, indicating that we might expect the adhesive strength to increase with increasing concentrations of additive. Due to the excessive amount of coupling agent used in the standard formulation, coupled with the finite glass surface area available for interaction, it is found that an increase in coupling agent concentration has a slightly negative impact on the adhesive strength.

A lack of coupling agent present in the size appears to produce more adhesion between the film and the glass. This is opposite to what we would expect, as the coupling agent is generally added to improve the bonding between the film and the glass. This phenomenon most likely arises due to the artificial environment in which the samples were prepared. To create a film which was peelable, it was necessary to produce a much thicker film than is normally used as a glass fibre size. To achieve this, the wet size was added in excess to flat rather than curved glass while also being in constant contact with the glass surface. During fibrisation, the individual fibres are sprayed with an aerosol of the size, most of which does not adhere to the fibres due to gravity and centrifugal forces encountered during winding. Because of this, a coupling agent is vital to ensure the maximum amount of size remains on the fibre for as long as possible. In this case, where only a small amount of size is used, the coupling agent would provide a much more important role which cannot be quantified using our peel test technique.

6.5 Cohesion

Samples were prepared as discussed previously in sections 3.2.4 & 6.2 and were mounted in the mechanical testing instrument as described in section 3.3.12. The samples were sheared laterally and the force required to shear the sample was measured. Each variation of the size was sheared five times to minimise the error and determine accurately the cohesive force of each dried size.

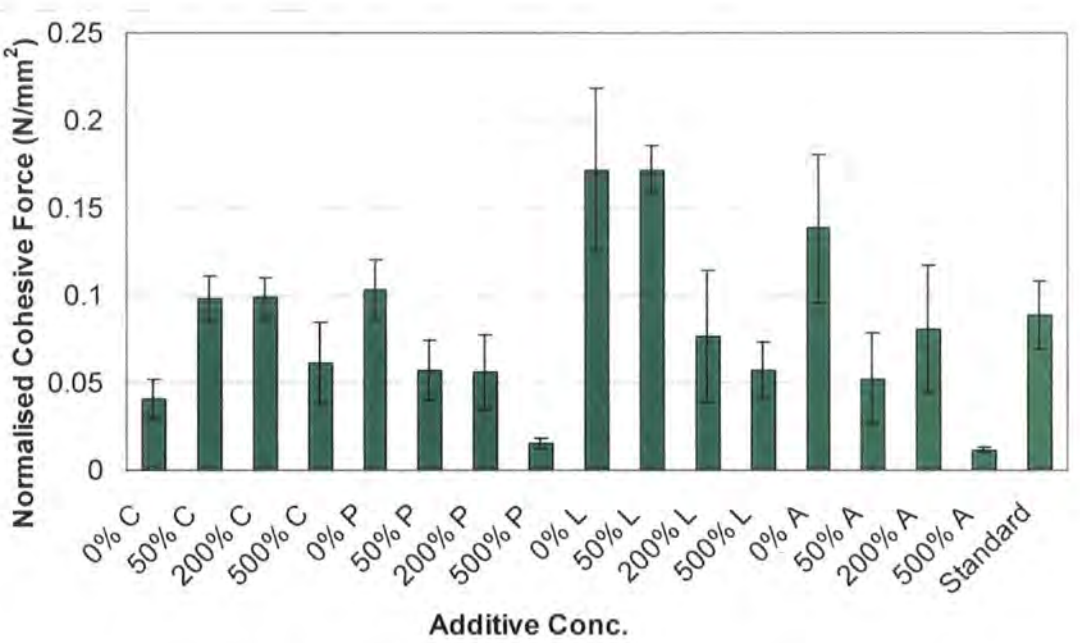

Figure 6.5 – Shear results for each variation of size formulated.

As for the adhesive study, a significant error in our results is present due to the difference in solid content, and therefore film thickness, of each variation of the size. To remove this error the results were normalised by dividing the cohesive strengths of each variation by the correspondent film thickness as determined by ESEM (see section 6.4 for film thickness values).

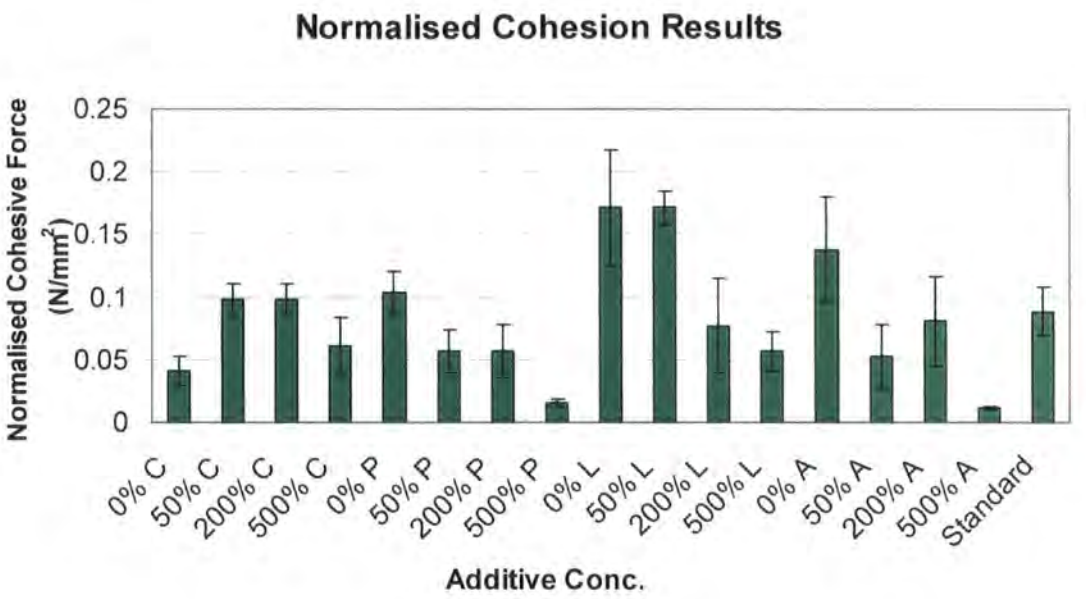

Figure 6.6 – Normalised shear results for each variation of size formulated

Although some trends can be observed from the results obtained, it must be explained that the associated error in this technique tends to mask all but the extreme cases of difference between strengths.

The sizes with the largest cohesive strengths appear to be those with lower than typical concentrations of lubricant and anti-static agent. Anti-static agents are typically specialised lubricants indicating that a lack of lubrication in the film produces an increase in bonding strength between the size and the glass. This is expected due to the inflexibility of the film, which is a consequence of the lack of lubrication present in the formulation.

The sizes with differing amounts of coupling agent present would be expected to produce the most obvious differences in cohesive strength. However, because the coupling agent is present in excess in the standard formulation coupled with the finite amount of glass surface area available for bonding, no real difference in cohesive strength can be observed for any of

the variations. The only exception to this trend is for the size which contains no coupling agent as this produces a weak cohesive strength film.

At extreme levels of component concentration (500%) it is observed that the cohesive strength reduces for all variations. This occurs due to the non-uniform nature of the film which is formed after drying. Upon the addition of five times the amount of a component additive, it appears that the deviance from the standard formulation is too great and the homogeneity of the film begins to reduce. When excessive amounts of plasticiser and anti-static agent are used in the formulation this was also found to occur, whereby the sample would not shear apart instantaneously, rather it tended to slide apart as though the site had not fully cured.

6.6 Conclusions

It has been observed that an excessive amount of any component in the size formulation produces an unsatisfactory size. Inhomogeneous films tend to form as can be observed from their cohesive strengths and wetting abilities.

The effect of wetting ability of water droplets on size films is less evident for the size with an excessive concentration of coupling agent. This is due to the species migrating to the glass interface during film formation, whereas for the other components it will generally migrate towards the air interface of the film causing a more inhomogeneous, hydrophilic surface.

The wetting ability of variations of the size appears to produce similar results when dropped in its liquid state on bare glass slides. This is most likely due to the large amount of water present in the size formulation dominating the wetting ability of the size droplet, obscuring any effects due to the variation in formulation.

Formulations of the size containing lower than typical component concentrations produce films with higher adhesive and cohesive strengths. A relationship appears to exist which indicates that less flexible films produce greater bonding to the glass surface.

A lack of coupling agent in the size formulation appears to produce a film which has weak cohesive strength, although it does still bind sufficiently well to the glass surface to allow the test to be carried out.

This variation also has a large amount of adhesive strength which is even larger than the standard formulation used in industry. The most likely

explanation for this phenomenon is due to the artificial manner in which the sample was prepared. It would be expected that a small amount of size would bind to a thin glass fibre much differently than an excess of size would to a flat glass size. Under these circumstances the role of the coupling agent is much more important to ensure that the size remains on the glass surface overcoming gravity and centrifugal forces. This is not the case for the sample investigated as the size remains in constant contact with the glass throughout.

Chapter 7

Conclusions

7.1 Conclusions

Batches of film-formers were created via emulsion polymerisation from a formulation supplied by Celanese. These film-formers were then incorporated into a formulation as supplied by St. Gobain Vetrotex which is used in industry to produce a working glass fibre size.

Initial studies were undertaken to determine the location of the constituent species present in the size to produce an image of its structure. The film-former formulation was then altered to produce a range of physical properties. The performance of sizes produced from these film-formers were then investigated in the areas of clarity, film formation, wetting ability and strength. Alterations to the size formulation was then undertaken to determine whether this produced any effect in the performance of the size over some of the same areas of investigation. The conclusions drawn are listed below:

- The coupling agent species present in the size formulation migrates to the glass interface of the size during drying.
- A minor amount of lubricant migrates to the air interface of the size during drying.
- Migration of species in the size only occurs during drying when the size is in its liquid state.
- The molecular weight and particle size of a film-former is directly related to the initiator and first stage monomer concentrations respectively.
- The molecular weight of a film-former does not alter the size's ability to form a continuous film if dried under suitable conditions.

- Film-formers with large particle sizes produce inhomogeneous films due to incomplete diffusion occurring during film formation.
- The inhomogeneity of films with larger particle sizes present produces an increasingly optically active film with an increased wet-out rate.
- The molecular weight and particle size of a film-former do not alter the corresponding sizes ability to wet a bare glass fibre due to the large amount of water present in the size formulation.
- A size can be redistributed following successive re-wetting and drying under certain conditions.
- The stiffness of a size is directly related to the molecular weight of the sizes film-former.
- An inhomogeneous, discontinuous size will be formed with excessive deviation from the size formulation.
- An excess of coupling agent is present in the standard size formulation.

7.2 Future Work

To conclude the thesis I would like to list a number of issues which I believe would be the natural route of progression should someone wish to continue research in this area. These are:

- Development of a more suitable method to measure the adhesion and cohesion of the sizes produced throughout.
- A more thorough investigation into the formulation changes mentioned in chapter 6. This would include a complete analysis of the sizes optical and film formation properties as carried out in chapter 5 to determine whether any further trends could be observed.
- An investigation into the sizes produced from the standard film-former using different additives. It would be interesting to produce sizes using a range of different additive materials, e.g. different lubricants, to determine the effect on the final properties of the overall size.
- An investigation using a different polymer based film-former to investigate how the type of polymer affects the overall properties of the complete size.

Bibliography

1. Vetrotex *Overview of Glass Fibres.*

2. Mark H.F.; Bikales N.; Overberger C.G.; Menges G.; Kroschwitz J.I., *Encyclopaedia of Polymer Science and Technology.* 2nd ed.; Wiley Interscience: Chichester, 1986; Vol. 6.

3. Vetrotex *Glass Fibres, New edition, according iso-norms*; 1993.

4. Schlachter F.E.L. US Patent 4737180. 1988.

5. Le Moigne S.; Boivent M.; Matzen G. US Patent 4615988. 1986.

6. de Dani A., *Glass Fibre Reinforced Plastics.* Newnes: London, 1960.

7. Farmer D.B. *Properties and Applications of Vinamul Glass Fibre Grades*; Vinamul.

8. Pittsburgh Plate Glass Co. GB Patent 1049517. 1966.

9. Phillips J.D. US Patent 4145201. 1978.

10. Hanna T.J. US Patent 4274853. 1979.

11. Higginbotham J.M.; Finck R.F.; Keck J.D.; Morrison M.W.; Fazio M.B.; Mercer D.T. US Patent 6065310. 2000.

12. Vetrotex *1500°C - The Quest for High Performance: Glass Fibre.*

13. Lowenstein K.L., *The Manufacturing Technology of Continuous Glass Fibres.* 2nd ed.; Elsevier: Amsterdam, 1983.

14. Darrichard L.D.; Plaisant J. US Patent 4433535. 1980.

15. Penn W.S., *GRP Technology.* MacLaren: London, 1966.

16. Gaymans R.J.; Wevers E., *Compos Part A* **1990,** 5(6), 663.

17. Ochelski S.; Kiczko A.; Gotowicki P., *Biuletyn Wojskowej Akademii Technicznej* **2005,** 54(11), 91 (AN - 2006:183825).

18. Panfilov N.A.; Abozin I.Y.; Kul'mis L.M.; Simina V.N., *Voprosy Materialovedeniya* **2002,** 3, 110 (CAN 139:70067).

19. Reynolds E.H.; Sweetland A.G.; Littler J.; Clarke D.R. GB Patent 915052. 1963.

20. Knuepfer B.; Schoettker M. DE Patent 4132390. DE 4132390, 1993.

21. Zellmer H. SE Patent 430908. 1983.

22. Hirata I.; Okada S.; Ito N.; Nozue A.; Otani M.; Yamazaki S.; Matoba, M. JP Patent 2003166162 (CAN - 139:37566). 2003.

23. Perez T.; Rebeca E. MX Patent 9910083 (CAN - 138:179256). 1999.

24. Weng Y.; Zhang, X.; Zhou W. CN Patent 1563190 (CAN - 143:368077). 2005.

25. Locatelli A., WO Patent 2002070246. **2002**.

26. Ainslie B.J.; Craig S.P. US Patent 4799946. 1989.

27. Seki T.; Sakai, T. JP Patent 2005079197 (CAN - 142:306123). 2005.

28. Wasylak J.; Dorosz D.; Kucharski J.; Kityk J. In Proceedings of SPIE - The International Society for Optical Engineering, 2003; SPIE: 2003; p 167.

29. Wagner P.A.; Ray R.I.; Little B.J.; Tucker W.C., *European Federation of Corrosion Publications* **1995,** 15, 143.

30. Laflin P. US Patent 4898769. 1989.

31. Klang E.; Richards D. In Proceedings of the International Conference on Composite Science and Technology, Durban, SA, 1996; Durban, SA, 1996; p 253.

32. Hong X.; Hua Y., *Huagong Xinxing Cailiao* **2005,** 33, 16 (CAN - 144:451215).

33. Kaushik A.; Singh, P.; Kaushik, J., *Int. J. Polym. Mat.* **2006,** 55(6), 425.

34. Poliksha A.M.; D'yakov S.P.; Kokolev N.V.; Gorbatskii I.I.; Vokhmyanin D.N.; Mulenkov B.P.; Karelin V.A.; Surovtsev G.N.; Vinokurov P.A. RU Patent 2150631 (CAN - 136:103700). 2000.

35. Johannson, O. K.; Stark, F. O.; Vogel, G. E.; Fleischmann, R. M., *J. Comp. Mat.* **1967,** 1, 278.

36. Sjögren A.; Joffe R.; Berglund L.; Mäder E., *Compos Part A* **1999,** 30, 1009.

37. Giannotta G.; Morra M.; Occhiello E.; Garbassi F.; Nicolais L.; D'Amore A., *Polym. Comp.* **1993,** 14, 224.

38. Tamaki Y.; Tomioka R. JP Patent 04338140 (CAN - 118:259778). 1992.

39. Kawabe T. JP Patent 04175247 (CAN 117:173341). 1992.

40. Garrett D.W., S. R. A. WO Patent 9201024. 1992.

41. Paul D.R.; Laura D.M.; Keskkula H.; Barlow J.W., *Polymer* **2002,** 43, 4673.

42. Schork F.J.; Gilmore C.M.; Poehlien G.W., *J. Appl. Polym. Sci.* **1993,** 48, 1449.

43. Schlehoefer B.; Luipoldhuette A.G., *Poliplasti e Plastici Rinforzati* **1971,** 19, 37 (CAN 75:6972).

44. Nascimento Buarque E. In Congresso Anual - Associacao Brasileira de Metalurgia e Materiais, 2004; Associacao Brasileira de Metalurgia e Materiais: 2004; p 1453 (CAN 144:110921).

45. Chang D.I.; Koh J.W., *Han'guk Chaelyo Hakhoechi* **1994,** 4, 219 (CAN 125:12256).

46. Farmer D.B.; McLennan A.J. US Patent 5364904. 1992.

47. Thimons T.V.; Swisher R.G.; Hou Y. US Patent 5437928. 1993.

48. Rammel G.E. US Patent 4584110. 1984.

49. Owens Corning Fiberglass Corp. GB Patent 896845. 1960.

50. Pittsburgh Plate Glass Co. GB Patent 919317. 1963.

51. Antle J.L.; Holman D.R. US Patent 2004191514. 2004.

52. Temple C.S.; Gaa P.C. WO Patent 9415884. 1994.

53. Klett M.W. WO Patent 9413473. 1994.

54. Martino G.T.; Hasuly M.J. US Patent 5120780. 1992.

55. Cowie J.M.G., *Polymers: Chemistry & Physics of Modern Materials*. 2nd ed.; Nelson Thornes: Cheltenham, 2002.

56. Beuche F., *Physical Properties of Polymers*. Interscience: New York, 1962.

57. Lovell P.A.; El Aasser M.S., *Emulsion Polymerisation and Emulsion Polymers*. Wiley Interscience: Chichester, 1997.

58. de Bruyn H. PhD Thesis. University of Sydney - PhD Thesis, 1999.

59. Kaufman H.S.; Falcetta J.J., *Introduction to Polymer Science and Technology*. Wiley Interscience: Chichester, 1997.

60. Smith W.V.; Ewart R.H., *J. Chem. Phys* **1948,** 16, 592.

61. Flory P.J., *Principles of Polymer Chemistry*. Cornell University Press: Ithica, 1953.

62. Klatte F. US Patent 1084581. 1914.

63. Mark H.F., *Encyclopaedia of Polymer Science and Engineering*. Wiley Interscience: Chichester, 1989.

64. Shawinigan Chem. Ltd. GB Patent 568884. 1945.

65. Mayne J.E.O.; Warson H.; Whitmore D.C. GB Patent 726927. 1955.

66. Yicheng Sun CN Patent 1350008 (CAN - 140:200591). 2002.

67. Iosif M.; Nicolaescu M.A. RO Patent 108800 (CAN - 132:322733). 1994.

68. Nakajima J. JP Patent 07207241 (CAN - 123:259150). 1994.

69. Ooishi M. JP Patent 05078541 (CAN - 119:74315). 1993.

70. Lee C.H.; Mallinson R.G., *J. Appl. Polym. Sci.* **1989,** 37, 3315.

71. Sarker S.; Adhikari M.S.; Banerjee M.; Konar R.S., *J. Appl. Polym. Sci.* **1990,** 39, 1061.

72. Lepizzera S.M.; Hamielec A.E., *Macromol. Chem. Phys.* **1994,** 195, 3103.

73. Makgawinata T.; El Aasser M.S.; Vanderhoff J.W.; Pichot C., *Acta Polym.* **1991,** 32, 10.

74. Urquiola M.B.; Dimonie V.L.; Sudol E.D.; El Aasser M.S., *J. Polym. Sci., Polym. Chem.* **1993,** 31, 1403.

75. Urquiola M.B.; Dimonie V.L.; Sudol E.D.; El Aasser M.S., *J. Polym. Sci., Polym. Chem.* **1996,** 30, 2619, 2931.

76. Keddie J.L.; Meredith P.; Jones R.A.L.; McDonald A.M., *Macromaolecules* **1995,** 28(8), 2673.

77. Butt H.J.; Korupka R.; Christensen B., *Colloid. Polym. Sci.* **1994,** 272(10), 1218.

78. Butt H.J.; Gerharz B., *Langmuir* **1995,** 11, 4735.

79. Joanicot M.; Wong K.; Macquet J., *Progr. Colloid. Polym. Sci.* **1990,** 81, 175.

80. Richard J., Dynamic viscoelastic properties of polymer latex films. In *Film formation in waterborne coatings*, Proder, W. U., Ed. ACS (Polymeric Materials) International Symposium Series no. 648: 1996; p 118.

81. Steward P.A.; Hearn J.; Wilkinson M.C., *Advances in Colloid and Interface Science* **2000,** 86, 195.

82. Bartsch E. Film formation from latex dispersions. http://www.uni-mainz.de/FB/Chemie/AK-Sillescu/htmlen/jahr/filmform.htm

83. Croll S.G., *J. Coat. Technol.* **1986,** 58(724), 41.

84. American society for testing materials, Standard test for minimum film formation temperature of emulsion vehicles. *ASTM O* **1993**, 2354.

85. Eckersley S.T.; Rudin A., *J. Coat. Technol.* **1990,** 67(780), 89.

86. Jenson D.P.; Morgan L.W., *J. Appl. Polym. Sci.* **1991,** 42, 2845.

87. Elgood B., *J. Oil Colour Chem. Assoc.* **1985,** 68, 164.

88. Sperry P.R.; Snyder B.S.; O'Dowd M.L.; Lesko P.M., *Langmuir* **1994,** 10, 2619.

89. Voyutskii S.S., *J. Polym. Sci.* **1958,** 32(125), 528.

90. Voyutskii S.S., Wiley Interscience: Chichester, 1963; Vol. 4.

91. Voyutskii S.S., *Rubber Chem. Technol.* **1964,** 37, 1153.

92. Bradford E.B.; Vanderhoff J.W., *J. Macromol. Chem.* **1966,** 1(2), 335.

93. Bradford E.B.; Vanderhoff J.W., *J. Macromol. Sci. Phys. B* **1972,** 6, 671.

94. Pramojaney N.; Poehlien G.W.; Vanderhoff J.W., *Drying* **1980,** 80(2), 93.

95. Pan S.X.; Davis H.T.; Scriven L.E. In Coatings conference proceedings, Atlanta, Georgia, 1996; TAPPI press: Atlanta, Georgia, 1996; p 115.

96. Iowa State University - Dept. of Materials Science and Engineering http://mse.iastate.edu/microscopy/ESEM.html (2006),

97. Seal Labs http://www.seallabs.com/edx.html

98. Neumann A.W.; Good R.J., *Surface and Colloid Science*. Plenum Press: New York, 1979; Vol. 2.

99. Quéré D., *Nature Materials* **2002,** 1, 14.

100. British Standards Institute, *BS EN 28510-2:1993* **1993**.

101. British Standards Institute, *BS ISO 4587:2003* **2003**.